

**NDOT Research Report**

**Report No. 493-12-803**

---

**Estimating Sediment Losses Generated from  
Highway Cut and Fill Slopes in the Lake Tahoe  
Basin**

---

**December 2014**

**Nevada Department of Transportation  
1263 South Stewart Street  
Carson City, NV 89712**



## Disclaimer

This work was sponsored by the Nevada Department of Transportation. The contents of this report reflect the views of the authors, who are responsible for the facts and the accuracy of the data presented herein. The contents do not necessarily reflect the official views or policies of the State of Nevada at the time of publication. This report does not constitute a standard, specification, or regulation.

University of Nevada, Reno

**Estimating Sediment Losses Generated from Highway Cut and Fill Slopes in the Lake Tahoe Basin**

A thesis submitted in partial fulfillment of the  
requirements for the degree of Master of Science  
in Hydrologic Sciences

By

Daniel L. Stucky

Dr. Keith E. Dennett/Thesis Advisor

December 2014



University of Nevada, Reno  
Statewide • Worldwide

THE GRADUATE SCHOOL

We recommend that the thesis  
prepared under our supervision by

**DANIEL L. STUCKY**

entitled

**Estimating Sediment Losses Generated from Highway Cut And Fill Slopes in the  
Lake Tahoe Basin**

be accepted in partial fulfillment of the  
requirements for the degree of

**MASTER OF SCIENCE**

Dr. Keith Dennett, Advisor

Dr. Eric Marchand, Committee Member

Dr. Paul Verburg, Graduate School Representative

Marsha H. Read, Ph. D., Dean, Graduate School

December, 2014

## ABSTRACT

Lake Tahoe's famed water clarity has gradually declined over the last 50 years, partially as a result of fine sediment particle (FSP, < 16 micrometers in diameter) contributions from urban stormwater. Of these urban sources, highway cut and fill slopes often generate large amounts of sediment due to their steep, highly-disturbed nature. Therefore, understanding the erosion mechanisms (rainfall-runoff and dry ravel), the magnitude of erosion rates and the particle-size distribution (PSD) of the eroded material from these highly disturbed slopes, as well as quantifying the load reductions achieved through slope stabilization practices, is critical to reducing sediment contributions to Lake Tahoe. Furthermore, accurate predictions of soil losses from these cut and fill slopes are required to establish baseline sediment loadings, assess the effectiveness of slope stabilization improvements and track the progress towards achieving Total Maximum Daily Load (TMDL) reduction milestones in the Lake Tahoe Basin. The Revised Universal Soil Loss Equation (RUSLE), Tahoe Basin Sediment Model (TBSM) and the Road Cut and Fill Slope Sediment Loading Assessment Tool (RCAT) are the most common soil erosion models used to predict sediment yields from disturbed slopes in the Lake Tahoe Basin; however, limited comparisons of the predictions from the various models to actual field data exist.

The primary objectives of this research were to (1) design and construct an inexpensive rainfall simulator capable of closely replicating the kinetic energy of natural rainfall and operating over steep terrain (2) use rainfall simulation data collected from a diverse set of 25 slopes adjacent to highways in the Lake Tahoe Basin to evaluate the predictive performance of the erosion models and determine significant correlations between the physical plot characteristics and the collected runoff and erosion data; (3) provide suggestions to improve the predictive performance of the models; and (4) use field measurements of dry ravel to quantify sediment yields and develop predictive equations to estimate this erosion phenomena.

The comprehensive correlation analyses of the rainfall simulation data indicated that surface cover, of all the physical characteristics of the slope site, most directly influenced the magnitude of erosion. In terms of broad comparisons, the slopes with volcanic soils (sandy loams) typically generated greater amounts of runoff and erosion than the slopes with granitic soils (sand and loamy sands) and exhibited finer particle size fractions in the bulk soil and runoff, resulting in four to ten times greater amounts of FSP soil

losses for comparable slopes. The fill slopes appeared to exhibit more noticeable and less predictable variations in the measured runoff and erosion parameters, presumably due to the unique characteristics of these slopes (e.g., foreign soil material, increased soil compaction and decreased surface roughness).

Using the Nash-Sutcliffe Model efficiencies ( $R^2_{eff}$ ) to evaluate the predictive performance of the selected models, the  $R^2_{eff}$  for the TBSM and RCAT were negative for both the total and FSP soil loss predictions, indicating that the mean of the observed soil losses from the rainfall simulations predicted the soil losses better than the TBSM and RCAT models. Conversely, the RUSLE model performed best in predicting both total soil losses ( $R^2_{eff} = 0.20$ ) and FSP soil losses ( $R^2_{eff} = 0.16$ ). The RUSLE performed most accurately in predicting the largest FSP sediment yields, while the TBSM performed best in predicting the smaller FSP sediment yields. Some potential improvements to the various sediment loss models include: using the bulk soil characteristics to estimate the FSP fraction of the runoff erosion (RUSLE), incorporating a slope-length factor to increase erosion rates on longer slopes (RCAT) and refine model soil parameters using calibration techniques and the soil, runoff and erosion data collected from the rainfall simulations performed during this research (TBSM).

The dry ravel collected from the field traps indicated that sediment yields are primarily slope dependent and may significantly increase when slope gradients exceed approximately 60%. Additionally, the PSD analyses revealed that the amount of fines in the bulk soil was similar to the amount in the dry ravel collected from the sediment traps (1:1 ratio), thus differing from the ratio of the FSP fraction observed during the rainfall simulation erosion and the FSP fraction of the bulk soil (1:5:1).

## ACKNOWLEDGEMENTS

I would like to express my sincere appreciation to my advisor, Dr. Keith Dennett, for his guidance, support and mentorship throughout this entire research process. Thanks also to my committee members, Dr. Paul Verburg and Dr. Eric Marchand, for their valuable contributions to this research. I want to recognize my employer Atkins, specifically my supervisor, Brian Janes, for his understanding, flexibility and complete support during this challenging time of pursuing my master's degree while working full-time as a civil engineer. Many thanks to Dr. Mark Weltz and Dr. Kossi Nouwakpo for sharing their expertise on the RUSLE, as well as Dr. William Elliot (Rocky Mountain Research Station, Moscow, Idaho) and Drea Traeumer (US Forest Service, Elk City, Idaho) for providing insight and direction on WEPP/TBSM modeling. Additionally, numerous graduate and undergraduate students at the University of Nevada-Reno contributed significant amounts of time and effort to this research. Shankar Gurung, Angel Lacroix, Jake Schill, Andrea Hlatky, Max Dugan and Bryan Byrne, thank you for all your hard work and dedication in ensuring that field and lab testing was performed at a high level.

Thank you to the Nevada Department of Transportation (NDOT) for their support of this research project. In particular, I want to acknowledge Matt Nussbaumer and Tyler Thew of the NDOT Hydraulics Section for their assistance in coordinating field testing, as well as their helpful input in making this a more successful project.

I want to end by recognizing my family support system. Without them, I would have never been able to achieve this goal. Thank you to my parents, Eric and Debbie Stucky, as well as my brother, Nick, and sister, Shata, and their respective families for always supporting my educational aspirations and encouraging me to achieve my goals. Most importantly, I would like to thank my wife, Ashley, for her constant, unwavering belief in me and support of my goals. Countless times during this process, when my roles as a full-time employee, father, husband and graduate student seemed overwhelming, she shouldered a bigger share of life's duties, lifted me up with words of encouragement and kept me focused on the end goal. Thank you. Lastly, I thank my beautiful and wildly entertaining daughter, Averi, for her ability to always put life's pressures in perspective with her innocence, curiosity and joy for life.

## TABLE OF CONTENTS

ABSTRACT .....	i
ACKNOWLEDGEMENTS .....	iii
TABLE OF CONTENTS .....	iv
LIST OF TABLES .....	vii
LIST OF FIGURES.....	viii
LIST OF ABBREVIATIONS AND ACRONYMS .....	x
Chapter 1 .....	1
INTRODUCTION .....	1
1.1 Background .....	1
1.2 Research Objectives .....	5
Chapter 2 .....	6
LITERATURE REVIEW .....	6
2.1 Overview .....	6
2.2 Soil Erosion Process.....	6
2.2.1 Dry Ravel .....	8
2.3 Soil Erosion and Water Quality in the United States .....	9
2.4 Lake Tahoe Total Maximum Daily Loads (TMDLs).....	10
2.4.1 Pollutant Load Reduction Model (PLRM) .....	10
2.5 History and Development of Soil Erosion Prediction Methods .....	11
2.6 Soil Erosion Prediction Models .....	16
2.6.1 Revised Universal Soil Loss Equation (RUSLE) .....	16
2.6.2 Modified Universal Soil Loss Equation (MUSLE) .....	23
2.6.3 Water Erosion Prediction Project (WEPP).....	24
2.6.4 Tahoe Basin Sediment Model (TBSM).....	32
2.6.5 Road Cut and Fill Slope Sediment Loading Assessment Tool (RCAT).....	33
2.7 Soil Erosion Model Evaluation Studies .....	37

2.8 Rainfall Simulations.....	38
2.8.1 Rainfall Simulator Types.....	38
2.8.2 Rainfall Kinetic Energy.....	39
2.8.3 Rainfall Intensity and Duration.....	43
2.8.4 Plot Size and Scaling.....	43
2.8.5 Uniformity.....	43
2.9 Lake Tahoe Rainfall Simulation-Based Soil Erosion Research.....	44
2.10 Particle Size Distribution Methods.....	49
2.11 Soil Textural Classification Systems.....	49
2.11.1 USDA Textural Soil Classification.....	50
Chapter 3.....	52
MATERIALS AND METHODS.....	52
3.1 Overview.....	52
3.2 Study Site Characteristics and Slope Selection.....	52
3.3 Rainfall Simulations.....	54
3.3.1 Design and Construction.....	55
3.3.2 Evaluation and Calibration.....	57
3.3.3 Field Testing Procedure.....	60
3.4 Dry Ravel Sediment Traps.....	64
3.4.1 Design and Construction.....	64
3.4.2 Field Testing Procedure.....	64
3.5 Particle Size Analysis and Soil Characterization.....	65
3.5.1 Site Soil Samples.....	67
3.5.2 Rainfall Simulation Runoff Sediment.....	70
3.5.3 Collected Dry Ravel.....	72
3.6 Selected Soil Erosion Models.....	72
3.7 Sensitivity Analysis of Soil Erosion Models.....	72

3.7.1 Model Sensitivity Parameters.....	73
3.8 Soil Erosion Modeling Approach.....	74
3.8.1 Revised Universal Soil Loss Equation (RUSLE) .....	75
3.8.2 Road Cut and Fill Slope Sediment Loading Assessment Tool (RCAT).....	77
3.8.3 Tahoe Basin Sediment Model (TBSM).....	77
3.9 Statistical Analyses .....	79
3.9.1 Regression Correlation Comparison Techniques .....	79
3.9.2 Model Evaluation Techniques.....	80
Chapter 4 .....	82
RESULTS AND DISCUSSION .....	82
4.1 Overview.....	82
4.2 Soil Erosion Model Sensitivity Analyses.....	82
4.3 Evaluation of Bulk Soil Characteristics .....	84
4.4 Rainfall Simulation Evaluation .....	85
4.4.1 Rainfall Simulation Runoff Assessment.....	90
4.4.2 Rainfall Simulation Erosion Assessment .....	95
4.4.3 Comparison of Results for Lake Tahoe Rainfall Simulation and Erosion Studies .....	103
4.5 Evaluation of Dry Ravel Monitoring .....	106
4.6 Soil Erosion Model Performance and Potential Improvements .....	111
4.6.1 Revised Universal Soil Loss Equation (RUSLE) .....	117
4.6.2 Tahoe Basin Sediment Model (TBSM).....	122
4.6.3 Road Cut and Fill Slope Sediment Loading Assessment Tool (RCAT).....	125
Chapter 5 .....	129
SUMMARY AND CONCLUSIONS .....	129
REFERENCES.....	134

**LIST OF TABLES**

Table 2.1. Lake Tahoe rainfall simulation characteristics .....	48
Table 2.2. Sediment particle size classification (USDA 1993) .....	50
Table 3.1. Locations of slope testing sites.....	54
Table 3.2. Summary of rainfall simulation plot characteristics .....	63
Table 3.3. Rainfall simulation site soil characteristics .....	68
Table 3.4. Dry ravel site soil characteristics.....	69
Table 3.5. Erosion model parameters for sensitivity analyses.....	74
Table 3.6. RUSLE and TBSM/WEPP site-specific soil parameters.....	79
Table 4.1. Erosion model sensitivity analyses.....	82
Table 4.2. Summary of bulk soil characteristics.....	85
Table 4.3. Summary of runoff and erosion measurements during rainfall simulations.....	86
Table 4.4. Summary of runoff and erosion parameters for rainfall simulations .....	88
Table 4.5. Comparison of erosion measurements from Lake Tahoe Basin erosion studies .....	104
Table 4.6. Summary of dry ravel monitoring .....	107
Table 4.7. Summary of observed and predicted soil loss from rainfall simulation plots.....	112
Table 4.8. Soil erosion model performance evaluation statistics .....	115

## LIST OF FIGURES

Figure 1.1. Lake Tahoe clarity depth measurements (UC Davis, 2013).....	1
Figure 1.2. Typical highway cut and fill slopes in the Lake Tahoe Basin.....	2
Figure 1.3. Schematic of typical mountain highway (CTIP, 2012).....	4
Figure 2.1. Hill slope soil loss, deposition and sediment yield (USDA-ARS, 1995b).....	7
Figure 2.2. The WEPP erosion model structure diagram (Ascough II et al., 1997).....	26
Figure 2.3. Runoff sediment yield dependence on granitic soil treatment and slope (Drake et al., 2010) ...	35
Figure 2.4. Rainfall velocity vs. fall distance for various drop diameters (van Boxel, 1998).....	41
Figure 2.5. Rainfall intensity-kinetic energy relationships (van Dijk et al., 2002).....	42
Figure 2.6. Comparison of soil classification systems (USDA 1993).....	50
Figure 2.7. USDA textural triangle (USDA 1993).....	51
Figure 3.1. Slope testing locations- overall site map.....	53
Figure 3.2. Typical rainfall simulator setup.....	57
Figure 3.3. Rainfall simulator piezometer head-rainfall intensity curve.....	59
Figure 3.4. Rainfall simulation site photographs.....	62
Figure 3.5. Dry ravel sediment trap installation.....	65
Figure 3.6. Vacuum filtration.....	66
Figure 3.7. Hydrometer testing.....	66
Figure 3.8. Laser particle size analyzer (DRI).....	66
Figure 3.9. Runoff hydrograph (RS 7-1).....	71
Figure 3.10. Sedigraph (RS 7-1).....	71
Figure 4.1. Variation of percent sand, silt and clay with cone penetrometer depth to refusal.....	89
Figure 4.2. Variation of runoff coefficient with percent silt in bulk soil.....	91
Figure 4.3. Variation of runoff coefficient with surface cover for cut slopes.....	93
Figure 4.4. Variation of runoff coefficient with slope gradient for cut slopes.....	93
Figure 4.5. Variation of runoff coefficient with percent organic matter in bulk soil for cut slopes.....	94
Figure 4.6. Variation of total equivalent soil loss with surface cover.....	95

Figure 4.7. Variation of total equivalent soil loss with percent organic matter in bulk soil .....	96
Figure 4.8. Variation of total equivalent soil loss with slope gradient .....	98
Figure 4.9. Variation of FSP in runoff with FSP in bulk soil .....	99
Figure 4.10. Variation of FSP in soil loss with silt content of bulk soil for cut slopes .....	100
Figure 4.11. Variation of FSP in soil loss with runoff coefficient.....	101
Figure 4.12. Variation of FSP in soil loss with surface cover .....	102
Figure 4.13. Rilling of cut slope along U.S. Highway 50.....	105
Figure 4.14. Dry ravel deposition cones along U.S. Highway 50 .....	107
Figure 4.15. Variation of sediment yield from dry ravel with ground slope .....	109
Figure 4.16. Variation of FSP in the collected dry ravel with FSP in bulk soil.....	110
Figure 4.17. Comparison of predicted total soil losses with observed total soil losses .....	113
Figure 4.18. Comparison of predicted FSP soil losses with observed FSP soil losses .....	113

**LIST OF ABBREVIATIONS AND ACRONYMS**

AASHTO	American Association of State Highway and Transportation Officials
ANSWERS	Aerial Nonpoint Source Watershed Environment Response Simulation
APEX	Agricultural Policy Environmental EXtender
ARS	Agricultural Research Service
BMP	Best Management Practices
CEC	Characteristic Effluent Concentration
CEC	Cation Exchange Capacity
CI	Confidence Intervals
CLIGEN	CLImate GENerator
CRC	Characteristic Runoff Concentration
CREAMS	The Chemical, Runoff and Erosion from Agricultural Management Systems
CWA	Clean Water Act
DEM	Digital Elevation Model
DRI	Desert Research Institute
DTR	Depth to Refusal
EPIC	Erosion Productivity Impact Calculator
FSP	Fine Sediment Particles (less than 16 microns in diameter)
HM	Hydrometer Method
IERS	Integrated Environmental Restoration Services
LCCP	Lake Clarity Crediting Program
LDM	Laser Diffraction Method
LWQCB	Lahontan Water Quality Control Board
MUSLE	Modified Universal Soil Loss Equation
NDEP	Nevada Division of Environmental Protection
NDOT	Nevada Department of Transportation
NPS	Non-Point Source

NRCS	Natural Resources Conservation Service
OFE	Overland Flow Element
PLRM	Pollutant Load Reduction Model
PM	Pipette Method
PNM	Pine Needle Mulch
PRISM	Parameter-elevation Regressions on Independent Slopes Model
PSD	Particle Size Distribution
PVC	PolyVinyl Chloride
RCAT	Road Cut and Fill Sediment Loading Assessment Tool
RMRS	Rocky Mountain Research Station
ROW	Right of Way
RUSLE	Revised Universal Soil Loss Equation
RUSLE1	Revised Universal Soil Loss Equation version 1
RUSLE2	Revised Universal Soil Loss Equation version 2
RUSLE (KNOMO)	RUSLE model simulations using site-specific soils data and empirical equations to estimate site-specific soil parameters
RUSLE (KNRCS)	RUSLE model simulations using soil parameters from Tahoe Basin NRCS Soil Survey
SCS	Soil Conservation Service
SLR	Soil Loss Ratio
SNOTEL	SNOWpack TELemetry
SWAT	Soil and Water Assessment Tool
SWMM5	Storm Water Management Model version 5
SWRRB	Simulator for Water Resources in Rural Basins
SWT	Storm Water Treatment
TBSM	Tahoe Basin Sediment Model
TBSM (PB)	TBSM model simulations using default parameters for the parent material/soil texture obtained from the TBSM Tahoe database

TBSM (SS)	TBSM model simulations using site-specific soils data and empirical equations to estimate site-specific soil parameters
TMDL	Total Maximum Daily Load
TSS	Total Suspended Solids
USBR	United States Bureau of Reclamation
USCS	Unified Soil Classification System
USDA	United States Department of Agriculture
USEPA	United States Environmental Protection Agency
USLE	Universal Soil Loss Equation
WEPP	Water Erosion Prediction Project

## Chapter 1

**INTRODUCTION****1.1 Background**

Lake Tahoe's world renowned water clarity has steadily decreased since Secchi depth clarity measurements commenced in the late 1960s, as shown in Figure 1.1 (UC Davis, 2013). Scientific research has revealed that fine sediment particles (FSP, < 16 microns in diameter) are the primary cause of clarity loss; urban stormwater runoff is thought to be responsible for nearly 70 percent of the FSP contributions to Lake Tahoe (NDEP, 2011). In order to reverse the decline in lake clarity, the Lake Tahoe Total Maximum Daily Load (TMDL) established load reduction milestones for each urban jurisdiction within the Tahoe Basin. The ultimate goal of the TMDL was to reduce the amount of phosphorus, nitrogen and FSP entering Lake Tahoe and restore deep water transparency to a 29.7 meters annual average Secchi depth, last measured in the late 1960s. The Lake Tahoe water clarity model suggested that the ultimate goal could take 65 years to achieve; therefore, the TMDL also established a 20-year interim goal, known as the Clarity Challenge, with the aim to reduce basin-wide FSP contributions by 32 percent and to reach an estimated corresponding Secchi depth reading of 24 meters (NDEP, 2011).

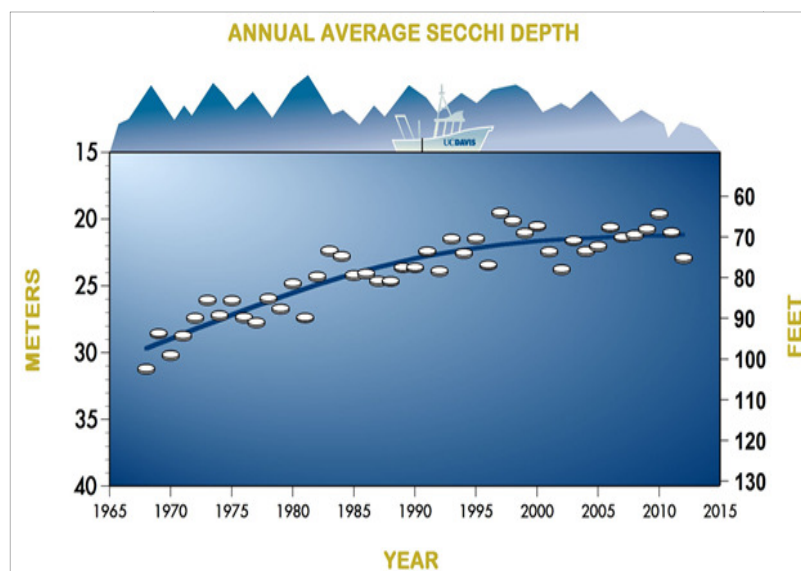


Figure 1.1. Lake Tahoe clarity depth measurements (UC Davis, 2013)

The Lake Clarity Crediting Program (LCCP) was developed to track overall progress towards meeting TMDL load reduction milestones through the use of Lake Clarity Credits. The program holds each

of the seven urban jurisdictions within the Tahoe Basin accountable, including the Nevada Department of Transportation (NDOT), by awarding annual Lake Clarity Credits based on pollutant load reductions achieved by each urban jurisdiction (LWQCB and NDEP, 2011). In order to receive credits through the LCCP, NDOT is required to estimate the quantities of FSP generated from right-of-way (ROW) by considering various factors such as road shoulder conditions, road abrasive application practices during winter weather, and pollutant recovery activities. Currently, the standard estimation tool recommended by the LCCP for evaluating pollutant load reductions and ultimately determining credits is the Pollutant Load Reduction Model (PLRM). The PLRM estimates pollutant loads generated from distributed sources characterized by specific land use conditions. However, there is currently no land use appropriate for simulating sediment contributions generated from major roadway cut and fill slopes, as these slopes exhibit unique characteristics (steep, highly disturbed, with minimal vegetative cover) that increase their vulnerability to significant erosion, as shown in Figure 1.2. The developers of the PLRM recommended that users evaluate the sediment contributions from these slopes externally using various nationally or regionally accepted soil loss models (PLRM, 2009).



Figure 1.2. Typical highway cut and fill slopes in the Lake Tahoe Basin

The current LCCP handbook (LWQCB and NDEP, 2011) proposes using the Cut and Fill Slope Sediment Loading Assessment Tool (RCAT) to estimate loads from cut and fill slopes. RCAT is a relatively new methodology based on soil erosion research and testing performed within the Lake Tahoe

Basin; however this research was largely based on milder slopes located on the west side of the Lake Tahoe Basin (Drake, McCullough, & Grismer, 2010). Therefore, it is unknown whether RCAT can be used to adequately predict the quantity of FSP for slopes located along roadways within NDOT's jurisdiction. Early comparisons of RCAT and other methods on NDOT cut and fill slopes has shown, in many cases, that RCAT estimates may be considerably lower than other methods. Additionally, RCAT does not currently incorporate an adequate procedure for evaluating slopes containing natural rock outcroppings or riprap covered slopes, a slope stabilization technique widely used by NDOT on previous water quality improvement projects within the Lake Tahoe Basin.

The Revised Universal Soil Loss Equation (RUSLE), developed by the United States Department of Agriculture (USDA), is another slope erosion prediction model historically used by NDOT on previous improvement projects. The RUSLE model also has limitations. RUSLE is an empirical model originally developed to predict soil losses from agricultural fields in the Midwest. Although RUSLE has been expanded in updated versions to estimate soil erosion by considering additional land uses, climatic conditions, and management practices, including rangelands, forests, mined lands, and construction sites across the United States, the method only estimates total sediment losses (Galetovic, Toy, & Foster, 1998). Further, it does not incorporate a direct method for estimating FSP and requires additional analyses or assumptions to determine FSP.

The Water Erosion Prediction Project (WEPP) is a process-based, continuous simulation computer model developed by the USDA that predicts soil detachment, transport, and delivery along a hill slope or through a channel or other impoundment facilities within a watershed. The Tahoe Basin Sediment Model (TBSM), developed in 2010, is the most recent WEPP interface and focuses specifically on the Lake Tahoe Basin. This version of the Disturbed WEPP predicts erosion from rangeland, forestland, and forest skid trails using climate, soil and management parameters customized for the Lake Tahoe Basin (Elliot & Hall, 2010). Although specific to the Tahoe Basin, the model still does not incorporate the relatively steep cut and fill slopes characteristic of NDOT roadways along the east shore of Lake Tahoe.

Steep, highly erodible cut and fill slopes occupy a significant portion of the NDOT ROW in the Tahoe Basin. Additionally, drainage conveyance facilities are typically located at the base of these cut slopes, often resulting in the transport of sediment into culverts and ultimately into Lake Tahoe. Figure 1.3 provides a schematic of the large cut and fill slopes and drainage facilities associated with a typical mountain highway. NDOT has spent millions of dollars on slope stabilization improvements and generally considers slope stabilization to be a cost effective tool for reducing erosion and sediment transport. The amount of Lake Clarity Credits that NDOT receives for their improvements is directly proportional to the amount of sediment generated from cut and fill slopes and reductions achieved from slope stabilization improvements. It is critical that NDOT have a consistent and reliable method for estimating sediment generated from cut and fill slopes within their jurisdiction. NDOT is concerned that the lack of an accurate soil loss prediction tool for NDOT-specific cut and fill slopes could result in fewer credits, potential fines imposed by the US Environmental Protection Agency (USEPA), additional regulations, and reduced funding for future improvement projects, possibly creating a disincentive for NDOT to implement stabilization improvements in the future.

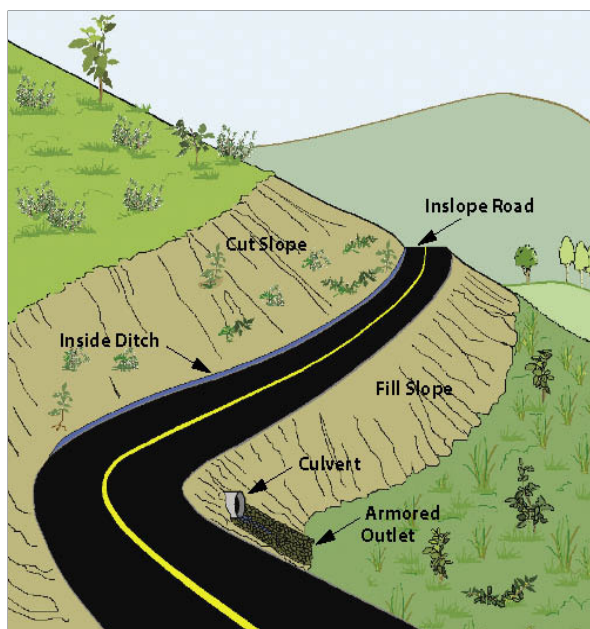


Figure 1.3. Schematic of typical mountain highway (CTIP, 2012)

## 1.2 Research Objectives

The primary objective of this research project was to compare RCAT, RUSLE, and TBSM and other suitable soil loss prediction models in order to identify the most appropriate method for determining the quantity of total sediment and FSP generated from highway cut and fill slopes located on the east side of Lake Tahoe along roadways maintained by NDOT. Additionally, this research will expand the current Lake Tahoe slope erosion dataset by incorporating NDOT-specific slopes. The results of soil erosion models and field testing will be used to propose potential modifications to these methods in order to provide more accurate and reliable predictions of the quantities of sediment generated from slopes within the Lake Tahoe Basin.

The specific objectives of this research project included the following:

- Identify soil erosion prediction models most appropriate for estimating sediment generation from highway cut and fill slopes within the Lake Tahoe Basin;
- Perform sensitivity analyses of the selected soil erosion methodologies to identify the most sensitive input parameters;
- Validate soil erosion model predictions for total and FSP soil loss using measured data obtained during rainfall simulations;
- Perform statistical analyses of various datasets to identify significant correlations between characteristics of rainfall simulation plots and runoff/erosion parameters;
- Provide recommendations or modifications to improve the accuracy of the various models tested; and
- Attempt to quantify soil losses resulting from dry ravel from a variety of NDOT slopes.

## Chapter 2

### LITERATURE REVIEW

#### 2.1 Overview

This chapter summarizes the detailed review of technical, engineering and scientific literature related to the soil erosion process, the impacts of soil erosion on water quality in the United States, the Lake Tahoe TMDL regulations, the development and structure of various soil erosion prediction models, an overview of previous studies evaluating soil erosion models, the use of rainfall simulators to study the rainfall-runoff and erosion process, a review of past erosion studies performed within the Lake Tahoe Basin, a description of particle size distribution testing methods, and a discussion of soil texture classification systems.

#### 2.2 Soil Erosion Process

Soil erosion represents the process by which soil material is detached and transported across the ground surface by wind, water, plants, humans, animals and/or other mechanisms. The three major water-induced soil erosion processes on hill slopes are the following (Galetovic et al., 1998): (1) the impact of raindrops on the ground surface; (2) unconfined, shallow overland flow (sheet flow or interrill erosion); and (3) concentrated runoff forming rills or small, ephemeral flow paths (rill erosion). Rill erosion results in considerably greater soil detachment rates and downstream sediment transport capacity in comparison to erosion caused by raindrop impact and subsequent interrill erosion (Renard, Foster, Weesies, McCool, & Yoder, 1997). At the watershed scale, gully and stream-channel erosion also contribute to the overall erosion process (USBR, 2006).

Erosion is a natural phenomenon, although the disturbance of the natural landscape by humans generally increases erosion relative to the natural erosion process. Soil erosion from construction sites and other highly-disturbed areas may generate average annual erosion rates of 100 to 200 tons per acre, resulting in nearly 1,000 times greater erosion rates than pre-construction rates (USEPA, 1992). In the Lake Tahoe Basin, disturbance from construction activities often degrades soil quality by removing nutrient rich topsoil from slopes. This slope disturbance, combined with the steep terrain, high elevation, and semi-

arid climate characteristics of the Tahoe Basin, inhibits vegetative growth and further exposes granitic and volcanic subsoils to erosion (Grismer & Hogan, 2004).

The terms soil loss and sediment yield are often used in literature, however these terms are not interchangeable. Soil loss refers to the soil material removed from a particular slope or slope segment caused by raindrop impact, interrill or rill erosion. Conversely, sediment yield describes the soil losses from slopes (rill and interrill erosion), plus erosion from streams and gullies, minus the sediment deposited in route to a point of interest (Galetovic et al., 1998). Figure 2.1 schematically distinguishes between the terms of soil loss, sediment deposition and sediment yield for a hill slope segment.

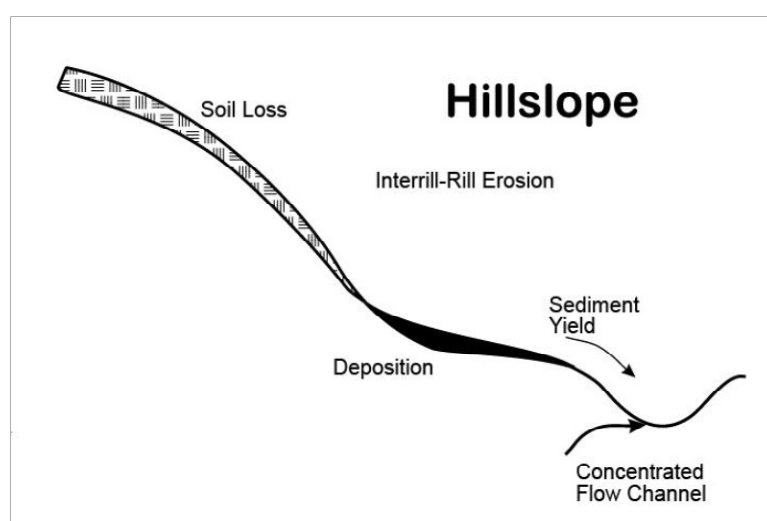


Figure 2.1. Hill slope soil loss, deposition and sediment yield (USDA-ARS, 1995b)

In addition to soil erosion resulting from rainfall and snowmelt runoff, wind and dry ravel erosion are other dominant erosive agents causing mass erosion, specifically in arid regions where soil is often dry and lacks protective vegetation (Gabet, 2003; Stallings, 1951). Dry ravel, discussed further in subsection 2.2.1, refers to the movement of sediment by means of bouncing, sliding or rolling down a hill slope in the absence of rainfall (Gabet, 2003).

Surface cover in the form of vegetation, rock, mulch, litter and other erosion protection materials can reduce the impacts of all types of erosive forces on the detachment and transport of soil particles, promote infiltration, and ultimately decrease soil erosion along a hill slope (Robichaud & Brown, 2002).

### 2.2.1 Dry Ravel

Dry ravel is a general term that describes the downward slope movement of sediment particles by forces other than rainfall. This erosion mechanism is considered a significant hill slope transport process, particularly in arid and semiarid environments containing dry, loose surface material (Gabet, 2003). Typically occurring on steep slopes with little ground cover, dry ravel is initially mobilized by animals or human disturbances, small vibrations and minor landslides (Anderson, Coleman, & Zinke, 1959; Krammes, 1965). Based on an evaluation of previous plot studies, dry ravel is often difficult to quantify and distinguish from wind erosion; therefore, dry ravel measurement studies typically quantify erosion from all non-water induced soil erosion processes (Sidle, Pearce, & O' Loughlin, 1985).

In separate studies evaluating dry ravel from steep hill slopes in California's San Gabriel Mountains, Anderson et al. (1959) and Krammes (1965) reported high sediment yields that generally increased nonlinearly with respect to slope. Anderson et al. (1959) observed that dry ravel erosion rates decreased during the wet season, attributing this seasonal decline to increased particle cohesion resulting from greater soil moisture.

Gabet (2003) examined sediment transport by dry ravel using flume experiments and field measurements from moderate to steep hill slope transects near Santa Barbara, California. In this study, Gabet (2003) used the hill slope measurements to calibrate a nonlinear, slope dependent transport equation for dry ravel of the following form:

$$q_d = \frac{\kappa}{\mu \cos \theta - \sin \theta} \quad \text{Equation 2.1}$$

where  $q_d$  = downslope mass flux ( $\text{kg m}^{-2} \text{yr}^{-1}$ )

$\kappa$  = constant (dimensionless)

$\mu$  = coefficient of kinetic friction (dimensionless)

$\theta$  = slope angle (degrees)

Additionally, the study furthered the seasonal observations from Anderson et al. (1959) by presenting an approach to predict the occurrence probability of dry ravel erosion throughout the year, based on a function of slope gradient and seasonal changes in soil moisture and particle cohesion.

### **2.3 Soil Erosion and Water Quality in the United States**

Soil erosion deteriorates the soil quality by removing important organic matter and nutrients which interferes with biological activity, resulting in decreased infiltration, plant growth and stability. In addition to the degradation of soil quality, soil erosion can also cause major water quality problems in surface waters and drainage ways, resulting in major environmental and economic impacts. Each year in the United States, more than 4 billion metric tons of soil are removed from the land surface by wind and water erosion, resulting in an approximately \$44 billion economic loss associated with the on-site and off-site environmental impacts of soil erosion (Pimentel et al., 1995).

Sediment is listed by the USEPA as the most significant non-point source (NPS) pollutant in the United States and the number one cause of pollution to rivers, streams, lakes and reservoirs (USEPA 1992). Soil erosion can impair surface water bodies through the following processes: (1) supplies excess nutrients to water bodies, specifically phosphorus and nitrogen, thus accelerating eutrophication; (2) reduces water quality by increasing turbidity, thus degrading aesthetics and habitat for fish and other aquatic species; (3) decreases conveyance capacity due to sedimentation within streambeds, potentially resulting in more frequent flooding; and (4) increases sediment related damages, causing economic impacts related to clean up and maintenance costs (USDA-NRCS, 2000).

In order to limit soil erosion and protect water quality in the United States, local, state and federal regulations have been established in an effort to reduce, control, and prevent soil erosion. The federal Clean Water Act (CWA) of 1972 established the basic framework for regulating pollutant discharges and water quality standards to all surface waters within the United States (USEPA, 1992). Specifically, the CWA requires states, territories and authorized tribes to establish water quality standards for all water bodies, identify impairments associated with these waterbodies, and determine TMDLs to fulfill these water quality standards (NDEP, 2011). In determining sediment related TMDLs, regulators require the use of comprehensive watershed modeling systems capable of simulating rill and interrill erosion, sediment transport, scour, deposition, gully and stream-channel erosion, and sedimentation in lakes, rivers and wetlands (USBR, 2006).

## **2.4 Lake Tahoe Total Maximum Daily Loads (TMDLs)**

Lake Tahoe is designated as an “Outstanding National Resource Water” by the USEPA. This prestigious designation requires strict protection of water quality and aesthetics through regulation of pollutant discharges (LWQCB and NDEP, 2011). Since measurements began in 1968, Lake Tahoe’s clarity has declined by nearly 30 feet as a result of increased basin development and tourism (NDEP, 2011). Based on the requirements of the CWA, California and Nevada established the Lake Tahoe TMDLs to address Lake Tahoe’s transparency and clarity impairments, which identifies fine sediment particles, nitrogen and phosphorus as the primary pollutants of concern responsible for the decline in water quality. The Lake Tahoe TMDL document identifies FSP as the primary cause of Lake Tahoe’s clarity loss and reports that urban stormwater runoff accounts for nearly 70 percent of the FSP contributions into Lake Tahoe (NDEP, 2011). The PLRM was developed to support the TMDL process by tracking pollutant load reductions from urban stormwater (PLRM, 2010a).

### **2.4.1 Pollutant Load Reduction Model (PLRM)**

The PLRM was developed in 2009 to provide a technical tool for designers and regulators to evaluate pollutant load reduction alternatives for stormwater quality improvement projects within the Tahoe Basin (PLRM, 2010a). The model integrates climate, soil, and land use databases specific to the Lake Tahoe Basin with USEPA’s Storm Water Management Model version 5 (SWMM5) to predict average annual loads for the various pollutants of concern defined in the Lake Tahoe TMDLs (PLRM, 2010a). Currently, the PLRM is the standard estimation tool recommended by the LCCP for establishing baseline loads, evaluating pollutant load reductions and ultimately determining Lake Clarity Credits used to provide accountability amongst the various urban jurisdictions within the Tahoe Basin in an effort to achieve the load reduction milestones established in the Lake Tahoe TMDLs (LWQCB and NDEP, 2011).

The Tahoe-specific PLRM database includes the following major components: precipitation and temperature data, groundwater parameters, Natural Resources Conservation Service (NRCS) soil properties for the Tahoe Basin, snow hydrology parameters, characteristic runoff concentrations (CRCs) for different land uses, characteristic effluent concentrations (CECs) for a variety of stormwater treatment (SWTs) facilities, and factors associated with the effectiveness of maintenance practices in reducing pollutant loads.

Using the customized Tahoe database and user supplied inputs, the PLRM generates a SWMM5 input file, then utilizes the SWMM5 engine to execute continuous simulations of rainfall, runoff, hydrologic routing and storage/treatment processes to ultimately produce pollutant load estimates (PLRM, 2010a).

The PLRM estimates pollutant load generation from distributed sources characterized by land use and specific land use conditions. Past monitoring and research efforts in the Tahoe Basin contributed to the development of CRCs, based on specific urban land use characteristics and conditions, for the pollutants of concern in the TMDLs for Lake Tahoe. The PLRM estimates pollutant loads for a catchment by multiplying the weighted CRCs based on land use by the computed runoff volume (PLRM, 2009). Of the specific urbanized land uses available in the PLRM, there is currently no land use appropriate for simulating sediment contributions from major roadway cut and fill slopes, as these slopes exhibit unique characteristics (e.g., steep, disturbed, and low vegetative or rock cover) increasing their vulnerability to significant erosion. The PLRM recommends that users evaluate these slopes externally using accepted soil loss models or other defensible prediction methods (PLRM, 2010b).

## **2.5 History and Development of Soil Erosion Prediction Methods**

Soil erosion data have been collected, analyzed and applied for nearly 100 years by engineers and scientists for a variety of different applications. The concept of using erosion plots to compute runoff and erosion on a unit-area basis is generally credited to the experiments of M.F. Miller and the Missouri Agricultural Experiment Station in the 1920s. Miller constructed a unit plot measuring 72.6 ft by 6 or 12 feet wide, which served as the “standard” for subsequent erosion-plot research (Galetovic et al., 1998).

Hugh Bennett, regarded as the “father of soil conservation,” served as the first director of the USDA Soil Conservation Service (SCS) and directed national attention towards the detrimental effects of soil erosion on farmers and the U.S. agricultural system, resulting in legislative action and the establishment of federal erosion experiment stations that generated much of the early erosion data in the United States (Helms, 2008).

The devastating soil losses, agricultural damages, and economic impacts resulting from the Dust Bowl era emphasized the importance of soil erosion research, ultimately leading to advancements in mathematical erosion prediction models. In the mid-1930s, H.L. Cook identified three major

variables that impacted soil erosion: 1) vulnerability of soil to erosion, 2) protection of soil by vegetative or rock cover, and 3) power and erosivity of rainfall and runoff. These initial efforts led to the first published mathematical equation by A.W. Zingg, who arithmetically described the effects of slope steepness and slope length on slope soil erosion. This prediction equation was further broadened in the early 1940s by D.D. Smith, to include factors representing cropping systems and management practices, eventually leading to a graphical method for determining recommended soil conservation practices across the Midwestern United States. In the late-1940s, after the end of World War II, Smith and D.M. Whitt continued to develop the erosion model by considering different factors representing soils, crops, slope lengths, and slope steepness, ultimately leading to the formation of an annual soil loss prediction equation. Despite the consideration of many factors, Smith and Whitt recognized the importance of including a rainfall factor to create a transferable prediction model applicable in other states. In 1946, the USDA-SCS re-evaluated the factors considered in the Smith and Whitt equation and added a rainfall factor, resulting in the Musgrave equation. The success of these initial state and regional erosion prediction equations resulted in the development of the National Runoff and Soil Loss Data Center at Purdue University by the Agricultural Research Service (ARS) for the purpose of compiling runoff and erosion data from across the United States (Renard et al., 1997). During this time, the use of rainfall simulations to collect large volumes of data evolved due to the inefficiencies and costliness associated with collecting sufficient amounts of soil-loss data from unpredictable natural events. Over time, the data assembled at the Data Center consisted of over 10,000 plot-years of soil loss and runoff data from natural and simulated rainfall events (Galetovic et al., 1998).

Using the large collection of data from the Data Center, W.H. Wischmeier and Smith developed the Universal Soil Loss Equation (USLE) in the early 1960s, primarily for croplands, to predict sheet and rill erosion based on the product of six different factors representing: 1) rainfall and runoff erosiveness; 2) soil erodibility; 3) slope length; 4) slope steepness; 5) cover-management practices; and 6) soil conservation practices. Although the USLE equation remained similar to earlier equations proposed by other researchers, the concepts, relationships and procedures used to evaluate erosion factors were more accurate and complete. The USLE was expanded in 1978 with an updated

version incorporating techniques for estimating site values from additional land uses, climatic conditions, and management practices, including rangelands, forests, mined lands, and construction sites. The USLE rapidly developed into the most significant and widely used soil erosion prediction model in the world (Renard et al., 1997).

The intent of the Revised Universal Soil Loss Equation, version 1 (RUSLE1), developed in the early 1990s, was to further supplement the six USLE factors used to calculate average annual soil loss by incorporating new research advancements in hydrology and erosion theory, expanding the soil erodibility and rainfall erosivity databases to the entire United States, and providing a computerized program to assist in calculations (Spaeth, Pierson, Wertz, & Blackburn, 2003).

The Revised Universal Soil Loss Equation, version 2 (RUSLE2), developed in 2001, represents the most current version in the development of the USLE. The RUSLE2 uses a more sophisticated mathematical approach to integrate the time varying equations that produce the erosivity, topographic, erodibility, cover-management and supporting practices factors, greatly improving over the mathematical approximations used in the USLE and RUSLE1. The RUSLE2 uses a hybrid approach of combining empirical equations with those derived from theory for erosion processes to estimate rates of rill and interrill erosion (USDA, 2001). During the evolution of the USLE to the RUSLE2, other significant erosion prediction models were developed.

In 1975, J.R. Williams transformed the USLE equation, developing the Modified Universal Soil Loss Equation (MUSLE) to predict sediment yield, by replacing the rainfall erosivity factor in USLE with a runoff energy factor based on the hypothesis that runoff is more influential in transporting sediment than rainfall (Smith, Williams, Menzel, & Coleman, 1984).

The Chemicals, Runoff, and Erosion from Agricultural Management Systems (CREAMS), Erosion Productivity Impact Calculator (EPIC), Agricultural Policy Environmental EXtender (APEX) and the Soil and Water Assessment Tool (SWAT) are examples of other models that were developed to evaluate water quality and other agricultural environmental impacts at a variety of different spatial scales. All of these models internally use the USLE and MUSLE methodologies to estimate erosion from rainfall

and runoff, but primarily focus on the environmental and economic impacts of agricultural management strategies (Gassman et al., 2005).

The CREAMS model was developed in 1980 by the USDA to evaluate non-point source pollution from field-sized areas. The model uses a physically-based platform to estimate runoff, erosion, plant nutrients and pesticide losses from agricultural lands across the United States (Knisel, 1980).

EPIC was developed in the early 1980s by the USDA to evaluate soil erosion impacts for 135 U.S. land resource regions. Consisting of nine components characterized by weather, soil, landscape, crop rotation and management system parameters, the field-scale model operates on a continuous basis using a daily time step performing long-term simulations. Similar to the CREAMS model, runoff volume is calculated using the SCS curve number method. The intent of the EPIC model was to predict crop yields by evaluating the impact of soil erosion and other factors on soil productivity (Williams, 1990).

The APEX model was developed in the 1990s to further the capabilities of EPIC by including whole farms and small watersheds. Although the model structure is similar to the EPIC model, farm management functions, specifically manure management, and the routing of water, sediment, nutrient and pesticides across complex landscapes represent the additional components of the APEX model (Williams & Izaurralde, 2006).

The SWAT model is a continuously simulated, physically-based model that evaluates the impacts of land management practices on sediment, water, and agricultural chemical routing, similar to the EPIC and APEX models, but is capable of modeling large, complex watersheds (Mukundan, Radcliffe, & Risse, 2010).

The Aerial Nonpoint Source Watershed Environment Response Simulation (ANSWERS), established in 1980, is a distributed parameter watershed model intended to estimate pollutant loads from agricultural watersheds (Beasley, Huggins, & Monke, 1980). The primary advantage of a distributed parameter model is the ability to simulate spatially and temporally variable watershed processes (Dillaha, Beasley, & Huggins, 1982).

The WEPP was developed in the 1980s by the USDA-ARS to replace empirically-driven erosion prediction models with a continuously simulated, physically-based model replicating soil erosion, including

infiltration, surface runoff, raindrop impact and flow detachment, sediment transport, deposition, plant growth, and residue composition (Tiwari, Risse, & Nearing, 2000). Rainfall, runoff, soil loss and soils data, collected from rainfall simulation tests performed on over 50 experimental sites across the United States, were used for model parameterization and testing and to develop predictive equations. In 1995, a graphical user interface was developed for the WEPP to assist users in performing simulations. A web-based WEPP GIS system (Geo WEPP) was created in 2001 that allows users to locate, automatically delineate a watershed based on digital elevation models (DEMs) and simulate any location in the U.S. Additional user interfaces have been developed for the WEPP model, including a suite of web-based user interfaces created by the USDA Forest Service Rocky Mountain Research Station (RMRS) in the early 2000s. This software package (FS WEPP) was developed to aid in the design of forest roads by predicting soil loss estimates from roads and timber harvesting areas, assess the impacts of fire on soil erosion and assist with fire fuel management systems (Flanagan et al., 2007). The TBSM, developed in 2010, is the most recent WEPP interface and focuses specifically on the Lake Tahoe Basin. This disturbed WEPP offshoot model predicts erosion from rangeland, forestland, and forest skid trails using climate, soil and management parameters customized for the Lake Tahoe Basin (Elliot & Hall, 2010).

In order to improve the predictive accuracy of the PLRM (see Section 2.4.1) for cut and fill slopes along roadways in the Lake Tahoe Basin, the RCAT was developed in 2010 to predict sediment yields, specifically FSP, from these highly-erodible slopes. The project objectives of the RCAT were to establish a simple, repeatable field assessment methodology and spreadsheet tool to assist erosion control and water quality planners and specialists working in the Tahoe Basin, designers and regulators to characterize, evaluate and estimate average annual total and fine sediment loadings generated from cut and fill slopes along roadways in the Tahoe Basin (Drake et al., 2010).

The selection of the most appropriate erosion model depends on the nature of the application. Empirically-based models, although not fully supported by fundamental hydrology and erosion theory, provide a simple structure easily applied to a variety of environmental conditions. Conversely, physically-based models tend to provide broader applicability and increased capabilities with the added expense of increased model complexity (Amore, Modica, Nearing, & Santoro, 2004). Overall, erosion models

represent predictive tools used to assess soil losses for conservation planning and as research tools to better understand the erosion process (USBR, 2006). Despite the high variability of erosion measurements from nearly identical plots, resulting in a predictive accuracy of +/- 50% for all erosion models (Elliot, Traeumer, Hall, & Brooks, 2013), these erosion models are commonly used for setting regulatory guidelines and standards (Grismer, 2010; LWQCB and NDEP, 2011).

## **2.6 Soil Erosion Prediction Models**

Based on a brief overview of the various soil loss prediction methods summarized in Section 2.4.1, the following sub-sections describe, in detail, the models previously used or considered to be most applicable for estimating soil erosion from the highly-disturbed highway cut and fill slopes present within the Lake Tahoe Basin.

### **2.6.1 Revised Universal Soil Loss Equation (RUSLE)**

This section describes the structure and the individual model parameters associated with the RUSLE, as well as the transformation of the original USLE into the current version.

The USLE was first introduced by the USDA in the USDA Agricultural Handbook 282 (Wischmeier & Smith, 1965) and later modified with the publication of the USDA Agricultural Handbook 578 (Wischmeier & Smith, 1978). Developed at the National Runoff and Soil Loss Data Center using a large collection of data from over 10,000 plot-years of soil loss and runoff data from 49 research different locations and supplemental data gathered across 16 states using 23 rainfall simulators, the USLE offered major improvements from preceding soil erosion equations. The original purpose of the USLE was to provide land conservation planners a tool to predict the average annual soil losses due to erosion for specific field areas depending on soil type, rainfall patterns, topography, cropping patterns and management practices. Although primarily intended to estimate rill and interrill soil erosion from agricultural areas with specific cropping and management systems, the USLE is also applicable to predicting soil losses from construction sites and other nonagricultural conditions (Wischmeier & Smith, 1978). The USLE is an index-based, empirically derived soil erosion model that predicts average annual soil losses resulting from sheet and rill erosion, using the following equation based on the product of six significant erosion factors (Wischmeier & Smith, 1965):

$$A = RKLSCP$$

Equation 2.2

where  $A$  = computed soil loss per unit area ( $\text{tons ac}^{-1} \text{ yr}^{-1}$ ),

$R$  = rainfall-runoff erosivity factor, see Section 2.6.1.1

$K$  = soil erodibility factor, see Section 2.6.1.2

$L$  = slope-length factor, see Section 2.6.1.3

$S$  = slope-steepness factor, see Section 2.6.1.3

$C$  = cover and management factor, see Section 2.6.1.4

$P$  = support practice factor, see Section 2.6.1.4

The USLE is based on the unit plot concept for establishing factor values. The unit or “standard” plot, used to experimentally determine factor values, measured 72.6 feet in length, consisted of a uniform length slope of 9 percent, and maintained a continuous fallow, tilled plot condition. The unit plot served as the base condition used to compare data from plots with different topographic, management and conservation practices (Renard, Yoder, Lightle, & Dabney, 2010).

The RUSLE1, released in 1997 with the publication of *USDA Agricultural Handbook 703*, retained the basic structure of the USLE. However, significant revisions were made to the algorithms used to calculate various factors based on further research developments since the introduction of the USLE. Additionally, RUSLE1 combined index- and process-based equations to create a hybrid model, differing from the solely empirically-based USLE. Similar to the USLE, RUSLE1 calculated erosion (soil detachment), not sediment yield or the transport of detached soil from the origin to another point in the watershed (Renard et al., 1997). RUSLE2, released in mid-2003, expanded the hybrid approach used in RUSLE1 by combining empirically-based and process-based erosion prediction technologies. Relationships based on modern theories of erosion processes (i.e., soil detachment, transport, deposition from rainfall impact and surface runoff) were incorporated in RUSLE2 when equations could not be developed from empirically-based data. However, the structure of the equation remains similar to USLE and RUSLE1. Using the validation erosion prediction technology developed for the USLE and RUSLE1, the RUSLE2 was derived and validated using more than 10,000 plot-years of natural runoff plots and an estimated equivalent of 2,000 plot-years of simulated rainfall data (USDA, 2001).

From hereinafter, RUSLE1 and RUSLE2 will be referred to as RUSLE. The following subsections describe the model parameters in RUSLE.

### 2.6.1.1 Rainfall-Runoff Erosivity Factor

The rainfall-runoff erosivity factor ( $R$ ) used in the RUSLE, derived using modern climate data, relates the impact of rainfall energy on erosion (Foster, Toy, & Renard, 2003). The analyses of large amounts of rainfall and soil erosion data revealed that soil loss is directly proportional to the product of total kinetic energy ( $E$ ) of a storm event and the storm's maximum 30-minute intensity ( $I_{30}$ ), given that all other factors, excluding rainfall characteristics, are held constant (Wischmeier & Smith, 1978). The rainfall kinetic energy per unit depth of rainfall,  $e_k$  (ft tons  $\text{ac}^{-1} \text{in}^{-1}$ ), is computed in the RUSLE by the following equation (Renard et al., 1997):

$$e_k = 1099(1 - 0.72e^{(-1.27I)}) \quad \text{Equation 2.3}$$

where  $i$  = rainfall intensity (in/hr)

The total rainfall energy of a single storm is calculated by the following equation (Galetovic et al., 1998):

$$E = \sum_{k=1}^p e_k d_k \quad \text{Equation 2.4}$$

where  $E$  = total rainfall energy of storm (ft tons  $\text{ac}^{-1}$ )

$d_k$  = depth of rainfall for  $k$ -th interval of the storm (in)

$p$  = total number of intervals in the storm

The total rainfall-runoff erosivity factor (hundreds of ft tons in  $\text{ac}^{-1} \text{hr}^{-1}$ ) over a specified time period, annually or for a single storm event, is calculated in the RUSLE by the following equation (Galetovic et al., 1998):

$$R = \frac{\sum_{i=1}^j (EI_{30})^i}{N} (10^{-2}) \quad \text{Equation 2.5}$$

where  $I_{30}$  = maximum 30-minute intensity (in/hr) for storm  $i$

$j$  = number of storms in an  $N$  time period

Annual rainfall-runoff erosivity factors for specific locations across the United States, assigned by state and county, are accessible from the NRCS RUSLE2 National Database (NRCS, 2008). In order to account for climate variability in counties with mountainous terrain, the NRCS RUSLE2 National Database

uses data obtained from the Parameter-Elevation Regressions on Independent Slopes Model (PRISM) database to organize erosivity values by precipitation depth zones that vary with elevation (NRCS, 2003).

The rainfall erosivity factor does not account for erosive forces produced by events other than rainfall, such as thaw, snowmelt and irrigation runoff. RUSLE established seasonal *EI* distributions for 84 climate zones in the western United States. In locations where winter precipitation is primarily snowfall, the winter months represent only a small percentage of the annual rainfall-runoff erosivity value. For the climatic zone encompassing the northern Sierra Nevada mountain range, the predominant snowfall months from November to May only account for approximately 13 percent of the annual erosivity value.

Although soil erosion from snowmelt events is considered much less significant than erosion from rainfall events (Ryan & Elliot, 2005), RUSLE provides procedures to account for snowmelt erosivity by using empirical relationships to increase the standard annual erosivity values. However, RUSLE recognizes the limitations with this approach and states that further research is required to identify the complexities associated with the redistribution of snow by drifting, sublimation, and reduced sediment concentrations in snowmelt on determining the erosive forces from snowmelt or rain on frozen soil (Renard et al., 1997).

#### **2.6.1.2 Soil Erodibility Factor**

The RUSLE soil erodibility factor (*K*) quantifies the vulnerability of soil to erosion from rainfall and runoff forces, independent of the effects of rainfall variations, slope, cover, and management practices (Renard et al., 1997). This factor is defined as the rate of erosion per unit of rainfall-runoff erosivity from the uniform plot, described in Section 2.6.1, performed on a particular soil. The conditions of this experimental unit plot produce RUSLE factor values of 1.0 for slope-length factor (*L*), slope-steepness factor (*S*), cover and management factor (*C*) and support practice factor (*P*), resulting in  $K = A/EI$  (Wischmeier & Smith, 1965). Therefore, soil erodibility is fundamentally viewed as the change in the soil per unit of applied external force or energy. The *K* factor represents the average annual value of the total soil and soil profile reaction to a large number of erosion and hydrologic processes (Renard et al., 1997).

For undisturbed soils, the soil erodibility factors are obtained from the published NRCS soil surveys for most major soil mapping units. These values range from approximately 0.02 to 0.64,

depending on the soil type (Galetovic et al., 1998). Soils containing high silt content typically result in high  $K$  values due to availability of easily mobilized fine sediment and vulnerability to surface crusting, resulting in increased runoff rates. Conversely, soils high in clay or sand content result in lower  $K$  values due to soil detachment resistance and high infiltration/low runoff rates, respectively (NRCS, 2003).

These soil erodibility values published by the NRCS reflect native organic-matter levels, not the organic matter levels resulting from management activities. Therefore, site specific  $K$  values for disturbed soils present on mined lands, construction sites or reclaimed lands should be estimated based on soil sampling and the use of the soil-erodibility nomograph, approximated by the following equation (Wischmeier & Smith, 1978):

$$K = (2.1 \times 10^{-4}(12 - OM) M^{1.14} + 3.25(s - 2) + 2.5(p - 3))/100 \quad \text{Equation 2.6}$$

where  $OM$  = percent organic matter content

$s$  = soil structure class (1 – 4) as defined in the NRCS *Soil Survey Manual* (USDA, 1993)

$p$  = soil permeability class (1 – 6) as defined in the NRCS *Soil Survey Manual* (USDA, 1993)

$M$  = particle-size parameter defined by the percent modified silt (0.1 - 0.002 mm) times the quantity of percent sand plus percent silt (> 0.002 mm)

### 2.6.1.3 Topographic Factor

The RUSLE combines the slope-length ( $L$ ) and slope-steepness ( $S$ ) factors into a combined topographic factor ( $LS$ ), which represents the expected ratio of soil loss from a field slope with a given slope steepness and length, relative to soil loss from a uniform plot, described in Section 2.6.1, under otherwise identical conditions. The slope length factor ( $L$ ) is expressed as follows (Wischmeier & Smith, 1978):

$$L = (\lambda/72.6)^m \quad \text{Equation 2.7}$$

where  $\lambda$  = slope length (ft), defined as the horizontal distance from the origin of overland flow to either the point of deposition or where the flow enters a defined channel

$m$  = variable slope length exponent

The slope length exponent ( $m$ ) relating the ratio of rill (caused by flow) to interrill (caused primarily by raindrop impact) erosion ( $\beta$ ) is calculated using the following equation (Renard et al., 1997):

$$m = \beta / (1 + \beta) \quad \text{Equation 2.8}$$

The ratio of rill to interrill erosion ( $\beta$ ) is determined by the following expression (Renard et al., 1997):

$$\beta = \frac{11.1607 \sin \theta}{3.0(\sin \theta)^{0.8} + 0.56} \quad \text{Equation 2.9}$$

where  $\theta$  = slope angle

If the soil is highly susceptible to rill erosion, specifically on steep, freshly prepared construction slopes, RUSLE recommends doubling the  $\beta$  value prior to calculating  $m$ . If the conditions of a slope favor interrill erosion, then RUSLE suggests multiplying the  $\beta$  value by 0.5 prior to calculating  $m$ .

For slopes exceeding 15 feet in length, RUSLE calculates the slope-steepness factor ( $S$ ) based on the following expressions dependent on slope gradient (Renard et al., 1997):

$$S = 10.8 \sin \theta + 0.03 \text{ for slopes } < 9\% \quad \text{Equation 2.10}$$

$$S = 16.8 \sin \theta - 0.5003 \text{ for slopes } \geq 9\% \quad \text{Equation 2.11}$$

Based on the assumption that rill erosion is insignificant on shorter slopes, the  $S$  factor is computed as follows for slopes shorter than 15 feet (Renard et al., 1997):

$$S = 3.0 (\sin \theta)^{0.8} + 0.56 \quad \text{Equation 2.12}$$

#### 2.6.1.4 Cover and Management Factor

RUSLE evaluates cover and crop management in a combined factor ( $C$ ), representing the ratio of soil loss from a slope under specific cover conditions to soil loss from the unit plot, as described in Section 2.6.1. Individual  $C$  values range from 0 (least erodible condition) to 1 (most erodible condition).  $C$  values represent weighted average soil loss ratios (SLRs), which vary annually depending on geographic location, cover conditions, management practices and the development of the vegetal cover during periods of erosive rainfall (Wischmeier & Smith, 1978). RUSLE computes SLRs or  $C$  factors based on the function of five subfactors (Renard et al., 1997):

$$C = PLU \cdot CC \cdot SC \cdot SR \cdot SM \quad \text{Equation 2.13}$$

where  $C$  = overall cover-management factor

$PLU$  = prior land use subfactor

$CC$  = canopy cover subfactor

$SC$  = surface cover subfactor

$SR$  = surface roughness subfactor

$SM$  = soil moisture subfactor

The  $PLU$  subfactor is a product of soil biomass and soil consolidation effects. In addition to specific equations calculating the  $PLU$  subfactor, RUSLE documentation contains tables identifying typical values used depending on land use condition (Renard et al., 2010). For highly disturbed slopes where topsoil is removed, thus decreasing soil biomass, organic matter and subsequently reducing the ability of the soil to resist erosive forces, the  $PLU$  subfactor is set equal to 1 (Galetovic et al., 1998).

The canopy-cover subfactor ( $CC$ ), expressed as the effectiveness of vegetative canopy in reducing rainfall impact energy on the soil surface, ranges from 0 to 1 and is defined in RUSLE by the following equation (Renard et al., 1997):

$$CC = 1 - F_c \exp(-0.1H) \quad \text{Equation 2.14}$$

where  $F_c$  = fraction of land surface covered by canopy

$H$  = distance that raindrops fall after striking the canopy (ft)

RUSLE defines the surface-cover subfactor ( $SC$ ) as cover that is in direct contact with the soil surface, including rocks, low vegetative cover at soil surface, crop residue, cryptogams, and other non-erodible material. This surface cover reduces erosion by limiting transport capacity of runoff, causing deposition in ponded areas. The effect of surface cover on soil erosion is given by (Renard et al., 1997):

$$SC = \exp[-b S_p (0.24/R_u)^{0.08}] \quad \text{Equation 2.15}$$

where  $b$  = empirical coefficient

$S_p$  = percentage of land covered by surface cover

$R_u$  = surface roughness (in)

Values of  $b$  vary depending on specific surface cover and the primary mechanism of soil loss (i.e., rill versus interill). A  $b$  value of 0.050 is recommended for lands dominated by rill erosion, such as for irrigation or snowmelt, and highly disturbed soils. A  $b$  value of 0.025 and 0.039 is recommended for fields dominated by interill erosion and rangeland conditions with the impacts of subsurface biomass removed, respectively. Surface roughness ( $R_u$ ), defined as the standard deviation of surface elevations, affects soil

erosion by decreasing the transport capacity and runoff detachment by reducing the flow velocity (Renard et al., 1997).

The surface roughness subfactor ( $SR$ ) is a function of the surface's random roughness which can reduce soil erosion and is based on the following equation (Renard et al., 1997):

$$SR = \exp[-0.66 (R_u - 0.24)] \quad \text{Equation 2.16}$$

The soil-moisture subfactor ( $SM$ ) accounts for the influence of antecedent soil moisture on infiltration and runoff, and ultimately soil erosion. When the soil profile is at field capacity, the  $SM$  value is equal to 1.0. Conversely, when the soil profile is near the wilting point, then the  $SM$  value is equal to 0 (Renard et al., 1997). In most instances,  $SM$  is assumed to equal 1, which means that soil moisture extraction from the surface vegetation has no significant impact on soil erosion (Renard et al., 2010).

Overall  $C$  values for “cut” and “fill” conditions vary due to differences in the characteristics of surface material. For cut slopes, soil remains in a relatively consolidated state and more resistant to erosion. Conversely, fill slopes contain loosened soils and reduced soil-aggregation size, therefore leaving the soil more susceptible to erosion (Galetovic et al., 1998).

### **2.6.1.5 Support Practice Factor**

Conservation practices used to slow the runoff of water and reduce soil erosion are incorporated in RUSLE through the support practice factor ( $P$ ). The  $P$  factor is defined as the ratio of soil loss with a specific support practice to the corresponding soil loss with upslope and downslope tillage (Wischmeier & Smith, 1978). For cultivated land, support practices include contouring, strip cropping, terracing, and subsurface drainage. In rangeland areas, support practices consist of soil disturbing practices near the contour, resulting in storage of moisture and runoff reduction (Renard et al., 1997). Generally, as land slope increases, contouring loses effectiveness, resulting in  $P$  values approaching 1.0. The support practice factor focuses primarily on agricultural field applications; thus, for most non-agricultural fields, the default value for the support practice factor is 1.0 (Wischmeier & Smith, 1978).

### **2.6.2 Modified Universal Soil Loss Equation (MUSLE)**

The MUSLE is a modified version of the USLE, developed by Williams (1975), that replaced the USLE rainfall erosivity factor,  $R$ , with a runoff energy factor. Williams noted the following improvements

of the MUSLE over the USLE: (1) greater accuracy because runoff is a superior contributor to sediment yield than rainfall; (2) ability to apply equation to individual storm events; and (3) obsolescence of the USLE sediment delivery ratios since the runoff factor accounts for sediment detachment and transport (Smith et al., 1984). The MUSLE equation takes the following form to predict sediment yield for small watersheds:

$$S = 95(QP_p)^{0.56}KLSCP \quad \text{Equation 2.17}$$

where  $S$  = sediment yield for a single event (tons)

$Q$  = total event runoff volume (ft<sup>3</sup>)

$P_p$  = event peak discharge (ft<sup>3</sup>/s)

$K$ ,  $LS$ ,  $C$ , and  $P$  = parameters from USLE, see Section 2.6.1

The MUSLE was compared to the USLE by evaluating each storm event in the MUSLE to determine an average annual sediment loss and comparing results to the USLE's average annual soil loss prediction. Although Williams' analysis revealed that the product of runoff volume and peak discharge for a single event produced more accurate results for large events than the USLE  $R$  factor, the MUSLE accuracy is heavily dependent on the accuracy of the hydrologic analysis (USBR, 2006).

### 2.6.3 Water Erosion Prediction Project (WEPP)

The USDA-ARS initiated the WEPP in 1985 with the objective of developing a "new-generation water erosion prediction technology" to replace the empirically-based USLE (Nearing, Foster, Lane, & Finkner, 1989). The WEPP erosion model, released in 1995 after ten years of extensive model parameterization and testing, represents a process-based, distributed parameter, continuous simulation model used to predict erosion from hillslopes and small watersheds (Flanagan, Gilley, & Franti, 2007; USDA-ARS, 1995b). The process-based element, based on the fundamental properties and governing equations of hydrologic and erosion mechanics science, offers broad applicability to a variety of hill slope and watershed conditions (USDA-ARS, 1995a). The continuous simulation feature accounts for variations in climatic, vegetative and soil conditions and can be used to estimate runoff and erosion on a daily time-step over a multi-year simulation period (Laflen, Lane, & Foster, 1991). In addition to the process-based structure and continuous simulation capabilities, the following features distinguish the WEPP model from

the USLE/RUSLE: (1) estimates the spatial and temporal distributions of soil loss; (2) simulates runoff and erosion from snowmelt; (3) models the entire erosion process (interrill and rill erosion, sediment transport and deposition) and (4) performs complex runoff and sediment routing to estimate watershed sediment yield (Flanagan et al., 2007; USDA-ARS, 1995a).

### **2.6.3.2 Model Structure of WEPP**

The WEPP erosion model is applicable to both hill slope and watershed applications. The hillslope application represents the most basic form of the WEPP erosion model and provides estimates of sediment yield at the base of a hill slope. This version is comparable to the USLE/RUSLE predictions, except that the estimates additionally consider sediment deposition along the hill slope (Lafren et al., 1991). The watershed application links hill slopes with channel sections and impoundments to route water and sediment to the watershed outlet (USDA-ARS, 1995a). However, this review focuses on the hill slope application of WEPP, as this version is most applicable to estimating sediment yield from cut and fill slopes in the Tahoe Basin.

The hill slope version of WEPP requires the following four input data files for model simulation: climate (see Section 2.6.3.3), plant/management (see Section 2.6.3.4), soil characteristics (see Section 2.6.3.5), and slope (USDA-ARS, 1995a). The slope input file defines the hill slope topographic parameters and requires user supplied information on slope orientation, length and steepness (USDA-ARS, 1995b). Hill slope profiles may include single or multiple overland flow elements (OFEs) to simulate non-uniform hill slopes. OFEs represent a unique spatial region comprised of a single soil, slope and vegetation (Flanagan, Frankenberger, & Ascough II, 2012).

The hill slope application of WEPP is comprised of nine conceptual hillslope components including climate generation, winter processes, irrigation, hydrology, soils, plant growth, residue decomposition, overland flow hydraulics, and erosion (USDA-ARS, 1995b). As shown in Figure 2.2, WEPP incorporates the distributed input parameters to continuously simulate the hydrologic and erosion processes and estimate the spatial and temporal distribution of erosion and sediment yield for a hill slope or small watershed (USDA-ARS, 1995a). The WEPP erosion model output includes erosion and runoff results, as well as information pertaining to the sediment characteristics of the runoff, including

composition, particle size distribution and sediment enrichment ratio (Ascough II, Baffaut, Nearing, & Liu, 1997).

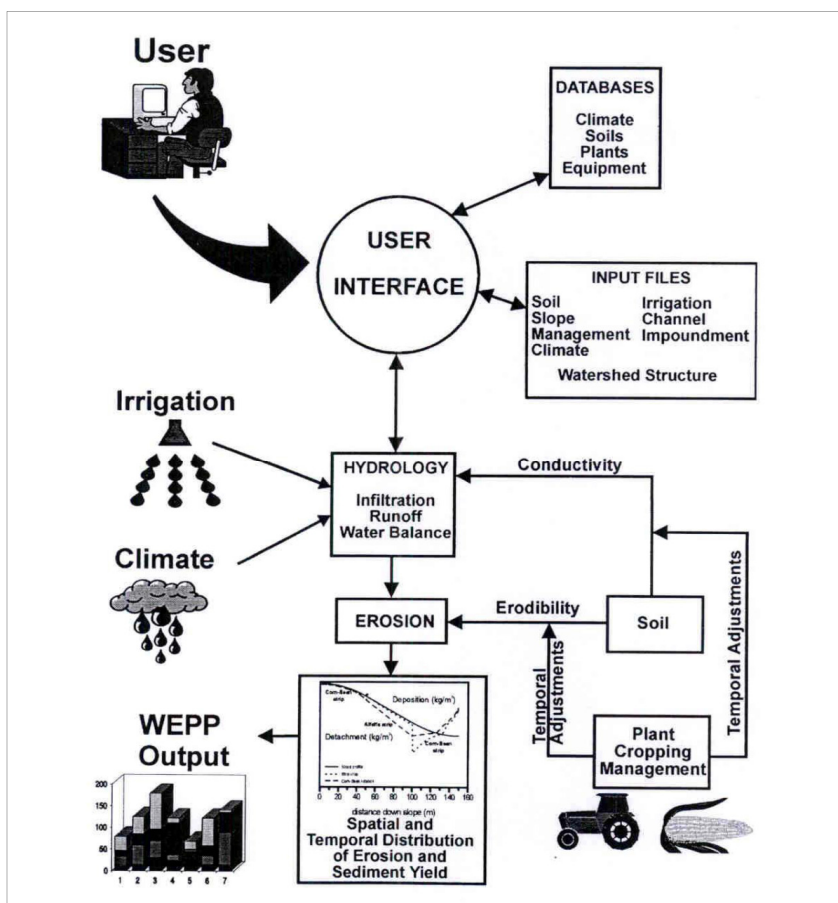


Figure 2.2. The WEPP erosion model structure diagram (Ascough II et al., 1997)

The following sub-sections briefly describe the significant hydrologic, plant growth and residue decomposition, soil, and erosion processes simulated in WEPP, as well as the governing equations used to model these processes.

### 2.6.3.3 Hydrologic Processes in WEPP

Hydrologic processes initiate the erosion process through raindrop energy splash detachment and by producing erosive runoff. The significant hydrologic processes included in WEPP consist of climate, infiltration, water balance and winter processes (USDA-ARS, 1995b).

The WEPP erosion model employs CLimate GENerator (CLIGEN), an external stochastic climate generation computer program, to construct climate data for use in model simulations. CLIGEN uses weather station statistics from over 2,600 locations across the United States to generate mean daily

precipitation, temperature, solar radiation, and wind values (USDA-ARS, 1995a). An internal disaggregation model converts daily climate data from CLIGEN into a simple, single peak storm pattern used by the infiltration and runoff components of the model (Flanagan et al., 2012). WEPP includes a large climate database, searchable by state and weather station, for use in model simulations (USDA-ARS, 1995b). For use in model validation efforts or design-storm erosion predictions, WEPP offers single-storm simulations that require climate related inputs of storm depth, storm duration, maximum intensity and percent duration to peak intensity (USDA-ARS, 1995a).

The hydrology component of WEPP includes infiltration, runoff, soil evaporation, plant transpiration, storage depression, and plant and residue interception of rainfall (USDA-ARS, 1995b). The infiltration process in the WEPP hill slope model is based on the Green-Ampt Mein Larson equation, expressed as (Copeland, 2009):

$$f = K_e \left( 1 + \frac{(\phi_e - \theta_i)\psi}{F} \right) \quad \text{Equation 2.18}$$

where  $f$  = infiltration rate (mm/hr)

$K_e$  = effective hydraulic conductivity (mm/hr)

$\phi_e$  = effective soil porosity ( $\text{mm}^3 \text{mm}^{-3}$ )

$\theta_i$  = initial soil water content (mm/mm)

$\psi$  = average wetting front capillary potential (mm)

$F$  = cumulative infiltration depth (mm)

The effective rainfall intensity,  $I_e$  (mm/hr), used to determine interrill soil detachment, is calculated from the following equation (Nearing et al., 1989):

$$I_e = \left[ \left( \int I^2 dt \right) / t_c \right]^{1/2} \quad \text{Equation 2.19}$$

where  $I$  = rainfall intensity (mm/hr)

$t$  = time (hr)

$t_c$  = total time during which the rainfall rate exceeds the infiltration rate (hr)

In determining surface runoff, WEPP uses either the kinematic wave equation or an approximate method that uses regression equations to compute peak runoff rate and runoff duration (USDA-ARS, 1995a). The hydraulic component of WEPP uses the surface runoff information to compute the hydraulic

shear forces exerted on the soil surface, which is ultimately used to estimate rill erosion estimates (Laflen et al., 1991).

The surface hydrology component in WEPP uses the climate, infiltration and plant growth information to maintain a daily soil water balance. The water balance component of WEPP uses a modified version of the Simulator for Water Resources in Rural Basins (SWRRB) to provide greater accuracy in estimating percolation and soil evaporation parameters (USDA-ARS, 1995a).

The winter processes component of the WEPP model simulates soil frost and thaw development, snowfall, snow accumulation and snowmelt. WEPP uses basic heat flow theory and daily temperature, solar radiation and precipitation data to estimate frost and thaw depths, which the model uses to adjust infiltration and erodibility parameters (USDA-ARS, 1995b). WEPP uses daily temperature data, disaggregated to hourly values, to partition precipitation data between rainfall and snowfall, as well as to determine snow accumulation and snowmelt (USDA-ARS, 1995a).

#### **2.6.3.4 Plant Growth and Residue Decomposition Processes in WEPP**

Plant growth reduces erosion by providing protective canopy and residue cover (Laflen et al., 1991). The plant growth component of WEPP uses a plant growth routine, based on the EPIC model, to simulate the temporal variability of plant variables, including plant height, litter cover, canopy cover, surface cover, leaf area index and exposed bare soil (USDA-ARS, 1995a). The residue decomposition component of WEPP estimates the decomposition process of residue above and below the ground surface (Laflen et al., 1991). These simulated plant/management parameters influence protective canopy and ground cover, soil hydraulic conductivity and soil erodibility values, therefore directly impacting runoff and erosion computations (USDA-ARS, 1995b). The effect of canopy and ground cover on reducing interrill erosion is estimated in WEPP using canopy and ground cover effect factors. The canopy effect,  $C_e$  (dimensionless), is calculated as (Nearing et al., 1989):

$$C_e = 1 - F_c e^{-0.34 H_c} \quad \text{Equation 2.20}$$

where  $F_c$  = fraction of soil protected by the canopy cover

$H_c$  = effective canopy height (m)

The ground cover effect,  $G_e$  (dimensionless), is determined as follows (Nearing et al., 1989):

$$G_e = e^{-2.5 g_i} \quad \text{Equation 2.21}$$

where  $g_i$  = fraction of soil protected by the ground cover

The WEPP database includes parameterized plant and residue conditions for a large number of cropland and rangeland plant/management strategies throughout the United States (Flanagan et al., 2012).

### 2.6.3.5 Soil Processes in WEPP

The soil processes component in WEPP includes numerous parameters that influence hydrologic and soil detachment processes (Laflen et al., 1991). These soil parameters include random roughness, oriented roughness, bulk density, wetting-front section, hydraulic conductivity, interrill erodibility, rill erodibility, and critical shear stress (USDA-ARS, 1995a).

The main WEPP parameter controlling infiltration and runoff is the effective hydraulic conductivity,  $K_e$  (mm/hr), which is approximated for soils with clay content of < 40% using the following expression (USDA-ARS), 1995a, 1995b):

$$K_e = -0.265 + 0.0086 \text{ SAND}^{1.8} + 11.46 \text{ CEC}^{0.75} \quad \text{Equation 2.22}$$

where  $\text{SAND}$  = percent sand content in the soil

$\text{CEC}$  = cation exchange capacity of the soil (meq/100g)

Considering the various soil components, the WEPP model is most sensitive to input values for interrill erodibility, rill erodibility and critical hydraulic shear (USDA-ARS, 1995b). The subsequent equations for these parameters apply to soils with > 30% sand content, similar to the types of soils present in the Lake Tahoe Basin, although these parameters can be approximated for a variety of soil conditions (USDA-NRCS, 2007; USDA-ARS, 1995b). The interrill erodibility parameter represents the resistance of the soil to detachment from raindrop impact energy, while the rill erodibility parameter characterizes the soil's resistance to detachment from concentrated rill flow (USDA-ARS, 1995a). Elliot, Liebenow, Laflen, & Kohl (1989) presented an equation to estimate the interrill erodibility parameter,  $K_i$  ( $\text{kg s}^{-1} \text{m}^{-4}$ ), by direct solution as follows:

$$K_i = 2728000 + 192100 \text{ VFS} \quad \text{Equation 2.23}$$

where  $\text{VFS}$  = percent very fine sand content (0.10 - 0.05 mm)

The rill erodibility parameter,  $K_r$  ( $\text{s m}^{-1}$ ), measures the soil resistance to detachment by concentrated rill flow and is approximated by the following equation (USDA-ARS, 1995b):

$$K_r = 0.00197 + 0.00030 VFS + 0.03863e^{-1.84 ORGMAT} \quad \text{Equation 2.24}$$

where  $ORGMAT$  = percent organic matter content

Critical hydraulic shear stress,  $\tau_c$  (Pa), is a threshold parameter where exceedance results in a rapid increase in soil detachment (USDA-ARS, 1995a). This threshold parameter is estimated as (USDA-ARS, 1995b):

$$\tau_c = 2.67 + 0.065 CLAY - 0.058 VFS \quad \text{Equation 2.25}$$

where  $CLAY$  = percent clay content ( $< 0.002$  mm)

The WEPP erosion model provides an extensive soils database, searchable by state and soil name, for direct input into the soils file (USDA-ARS, 1995b). Additionally, the program allows flexibility for the user to generate soil input files based on site-specific data or data provided by the NRCS soil surveys. Specific soil properties available for input include soil texture (percent rock, sand, very fine sand, and clay), organic matter content, and cation exchange capacity (Flanagan et al., 2012).

#### 2.6.3.6 Erosion and Deposition Processes in WEPP

The erosion component of WEPP differentiates between interrill and rill erosion and computes the net detachment and deposition using the steady-state continuity equation, of the form (Tiwari et al., 2000):

$$dG/dx = D_f + D_i \quad \text{Equation 2.26}$$

where  $x$  = distance downslope (m)

$G$  = sediment load ( $\text{kg s}^{-1} \text{m}^{-1}$ )

$D_f$  = rill erosion rate ( $\text{kg s}^{-1} \text{m}^{-2}$ )

$D_i$  = interrill erosion rate ( $\text{kg s}^{-1} \text{m}^{-2}$ )

Sediment detachment from interrill areas is supplied to rill channels, based on a function of slope and surface roughness. Interrill erosion is a function of effective rainfall intensity ( $I_e$ ) and the interrill erodibility parameter, which is determined from a combination of parameters, including the effects of canopy cover and ground cover on reducing interrill erosion. The interrill erosion rate ( $D_i$ ) is determined independently of slope length and computed by the following equation (Nearing et al., 1989):

$$D_i = K_i I_e^2 C_e G_e (R_s / w) \quad \text{Equation 2.27}$$

where  $K_i$  = interrill erodibility ( $\text{kg s}^{-1} \text{m}^{-4}$ ), see Equation 2.23

$I_e$  = effective rainfall intensity (mm/hr), see Equation 2.19

$C_e$  = canopy cover effect, see Equation 2.20

$G_e$  = ground cover effect, see Equation 2.21

$R_s$  = spacing of rills (m)

$w$  = computed rill width (m)

The rill erosion rate ( $D_f$ ) is positive for detachment and negative for deposition. In the case that (1) the sediment transport capacity is greater than the sediment load and (2) the hydraulic shear stress exerted by the flow exceeds the critical shear stress of the soil, the rill detachment ( $D_f$ ) can be estimated as follows (Tiwari et al., 2000):

$$D_f = D_c (1 - G/T_c) \quad \text{Equation 2.28}$$

where  $D_c$  = rill detachment capacity ( $\text{kg s}^{-1} \text{m}^{-4}$ ), see Equation 2.24

$T_c$  = sediment transport capacity ( $\text{kg s}^{-1} \text{m}^{-1}$ ), see Equation 2.31

If the critical shear stress of the soil is exceeded, then WEPP computes the rill detachment capacity ( $D_c$ ), expressed as (Nearing et al., 1989):

$$D_c = K_r (\tau_f - \tau_c) \quad \text{Equation 2.29}$$

where  $K_r$  = rill erodibility ( $\text{s m}^{-1}$ ), see Equation 2.24

$\tau_f$  = flow shear stress acting on soil particles (Pa)

$\tau_c$  = critical hydraulic shear stress of the soil (Pa), see Equation 2.25

In the case where the hydraulic shear stress exerted by the flow is less than the critical shear stresses of the soil, then the rill detachment equals zero. In the case where the sediment load exceeds the sediment transport capacity, then deposition occurs and can be calculated as (Nearing et al., 1989):

$$D_f = (V_f/q) (T_c - G) \quad \text{Equation 2.30}$$

where  $V_f$  = effective fall velocity of the sediment (m/s)

$q$  = flow discharge per unit width ( $\text{m}^2/\text{s}$ )

WEPP uses a modified version of the Yalin equation to compute the sediment transport capacity ( $T_c$ )

$$T_c = k_t \tau_f^{3/2} \quad \text{Equation 2.31}$$

where  $k_t$  = transport coefficient

$\tau_f$  = hydraulic shear acting on the soil flow (Pa) based on a function downslope distance (x)

#### **2.6.4 Tahoe Basin Sediment Model (TBSM)**

The TBSM, developed in 2010, is the most recent of the USDA Forest Service online interfaces to the WEPP erosion prediction technology. Customized for the Lake Tahoe Basin, the TBSM predicts average annual runoff, erosion (total and fine sediment) and phosphorus delivery from upland forest hillslopes using climate, soil and management parameters specific to the Tahoe Basin (Elliot & Hall, 2010). Specific forested land use applications include low and high severity prescribed fire and wildfire areas, forest harvest operations, ski runs and snow-making corridors, cut and fill slopes, various forest access roads, and revegetated, mulched, and tilled disturbed surfaces (Elliot et al., 2013). Based on the same fundamental processes and equations of hydrologic and erosion mechanics science used in WEPP (described in Section 2.6.3), TBSM simplifies the application of WEPP to the specific conditions of the Tahoe Basin. The Tahoe experimental database is based primarily on research data formulated from rainfall simulation-based runoff and erosion studies on forest roads, undisturbed and disturbed forest hill slopes (Foltz, Elliot, & Wagenbrenner, 2011; Grismer & Hogan, 2004, 2005a, 2005b). TBSM requires the modeler to input the site characteristics for model simulation including climate, topography, vegetation/treatment managements, surface cover, soil texture, and percent rock in soil (Elliot et al., 2013).

TBSM employs the use of Rock:Clime (version 2010.05.08) to generate climate parameters files which consider daily precipitation, temperature, solar radiation, time-to-peak distributions and wind data. Rock:Clime features a format similar to the data generated by CLIGEN, discussed in Section 2.6.3.3, and is fully compatible with the WEPP erosion model. TBSM provides climate station parameter values for the seven SNOWpack TELEmetry (SNOTEL) sites in the Tahoe Basin. Rock:Clime allows flexibility for modelers to modify the available SNOTEL site climates, using data generated by PRISM, to create custom climates for specific locations in the Tahoe Basin (Elliot et al., 2013).

The required topographic inputs for the TBSM include horizontal slope length (1.5 – 1,200 ft) and percent gradient (0 – 100 percent). To represent non-uniform hillslopes, TBSM can accommodate two OFEs (described in Section 2.6.3.2) : an “upper element” and “lower element” (Elliot et al., 2013).

TBSM provides fourteen categories of vegetation/treatments, similar to WEPP plant/management files (described in Section 2.6.3.4), parameterized for the Tahoe Basin using available research data. The fourteen available vegetation and treatment managements include mature forest, young forest, shrubs, good grass, poor grass, bare, low severity fire, high severity fire, burn pile, mulch only, mulch and till, low traffic road, high traffic road and skid trail (Elliot et al., 2013). These vegetation treatments influence plant height, spacing, leaf area index, root depth, biomass, interrill and rill erodibility, hydraulic conductivity and radiation energy to biomass conversion ratio (Elliot & Hall, 2010). TBSM provides default percent cover values for each treatment, however the user is encouraged to modify these values based on specific site conditions. Percent cover (0 – 100 percent) includes the percent of vegetation, rock and residue covering the soil surface. Surface cover, considered one of the more sensitive parameters in TBSM/WEPP, protects the hill slope from erosive rainfall and typically provides increased infiltration capacity, thus further reducing erosion by reducing runoff (Elliot et al., 2013).

TBSM includes four soil textures parameterized from Tahoe Basin research data and soil analyses including granitic, volcanic, alluvial, and rock/pavement. The soil properties include critical shear stress, interrill erodibility, rill erodibility and hydraulic conductivity (described in Section 2.6.3.5). These soil properties change for a given soil texture based on the paired treatment type, thus resulting in a total of 56 (4 soil textures x 14 treatments) possible unique soil texture/treatment combinations. Soil texture is also considered as one of the more sensitive parameters in TBSM/WEPP in relation to runoff and erosion estimates. To account for the impact of subsurface rocks in reducing hydraulic conductivity, TBSM requires the user to input the percent of rock fragments (0 – 50) in the upper soil. An increase in percent rock proportionally decreases hydraulic conductivity, resulting in increased runoff and rill erosion (Elliot et al., 2013).

#### **2.6.5 Road Cut and Fill Slope Sediment Loading Assessment Tool (RCAT)**

In an effort to improve the understanding of sediment generation from roadway cut and fill slopes within the Lake Tahoe Basin, the RCAT was developed in 2010 by Integrated Environmental Restoration Services (IERS). RCAT provides a simple, repeatable field assessment methodology and spreadsheet tool designed to estimate runoff volume, total and FSP sediment yields from uniform, small scale (< 1 acre)

roadway cut and fill slopes (Drake & McCullough, 2010). The ultimate purpose of the RCAT was to supplement the PLRM's current land use database, as mentioned in Section 2.4.1, by providing a new land use category representing the unique conditions of the steep, highly disturbed slopes present within the Tahoe Basin (Drake & McCullough, 2010). Although RCAT has yet to be fully integrated with the PLRM, due to project scope limitations and complexities associated with creating a new PLRM module, RCAT provides a procedure for incorporating output into PLRM by calibrating PLRM sediment loading outputs to RCAT loading estimates (Drake et al., 2010). This quasi-integration allows for the modeling of pollutant reductions in the PLRM associated with cut and fill slope connectivity to downstream stormwater treatment facilities (e.g., infiltration basins, cartridge filters, etc.).

In formulating the runoff and erosion relationships used in the RCAT, the developers conducted rainfall simulations at cut and fill slopes to supplement existing runoff and erosion data compiled from over 900 rainfall simulations conducted by Grismer, Ellis, & Fristensky (2008) and Grismer & Hogan (2004, 2005a, 2005b) in the Tahoe Basin between 2002 and 2009. Using these data, non-linear regression exponential equations were developed to predict sediment yield (mass of sediment per unit runoff) for each soil type (granitic and volcanic) and treatment type (bare, grass/mulch covers, incorporated soil amendments and native vegetation) as a function of slope gradient, as shown in Figure 2.3 (Drake et al., 2010).

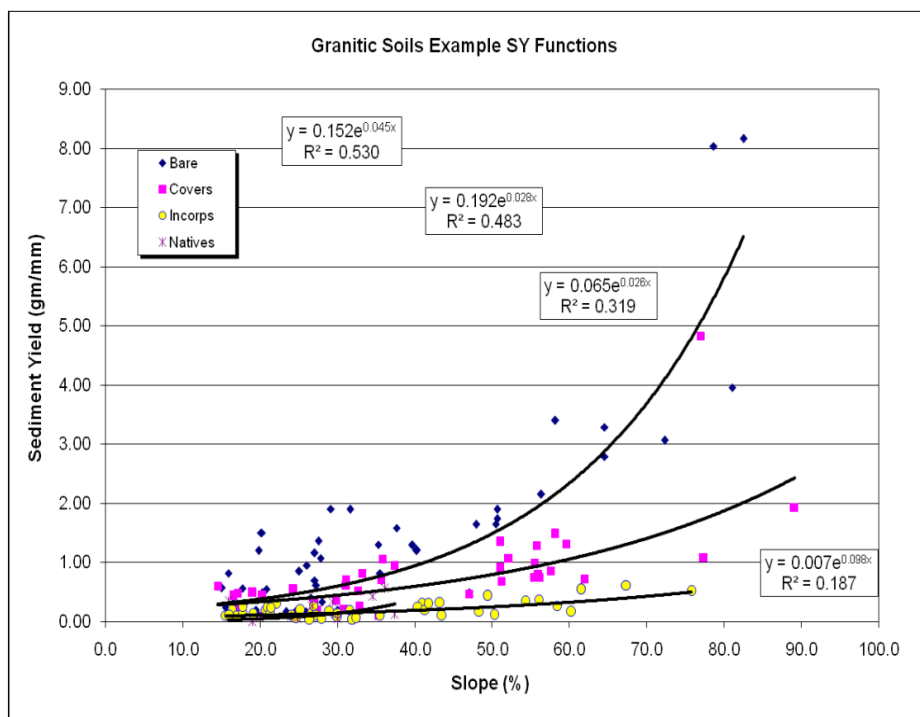


Figure 2.3. Runoff sediment yield dependence on granitic soil treatment and slope (Drake et al., 2010)

Direct field measurements are required for input into the RCAT spreadsheet tool which include slope gradient (1 to 90 percent), slope area, percent total cover, mulch/litter depth, soil moisture, and cone penetrometer depth to refusal (DTR). RCAT provides guidelines for all field measurements and recommends the use of 1 square meter quadrants, constructed of polyvinyl chloride (PVC) pipe, to create visual transects to guide field measurements and ensure variation in slope characteristics is adequately represented (Drake & McCullough, 2010). In addition to these direct field measurements, the user is required to input precipitation depth and soil type.

The RCAT incorporates field measurements of percent total cover and mulch/litter depth into a surface cover index (SC) to account for the effectiveness of vegetative canopy and surface cover in reducing the energy of rainfall striking the soil surface and the sediment transport capacity of runoff, using the following equation (Drake & McCullough, 2010):

$$SC = d_{ML} \frac{TC}{100} \quad \text{Equation 2.32}$$

where  $d_{ML}$  = mulch/litter depth (in)

$TC$  = total cover (%)

Total cover in RCAT refers to the debris cover first contacted by raindrops and includes plants (< than 3 feet tall), mulch/litter, rocks, gravel, logs, pine cones, and other types of woody debris. Percent total cover is visually estimated to the nearest 25 percent, using quadrants, and inputted into the RCAT spreadsheet. To determine mulch/litter depth, the user is required to sub-divide the quadrant into sections and obtain nine measurements of mulch/litter depth using a ruler. Each reading is inputted into the RCAT spreadsheet tool to obtain an average value for the slope (Drake & McCullough, 2010).

Cone penetrometer DTR measurements reflect soil strength and provide insight to the depth to restricting layers, therefore indirectly measuring soil hydraulic conductivity and infiltration capacity when combined with soil moisture measurements (Drake et al., 2010). RCAT recommends determining soil moisture levels prior to obtaining cone penetrometer DTR measurements, as cone penetrometer DTR measurements executed at soil moisture levels exceeding 15% are not comparable to measurements at lower moisture levels, therefore potentially skewing results. RCAT provides guidelines to determine soil moisture content using either a soil moisture measurement device or a “feel test”. The cone penetrometer records the penetration depth reached for a corresponding dial reading of approximately 350 pounds per square inch (psi). Similar to the mulch/litter depth procedure, the cone penetrometer DTR measurements require nine readings per quadrant to eventually determine the average value for the slope (Drake & McCullough, 2010).

RCAT requires users to input soil type (granitic or volcanic), as Lake Tahoe erosion studies by Grismer & Hogan (2004, 2005) revealed that volcanic soils typically generate greater sediment yields relative to granitic soils for all slope gradients and cover types. Parent materials of soil types for all soil mapping units in the Lake Tahoe basin are accessible from the Tahoe Basin NRCS Soil Survey. The majority of the northern and western portion of the Lake Tahoe Basin is comprised of volcanic soil types, while the eastern portion is composed primarily of granitic soils (USDA-NRCS, 2007).

In estimating the FSP fractions of the sediment loads, RCAT uses PSD data obtained from both recent and past Lake Tahoe rainfall simulations. This data revealed that runoff PSDs are primarily dependent on soil type and treatment type and not dependent on slope gradient (Drake et al., 2010).

Although not specifically described in RCAT documentation, values of average annual precipitation depth can be obtained from a variety of different sources. However, in order to be consistent with the PLRM, the user should use the average annual precipitation estimates contained in the PLRM hydrologic database (Met Grid cells) for RCAT sediment yield analysis. Location specific precipitation data within the Tahoe Basin associated with PLRM Met Grid cells is extrapolated based on relationships derived from PRISM. In determining the annual runoff fraction, used in RCAT to determine average annual runoff and ultimately sediment yield, a relationship was determined based solely on slope using a square root relationship between runoff fraction and slope angle. Based on a previous study by Heyvaert, Parra, Strassenburgh, & Townsend (2008) that determined stormwater runoff from a range of urban and suburban slopes, the maximum runoff fraction associated with very steep slopes (90 percent) was set at 15 percent in RCAT. Using this data, RCAT runoff fractions ( $R_F$ ) range non-linearly from 5 to 15 percent of the total precipitation for slopes ranging from 10% to 90%, as expressed by the following equation (Drake et al., 2010):

$$R_F = 0.1581 \left( \frac{S}{100} \right)^{1/2} \quad \text{Equation 2.33}$$

where  $S$  = slope (%)

The RCAT presents an example for predicting the sediment yield for a 20-year, 1-hour storm event, a typical design storm used in the Tahoe Basin. Thus, RCAT can be used to determine sediment yield from individual storms and design storms.

In the RCAT, the surface cover index value is used with the combination of various ranges of cone penetrometer DTR, soil type and average slope to determine the sediment yield of a particular area. The precipitation depth, runoff fraction and slope area are used to calculate runoff volume and ultimately determine the sediment load (total and FSP) from the area.

## **2.7 Soil Erosion Model Evaluation Studies**

Tiwari et al. (2000) compared measured erosion data from 20 natural rainfall plots with erosion predictions from both the WEPP and USLE/RUSLE prediction methodologies. The overall results indicated that USLE/RUSLE consistently predicted soil loss better than WEPP, however WEPP performed as well or better at 85 percent of the sites. Spaeth et al. (2003) evaluated the USLE and RUSLE using

rainfall simulation data on a diverse set of rangeland vegetation types. The USLE consistently over predicted soil loss, while the RUSLE tended to under predict soil loss based the results of the Nash-Sutcliffe model efficiencies. In a study applying RUSLE and WEPP erosion models to three Sicilian basins, in order to determine the predictive accuracy, Amore et al. (2004) reported that WEPP best estimated measured sediment volumes in collection reservoirs. Larsen & MacDonald (2007) compared the sediment yield predictions from the RUSLE and Disturbed WEPP models versus collected data from wildfire areas in the Colorado Front Range Mountains. The study concluded that both models performed poorly, however the WEPP predicted sediment yields slightly better than the RUSLE. In a case study on roadway cut slopes in El Dorado County, California, Drake et al. (2010) compared sediment loading predictions from the RUSLE and the RCAT. The results revealed that the annual sediment yields from the RCAT were approximately five times greater than the estimates generated from RUSLE.

## **2.8 Rainfall Simulations**

The understanding of runoff, infiltration and soil erosion has been greatly enhanced through the use of rainfall simulations. Although data collected from natural rainfall events is preferable, the unpredictability of natural rainfall leads to difficulties and inefficiencies with collecting sufficient amounts of data to develop statistically supported relationships. Rainfall simulations offer an efficient, controlled and repeatable method of gathering large amounts of data over a variety of environmental conditions (Thomas & Swamt, 1989).

The effective design of a rainfall simulator addresses the following key characteristics: (1) accurate replication of natural rainfall kinetic energies by considering drop size, fall height and corresponding fall velocity; (2) the capability to simulate specific design storms through the control of rainfall intensity and storm duration; (3) continuous and uniform rainfall distribution over the plot area; (4) effective design that considers portability, water availability, wind protection and manageability on difficult terrain; and (5) an effective runoff collection system (Battany & Grismer, 2000a).

### **2.8.1 Rainfall Simulator Types**

The two primary types of rainfall simulators generally used for soil erosion research are spray nozzles and drop-formers. The spray nozzle types of rainfall simulators produce a fan spray, generating

large drop size distributions. The wide range of emitted drop sizes generally requires the use of high frame-rate cameras and blotting paper to determine the drop size distribution and corresponding fall velocities needed to calculate the raindrop kinetic energy (Abudi, Carmi, & Berliner, 2012). These spray nozzles typically operate at high intensities and pressures that generate an initial velocity at the raindrop outlet, resulting in shorter fall distances required to achieve terminal velocities (Navas, Alberto, Machín, & Galán, 1990). Drop-former type rainfall simulators typically operate at lower pressures and generate a repeatable drop pattern and a single drop size dependent on the system pressure and the orifice size of the emitter. The narrow range of drop sizes produced by drop-formers means the kinetic energy of the drops depends primarily on the height of the drop-forming mechanism above the ground surface (Battany & Grismer, 2000a). Despite the large amounts of erosion data gathered from numerous rainfall simulation-based studies, there is currently no standardized design for rainfall simulators or testing methodology for measuring erosion rates; this often results in difficulties when attempting to compare results from different studies (Grismer, 2012).

### 2.8.2 Rainfall Kinetic Energy

The raindrop impact energy or kinetic energy colliding with the land surface results in the detachment of soil particles and represents the initiation of the rainfall runoff and erosion process and is an important parameter for characterizing the erosion processes (Battany & Grismer, 2000a). Rainfall kinetic energy is often considered the primary indicator of rainfall erosivity and is typically reported in rainfall simulation-oriented studies (van Dijk, Bruijnzeel, & Rosewell, 2002). The kinetic energy,  $KE$  (J), of rainfall is a function of the drop size and the impact velocity of the raindrop, and can be estimated as follows:

$$KE = \frac{1}{2}mv^2 \quad \text{Equation 2.34}$$

where  $m$  = mass of raindrop (kg)

$v$  = velocity of the raindrop (m/s)

The mass of the raindrop (kg) can be expressed as a function of raindrop diameter, assuming a spherical drop shape:

$$m(D) = \frac{\pi}{6} \rho D^3 \quad \text{Equation 2.35}$$

where  $D$  = diameter of raindrop (mm)

$\rho$  = density of water ( $\text{kg mm}^{-3}$ )

The drop size distribution of natural rainfall depends on various storm characteristics, including storm type (e.g., orographic, convective, drizzle below clouds, etc.) and rainfall intensity (van Dijk et al., 2002).

Natural rainfall drop sizes generally range from 1 to 7 mm in diameter (Chow, Maidment, & Mays, 1988).

Low intensity natural rainfall events (< 10 mm/hr) typically produce median drop sizes of < 1 mm, while high intensity storms (> 10 mm/hr) may yield median drop sizes between 2 and 3 mm in size (Laws & Parsons, 1943).

Natural raindrops reach terminal velocity prior to impacting the ground surface due to their significant fall height from the atmospheric level. To determine the terminal velocity of rainfall, various researchers established power law equations, based on drop size and velocity measurements of natural rainfall, which calculate the terminal velocity as a function of the raindrop diameter. A relationship presented by Beard (1976) is given as:

$$v_D = 0.0561D^3 - 0.912D^2 + 5.03D - 0.254 \quad \text{Equation 2.36}$$

where  $v_D$  = terminal velocity of raindrop (m/s)

$D$  = diameter of raindrop (mm)

Rainfall simulations typically produce raindrops from heights less than 10 feet above the ground surface. As a result, the majority of drops do not reach their terminal velocity prior to impact. Inadequate fall height is a common shortcoming of rainfall simulators, resulting in low raindrop kinetic energy (Battany & Grismer, 2000a). Additionally, the effects of raindrop shape distortion result in the necessity of complex mathematical equations to describe the relationship between fall velocity and drop diameter. The numerical model, developed by van Boxel (1998) and graphically shown in Figure 2.4, uses physical principles to relate fall velocity, fall height and raindrop diameter. This model assists in determining the fall speed and, indirectly, the kinetic energy of raindrops generated by rainfall simulators.

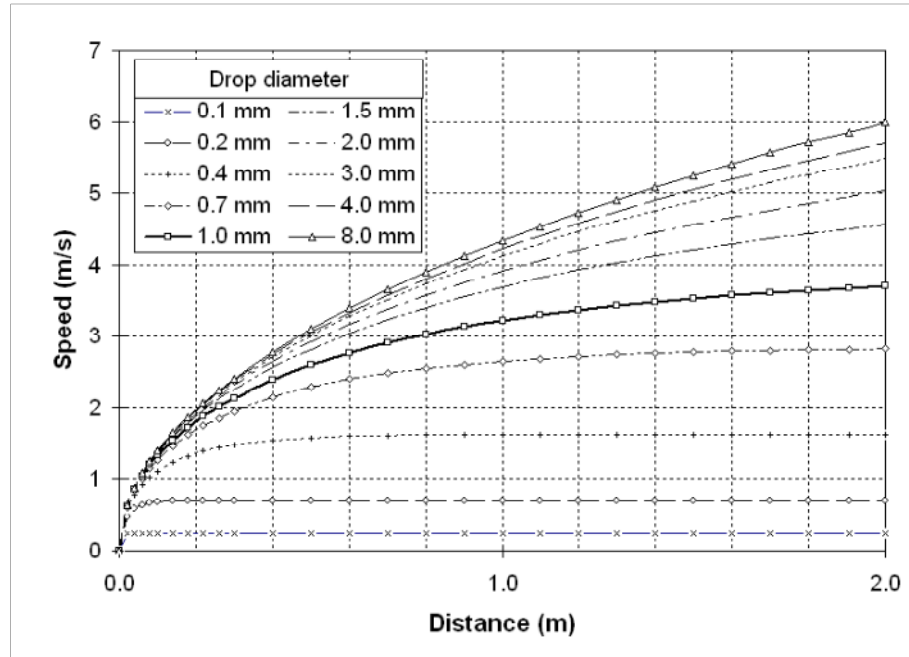


Figure 2.4. Rainfall velocity vs. fall distance for various drop diameters (van Boxel, 1998)

For comparative purposes, the kinetic energy is often expressed in either volume specific terms (kinetic energy content) or time specific terms (power). The kinetic energy content or the kinetic energy per unit rainfall depth is expressed as (van Dijk et al., 2002):

$$e_K = \frac{1}{2} \rho \sum_{i=1}^k f_i v_i^2 \quad \text{Equation 2.37}$$

where  $e_K$  = kinetic energy content ( $\text{J m}^{-2} \text{mm}^{-1}$ )

$\rho$  = mass density associated with 1 mm of rainfall ( $\text{kg m}^{-2} \text{mm}^{-1}$ )

$f_i$  = mass fraction of raindrops in size class  $i$

$v_i$  = velocity of the raindrops in size class  $i$  (m/s)

To directly measure kinetic energy is costly and cumbersome; therefore, it is usually related to rainfall intensity using mathematical equations (Sanchez-Moreno, Mannaerts, Jetten, & Löffler-Mang, 2012).

Numerous studies have established mathematical relationships between rainfall intensity and kinetic energy content, typically in the form of a power-law, exponential, and logarithmic equations, as shown in Figure 2.5. The data used to derive these equations are commonly based on the drop size distribution and terminal velocity measurements made by Laws & Parsons (1943) at Washington, D.C. under near standard conditions (air pressure = 1 bar, air temperature = 20° C). Based on Figure 2.5, typical kinetic energy

content values range from approximately  $10 \text{ J m}^{-2} \text{ mm}^{-1}$  to an upper limit of  $30 \text{ J m}^{-2} \text{ mm}^{-1}$  (van Dijk et al., 2002). Van Dijk et al. (2002) reviewed 19 studies with published rainfall data gathered at 24 different locations throughout the world to develop relationships between rainfall intensity and kinetic energy and concluded that the average minimum and average maximum values of kinetic energy content were  $11.1$  and  $29.9 \text{ J m}^{-2} \text{ mm}^{-1}$ , respectively.

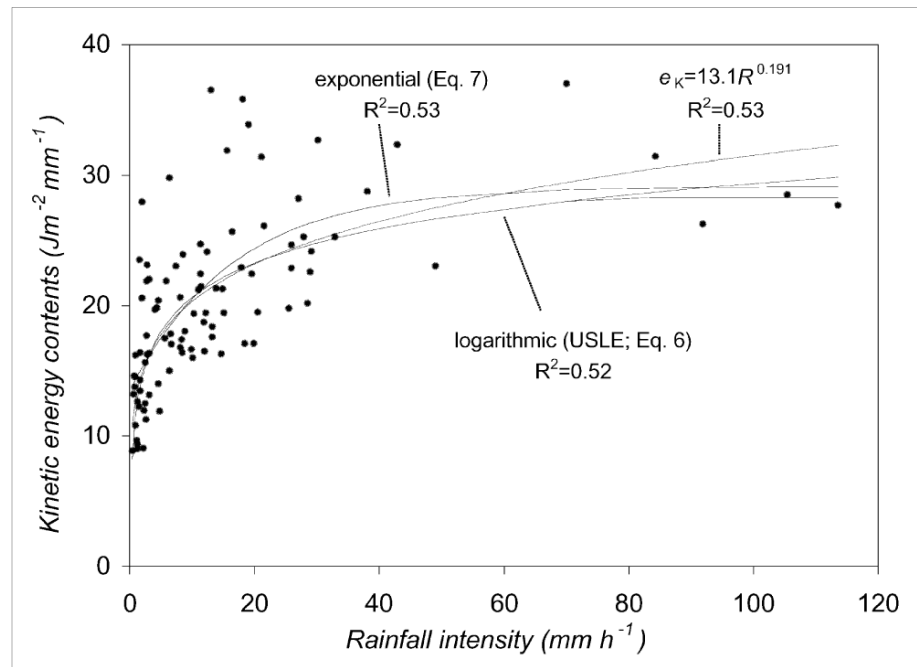


Figure 2.5. Rainfall intensity-kinetic energy relationships (van Dijk et al., 2002)

Additionally, the rainfall kinetic energy component is frequently expressed on a kinetic energy per unit time basis, termed as raindrop power and calculated as follows (Abudi et al., 2012):

$$EK = I e_K \quad \text{Equation 2.38}$$

where  $EK$  = raindrop power ( $\text{J m}^2 \text{ hr}^{-1}$ )

$I$  = rainfall intensity (mm/hr)

Based on the results of Figure 2.5, raindrop power values range from approximately  $10 \text{ J m}^{-2} \text{ hr}^{-1}$  to  $3,600 \text{ J m}^{-2} \text{ hr}^{-1}$  for rainfall for rainfall intensities of  $1$  and  $120 \text{ mm/hr}$ . Madden, Wilson, & Ntchimpera, (1998) used an electronic sensor to measure raindrop power for 85 rainfall events occurring in Ohio between 1996 and 1997. The measured storms, with average intensities ranging from  $0.1$  to  $42 \text{ mm/hr}$ , produced raindrop powers within the range of  $0$  to  $3,000 \text{ J m}^{-2} \text{ hr}^{-1}$ .

### 2.8.3 Rainfall Intensity and Duration

The configuration of rainfall simulators to replicate the varying intensities experienced during a natural storm event is often impractical without the use of sophisticated control mechanisms to create non-uniform hyetographs throughout the simulation period (Sawatsky et al., 1996). Therefore, rainfall simulators typically operate using statistically determined rainfall intensities and durations from extreme historical events (i.e., 25-, 50- or 100-year events) for a specific locale (Hamed et al., 2002). Rainfall simulations often exceed the duration of the design storm event and are typically performed for a specified time period or until steady-state runoff is achieved (Foltz et al., 2011; Grismer & Hogan, 2004, 2005a, 2005b).

### 2.8.4 Plot Size and Scaling

The majority of rainfall simulations used for runoff and soil erosion studies encompassed plot areas  $< 1.5 \text{ m}^2$ , including typical run lengths of  $< 1 \text{ m}$  (Cerde, 1999). These short run lengths indicate that soil erosion measurements only reflect interrill erosion, not the more significant rill erosion, as rill erosion is considered to occur at slope lengths exceeding 4 m (Renard et al., 1997). Therefore, runoff-soil loss relationships established from small plot rainfall simulations are considered scale-dependent and generally underestimate soil losses when applied to larger areas with longer run lengths (Hamed et al., 2002).

### 2.8.5 Uniformity

Rainfall simulators need to apply a uniform distribution of raindrops over the plot area. To estimate the spatial variability of rainfall over the plot surface, rainfall simulators are typically calibrated using tests performed in laboratory settings (Hignett, Gusli, Cass, & Besz, 1995). Various containers, distributed randomly throughout the plot, collect simulated rainfall during a series of runs (Thomas & Swamt, 1989). From this collected data, the uniformity coefficient ( $CU$ ) is used to quantitatively describe the rainfall uniformity, as follows (Christiansen, 1942):

$$CU = 100 \left( 1.0 - \frac{\sum x}{mn} \right) \quad \text{Equation 2.39}$$

where  $x$  = deviation of individual observations from the mean

$m$  = mean value

$n$  = number of observations

In a study evaluating the suitability of various rainfall simulators for erosion testing, Pérez-Rodríguez et al. (2009) noted that acceptable event simulations typically achieve CU values greater than 80%.

## **2.9 Lake Tahoe Rainfall Simulation-Based Soil Erosion Research**

This section summarizes the recent history of rainfall simulation-based erosion studies in the Lake Tahoe Basin. The main design features of the rainfall simulators (e.g., fall height, plot size, and rainfall simulator type) and the characteristics of the simulated rainfall (e.g., median drop size, rainfall intensity, duration, and kinetic energy) used in these Tahoe-specific studies are summarized in Table 2.1, located at the end of this section.

Prior to the research performed by Munn (1974), limited quantitative site-specific infiltration, runoff and sediment transport data existed in the Tahoe Basin, primarily due to site accessibility constraints and the labor and time intensive nature of performing rainfall simulations and erosion measurements in alpine watersheds (Guerrant, Miller, Mahannah, & Narayanan, 1990). Munn (1974) used high intensity, 15-minute duration storm simulations to evaluate the erosion characteristics of seven different soil types in the Lake Tahoe Basin. This study, conducted on both undisturbed natural and disturbed plots and slope gradients ranging from 0 to 60 percent, concluded that the major variables influencing soil erosion were slope gradient and soil texture.

In a study assessing the practicality of four different types of rainfall simulators and their ability to characterize infiltration on the Cagwin soil series (granitic) in the Tahoe Basin, Guerrant et al. (1990) concluded that the modular, drop-former type (formed using 500 hypodermic needles) performed best, considering water consumption, transportability, labor requirement and other considerations related to the steep, sub-alpine environment. Furthering this evaluation, Guerrant, Miller, Mahannah, & Narayanan (1991) used the modular-type rainfall simulator to assess infiltration, runoff and erosion for the Cagwin soil series. The rainfall simulations were performed on four different types of plot conditions (two disturbed and two natural) and slope gradients ranging from 0-15, 15-30 and > 30 percent. The study discovered that the slope significantly affected erosion rates and had a lesser impact on infiltration and runoff, while plot condition had the greatest effect on infiltration and runoff.

Naslas, Miller, Gifford, & Fernandez (1994) used a rainfall simulator, similar to the one used by Guerrant et al. (1990 and 1991), to investigate the impacts of soil type, plot condition and slope gradient on infiltration, runoff and interrill surface erosion in the Tahoe Basin. These rainfall simulations were applied to three slope gradients (<15, 15-30, and >15 percent), two soil types (Meeks and Umpa) and four plot conditions (two natural and two disturbed). The researchers concluded that soil type, plot condition, slope and duration of the simulation all represent important factors in understanding the magnitude of erosion.

In a series of Lake Tahoe erosion studies, Grismer & Hogan (2004, 2005a, 2005b) used rainfall simulations, based on drop-former design developed by Battany & Grismer (2000a), to assess the effectiveness of revegetation and mulch treatments for erosion control on increasing infiltration and reducing erosion at several roadway cut slopes and ski runs throughout the Tahoe Basin. In the first phase, Grismer & Hogan (2004) performed a preliminary method assessment by conducting rainfall simulation testing at eight sites having various soil types (two volcanic, five granitic, and one mixed soil type) with slopes ranging from 48 to 72 percent. The authors reported that runoff rates, sediment concentrations, and sediment yields for volcanic soils were greater than those from granitic soils. Additionally, the investigators stated that pine needle mulch (PNM) cover treatments substantially reduced erosion from all plots. In the second phase of the evaluation, Grismer & Hogan (2005a) performed rainfall simulations on bare slopes to establish a basis of comparison to the revegetated slopes analyzed in the first phase and subsequent third phase. Plot conditions consisted of bare and some “native”, relatively bare, undisturbed plots on granitic and volcanic soils with slopes ranging from 28 to 78 percent and 22 to 61 percent, respectively. The PSD analyses revealed that runoff from plots with granitic soil typically contained larger grain sizes than volcanic soils. In terms of soil loss per unit runoff, sediment yields ranged from 1 to 12 g m<sup>-2</sup> mm<sup>-1</sup> and 3 to 31 g m<sup>-2</sup> mm<sup>-1</sup> for granitic and volcanic soils, respectively. In the third and final phase of the infiltration and erosion evaluation series, Grismer & Hogan (2005b) conducted rainfall simulations on revegetated/mulched disturbed slopes and mulch-lined “native” covered slopes of both the granitic and volcanic origin. The slopes evaluated had gradients ranging from 30 to 70 percent. The results of this study were consistent with those of the previous phases in that sediment yields for volcanic soils were typically

higher than yields from granitic soil plots, ranging from 0.3 to 3 g m<sup>-2</sup> mm<sup>-1</sup> and 2 to 12 g m<sup>-2</sup> mm<sup>-1</sup>, respectively.

Grismer, Ellis, & Fristensky (2008) added to the previous erosion work performed by Grismer & Hogan (2004, 2005a, 2005b) and evaluated the impact of slope gradient on runoff sediment PSDs and sediment yield for a variety of soil types and plot conditions. The researchers concluded that runoff rates generally increased with increasing slope for all soil types and plot conditions and noted that volcanic soils resulted in 3 to 4 times greater sediment yields relative to granitic soils, thus supporting previous findings by Grismer & Hogan (2004, 2005a, 2005b). Additionally, the investigators determined that granitic soils produced larger particle sizes in bulk soil and runoff samples than volcanic soils.

In research related to evaluating the long-term impacts of revegetation and soil restoration efforts on improving infiltration and reducing erosion, Grismer, Schnurrenberger, Arst, & Hogan (2009) performed multi-year hydrologic and vegetation monitoring on 120 plots covered with various soil restoration treatments. Using rainfall simulations to determine infiltration, runoff and erosion characteristics, the researchers concluded that PNM cover was most effective in reducing runoff and erosion in the short term. However, successful plant establishment may be the most important feature in increasing infiltration and limiting erosion in the long term.

In developing the erosion prediction relationships used in the RCAT, described in Section 2.6.5, Drake et al. (2010) performed rainfall simulations on roadway cut slopes in the Tahoe Basin to supplement the previous runoff, erosion and runoff sediment PSD data collected by Grismer & Hogan (2004, 2005a, 2005b) and Grismer et al. (2008). The authors noted that PSDs from runoff samples were primarily dependent on soil type and treatment/vegetation, not slope dependent as previously reported by Grismer et al. (2008).

Rice & Grismer (2010) conducted rainfall simulations to research the impacts of surfactant treatments on infiltration, runoff, and sediment yields. These rainfall simulations were performed within the Tahoe Basin at four relatively undisturbed, native, forested sites with slopes ranging from 10 to 15 percent. Sediment yields per unit runoff for the untreated water simulations ranged from 0.2 to 0.9 g m<sup>-2</sup> mm<sup>-1</sup> and 1.0 to 1.2 g m<sup>-2</sup> mm<sup>-1</sup> for volcanic and granitic soil types, respectively. Granitic soil sites

typically produced higher infiltration rates than volcanic sites. The authors indicated that runoff sediment PSDs were generally smaller than values reported by Grismer et al. (2008), noting that although several factors influence PSD, soil cover may be most effective in minimizing the transport of larger particles.

In an effort to improve understanding of Tahoe-specific runoff and erosion parameters for WEPP erosion modeling, Foltz, Elliot, & Wagenbrenner (2010) and Foltz et al. (2011) performed rainfall simulations on forest access roads ranging from 2 to 10 percent for both granitic and volcanic parent material origins. Hydrographs and sedigraphs from the simulations revealed that each location generated runoff within the first 3 minutes and initial sediment concentrations typically peaked early during the simulation followed by decreasing concentrations, behavior typical of forest roads where loose surface material is flushed quickly by initial runoff. These relatively bare, highly erodible surface roads produced similar median runoff particle sizes for both granitic and volcanic soils, differing from results reported in previous studies by Grismer & Hogan (2005a) and Grismer et al. (2008) where granitic soils generated significantly larger runoff particle sizes than volcanic soils.

Table 2.1. Lake Tahoe rainfall simulation characteristics

Rainfall Simulation Study Reference	<sup>2</sup> Rainfall Simulator Type (DF or SN)	Plot Size (W x L, m)	Plot Area (m <sup>2</sup> )	Fall Height (m)	Median Drop Size, D <sub>50</sub> (mm)	Applied Rainfall Intensity (mm/hr)	Duration (min)	Rainfall KE Contents (J m <sup>-2</sup> mm <sup>-1</sup> )	Rainfall Power (J m <sup>-2</sup> hr <sup>-1</sup> )	% of Natural KE
Munn (1974)	DF	0.61 x 0.61	0.37	2.5	NR	127	15	NR	NR	NR
Guerrant et al. (1991)	DF	0.6 x 0.76	0.46	1.4	2.5	80	15	NR	NR	30
Naslas, Miller, Gifford, & Fernandez (1994)	DF	0.6 x 0.76	0.46	3.5	2.5	90	60	NR	NR	70
Grismer & Hogan (2004)	DF	0.8 x 0.8	0.64	NR	2.1	60	60 or steady-state	NR	NR	70
M. E. Grismer & Hogan (2005a)	DF	0.8 x 0.8	0.64	NR	2.1	60	60 or steady-state	NR	NR	70
M. E. Grismer & Hogan (2005b)	DF	0.8 x 0.8	0.64	NR	2.1	60	60 or steady-state	NR	NR	70
M. E. Grismer et al. (2008)	DF	0.8 x 0.8	0.64	NR	2.1	60-100	60 or steady-state	NR	NR	NR
M E Grismer et al. (2009)	DF	0.8 x 0.8	0.64	1.0	2.1	60-120	30-40 or steady-state	NR	NR	NR
Drake, Mccullough, & Grismer (2010)	DF	0.8 x 0.8	0.64	1.0	2.1	119	45 or steady-state	10.3	1,220	NR
Rice & Grismer (2010)	DF	0.8 x 0.8	0.64	1.0	2.1	120	Steady-state	NR	NR	NR
R. B. Foltz et al. (2010)	SN	1.0 x 1.0	1.00	3.0	NR	86	50	20.0	1,720	NR

<sup>2</sup> DF and SN denotes drop-former and spray nozzle types of rainfall simulators, respectively  
 NR- not reported in literature

### **2.10 Particle Size Distribution Methods**

The PSD of the soil material provides valuable information on the physical and chemical properties of the soil, as well as the soil's vulnerability to erosion (Brown, 2003; Galetovic et al., 1998). The sand fraction of the soil material is typically determined by means of mechanical sieving, a procedure which separates particle sizes by passing soil material through various sieve sizes, defined by the size of the square openings, stacked on top of one another (Ferro & Mirabile, 2009). The smallest sieve size captures the 50 micron particle size; therefore, other techniques are required to determine PSDs for particles smaller than this threshold. These techniques consist of classical sedimentation methods (hydrometer, HM or pipette, PM), as well as various "new age" techniques (laser diffraction, LDM) initially developed for analyzing powders and gels in industrial applications (Ferro & Mirabile, 2009). The sedimentation methods are time intensive and require relatively large sample sizes (10 – 20 g for PM and 50 g for HM); while the LDM requires smaller sample sizes (< 1 g) and minimal analysis time, at the expense of higher costs (Eshel, Levy, Mingelgrin, & Singer, 2004). Eshel et al. (2004) compared the PM to the LDM for 42 soil samples from California and reported that the LDM generally yielded a smaller clay fraction and a higher proportion of silt in comparison to the PM. In an study comparing the HM to the LDM for 30 different soil samples, Ferro & Mirabile (2009) observed that the HM typically overestimated the clay fraction in comparison to the LDM, although reported that estimates of sand fractions were generally equal.

### **2.11 Soil Textural Classification Systems**

Soil texture refers to the proportionate distribution of different soil mineral particle sizes. The three major soil classification systems used by geologists and engineering professionals consist of the Unified Soil Classification System (USCS), American Association of State Highway and Transportation Officials (AASHTO) System and the USDA Textural Classification System. One significant difference between the three classification systems are the cutoff sizes for different particle size classes, as shown in Figure 2.6. Additionally, the USCS and AASHTO systems consider other properties (e.g., liquid limit and plasticity index) in determining soil classification, while the USDA system depends entirely on particle size (Brown, 2003). The USDA textural classification system is the method used to classify the soil textures

used in most erosion models, including the RUSLE and WEPP erosion prediction models (Flanagan et al., 2012; Galetovic et al., 1998).

<b>U.S.D.A.</b>	CLAY	SILT		SAND				GRAVEL			COB- BLES	STONES
		fi.	co.	v.fi.	fi.	med.	co.	v.co.	fi.	med.		
		.002	.05					2			76	250mm
<b>INTER- NATIONAL</b>	CLAY	SILT	SAND				GRAVEL	STONES				
			fi.	co.								
		.002	.02			2	20mm					
<b>UNIFIED</b>	SILT OR CLAY		SAND				GRAVEL		COBBLES			
			fi.	med.	co.	fi.	co.					
			.074			4.76	76mm					
<b>AASHO</b>	CLAY	SILT	SAND			GRAVEL OR STONES			BOULDERS			
			fi.	co.		fi.	med.	co.				
		.005	.074			2	76mm					
<b>PHI SCALE</b>												
		.00195	.0078	.031	.125	.5	2	8	32	128	512mm	

Figure 2.6. Comparison of soil classification systems (USDA 1993)

### 2.11.1 USDA Textural Soil Classification

The USDA subdivides soil mineral particles into classes or size “separates” defined by particle size limits expressed in millimeters. Table 2.2 shows the eight size separates for the minerals less than 2 millimeters in size.

Table 2.2. Sediment particle size classification (USDA 1993)

Class Name	Particle Size (mm)
Rock Fragments	> 2.0
Very Coarse Sand	2.0 – 1.0
Coarse Sand	1.0 – 0.5
Medium Sand	0.5 - 0.25
Fine Sand	0.25 – 0.10
Very Fine Sand	0.10 – 0.05
Silt	0.05 – 0.002
Clay	< 0.002

The USDA determines the soil texture based on the weight proportion of the separates for mineral particles less than 2 millimeters in diameter. Laboratory PSD analyses, using a combination of methods discussed in Section 2.10, are used to determine weight proportions. There are twelve major textural classes defined in the USDA system: sand, loamy sands, sandy loams, loam, silt loam, silt, sandy clay loam, clay loam, silty clay loam, sandy clay, silty clay, and clay. Additional subclasses of sand, loamy sands and sandy loams are determined based on the proportion of individual sand separates. The compositions (percentages of sand,

silt and clay content) of these basic textural classes are defined by the USDA Textural Triangle shown in Figure 2.7 (USDA 1993).

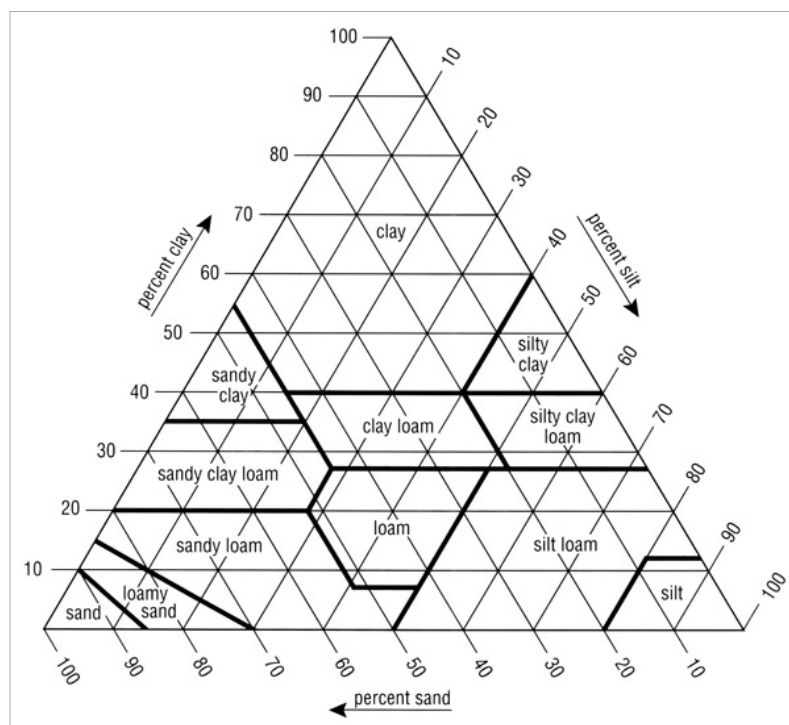


Figure 2.7. USDA textural triangle (USDA 1993)

Mineral particles exceeding 2 millimeters are analyzed separately from the soil separates.

Depending on their shape and size, rock fragments are classified into the following classes: gravel (2.0 – 75 mm), cobbles (75 – 250 mm), stones (250 – 600 mm) and boulders (> 600 mm). Depending on the weight or volume percentages, the adjectival form of the class name of the rock fragments is used as a modifier of the textural names. In the case of a sandy loam soil containing rock fragments dominated by the gravel class, the following adjectival terms are used to describe the textural class: “gravelly” sandy loam (15 to 35 percent), “very gravelly” sandy loam (35 to 60 percent). No adjectival term is used when the dominant rock fragment is less than 15 percent (USDA 1993).

## Chapter 3

### **MATERIALS AND METHODS**

#### **3.1 Overview**

This chapter describes the materials and methods used to perform rainfall simulations, collect and analyze runoff samples to quantify erosion, quantify dry ravel erosion, determine the PSDs of bulk soils and the percentages of FSP in the runoff sediment, analyze relationships between soil losses and site characteristics, perform sensitivity analyses on selected soil erosion models, evaluate soil erosion models and estimate average annual sediment yields from tested slopes.

#### **3.2 Study Site Characteristics and Slope Selection**

Lake Tahoe is a large alpine lake located on the California-Nevada border, approximately 25 miles southwest of Reno, Nevada (see Figure 3.1). Multiple field visits, performed in the spring of 2013, identified 29 potential sites for rainfall simulation testing and sediment trap collection. All sites were located adjacent to roadways owned and/or maintained by NDOT within the Lake Tahoe Basin (i.e., State Route 28, State Route 431 and U.S. Highway 50). A discussion between UNR, Atkins and NDOT was held on July 2, 2013 and the preferred slopes were identified for rainfall simulation testing and installation of dry ravel sediment traps. A total of 15 sites were selected for field testing with the intent to represent a wide range of slope characteristics including slope gradient, soil type, cut and fill slopes, vegetative cover, canopy cover, riprap, rock outcroppings, and the depth and coverage of mulch and litter. Accessibility and safety were other major factors considered when selecting suitable sites. A total of 25 rainfall simulations were performed and a total of 8 dry ravel sediment traps were installed at the base of various slopes. See Figure 3.1 and Table 3.1 for a map of overall testing locations and location details, respectively.

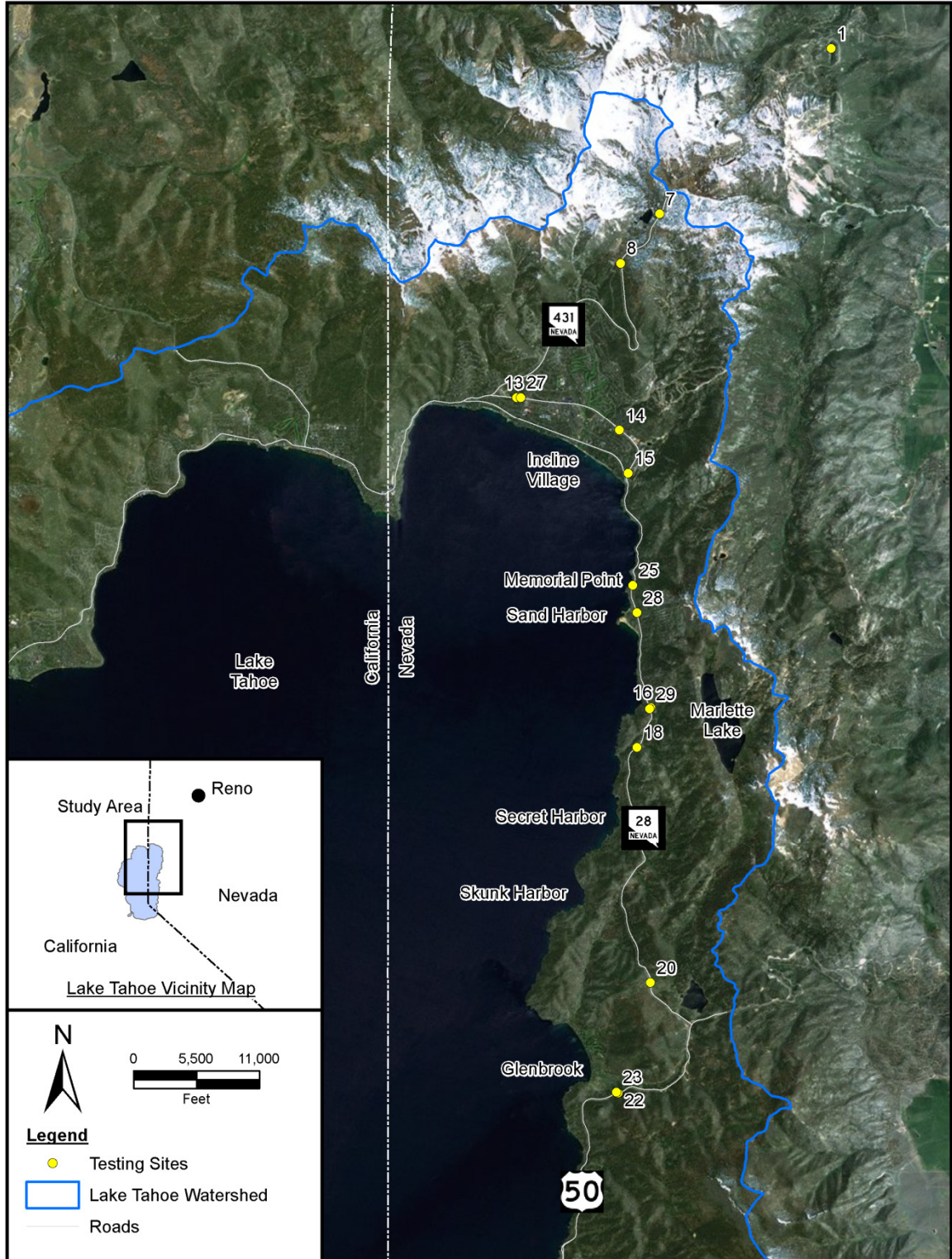


Figure 3.1. Slope testing locations- overall site map

Table 3.1. Locations of slope testing sites

Site ID	NDOT Roadway	Slope Type	USGS Elevation (ft)	Aspect	<sup>1</sup> Field Testing Type/ID	Latitude (N)	Longitude (W)
1	SR 431	Cut	7620	N	DR 1	39.3355	119.8710
7	SR 431	Fill	8360	NW	RS 7-1	39.2951	119.9232
					RS 7-2	39.2952	119.9231
8	SR 431	Cut	8120	E	RS 8-1	39.2833	119.9348
					RS 8-2	39.2832	119.9348
					DR 2	39.2833	119.9347
13	SR 28	Cut	6400	N	RS 13-1	39.2506	119.9659
					RS 13-2	39.2507	119.9660
14	SR 28	Cut	6420	SW	RS 14-1	39.2418	119.9319
					RS 14-2	39.2418	119.9318
15	SR 28	Cut	6320	W	RS 15-1	39.2333	119.9313
					RS 15-2	39.2332	119.9313
					DR 3	39.2331	119.9315
					DR 4	39.2323	119.9319
16	SR 28	Cut	6440	W	RS 16-1	39.1766	119.9236
					RS 16-2	39.1767	119.9236
18	SR 28	Cut	6460	NW	RS 18-1	39.1670	119.9278
					RS 18-2	39.1670	119.9277
20	SR 28	Fill	6920	E	RS 20-1	39.1105	119.9224
					RS 20-2	39.1104	119.9224
22	US 50	Cut	6520	N	RS 22-1	39.0840	119.9314
					RS 22-2	39.0840	119.9315
					RS 22-3	39.0840	119.9315
					DR 8	39.0838	119.9327
23	US 50	Cut	6520	S	DR 7	39.0842	119.9322
25	SR 28	Cut	6260	W	RS 25-1	39.2068	119.9290
					RS 25-2	39.2060	119.9296
27	SR 28	Cut	6420	S	RS 27-1	39.2508	119.9649
					RS 27-2	39.2508	119.9648
28	SR 28	Fill	6260	E	RS 28-1	39.1995	119.9283
					RS 28-2	39.1996	119.9283
					DR 5	39.1995	119.9282
29	SR 28	Fill	6420	W	DR 6	39.1764	119.9239

<sup>1</sup> RS and DR denotes rainfall simulation and dry ravel sediment trap installation sites, respectively

### 3.3 Rainfall Simulations

In order to assess various soil erosion estimation methodologies, numerous slope erosion measurement methods were considered including rainfall simulations, silt fences and other natural rainfall erosion plot measurement techniques. Silt fencing is a common best management practice (BMP) used to control sediment at construction sites, as well as an inexpensive technique used to measure hillslope soil erosion (Robichaud & Brown, 2002). However, the effectiveness of silt fences in trapping fine sediment has been widely evaluated. In a comprehensive review of silt fence sediment removal efficiency studies, Faucette et. al (2008) reported that trapping efficiency considerably declines as particle size decreases,

concluding that 92% of the total suspended solids (TSS), composed of grain sizes significantly smaller than the smallest silt fence opening (210 microns), were normally not trapped. Since the current research project focuses on quantifying fine sediment particles, the silt fence was not considered a viable soil erosion measurement technique.

Due to project schedule constraints, field accessibility issues, and the temporal and spatial variability of natural rainfall in the Lake Tahoe Basin, rainfall simulations were considered the most effective measurement method to validate the soil erosion model results for individual storm events. Rainfall simulations have been used for model evaluation in numerous studies (see Section 2.7), including studies by Spaeth, Pierson, Weltz, & Blackburn (2003) and Pudasaini et al. (2004) who used rainfall simulation data on various rangeland vegetation types and construction sites, respectively, to evaluate the prediction accuracy of the RUSLE. Historically, rainfall simulation has led to significant developments in hill slope erosion and runoff research and provides a repeatable method for collecting large amounts of data from a variety of different site conditions (Galetovic et al., 1998).

As discussed in Section 2.8, an effective rainfall simulator design must consider kinetic energy, drop size, fall height and raindrop fall velocities to accurately simulate natural rainfall conditions. Additionally, rainfall simulators should feature the ability to simulate specific design storms and apply uniform rainfall over the plot area (Abudi et al., 2012).

### **3.3.1 Design and Construction**

A portable field rainfall simulator, constructed of polyethylene drip line and 1/2 gallon per hour (gph) drip emitters, was designed and developed for this research project (see Figure 3.2). The drop-former type of mechanism consisted of a gridded system with 425 drip buttons spaced at approximately 2.5 inch on center and covering a 42.5 inch wide by 50.5 inch long plot. The rainfall grid was attached to an aluminum frame (48 inch wide by 75 inch long) for support using metal ties and 1 inch diameter PVC pipe. Steel rebar was inserted vertically within the hollow aluminum frame to allow each of the four legs to be adjusted in height and leveled to accommodate different slope gradients. The rainfall simulator was positioned at a fixed height of 8 ft (~2.5 m) above the ground at the upslope end. The height at the down slope end varied depending on the slope gradient and

associated height of the rebar extensions. For a 1.5:1 slope (67%), the rainfall grid at the downstream end stood approximately 12 ft (~3.5 m) above the ground. When necessary, large tarps were attached to the exterior frame of the rainfall simulator to protect the plot and falling raindrops from wind disturbance.

A generator powered a small submersible pump that supplied water from a 55-gallon water tank, located at the base of the rainfall simulator, to each of the four corners of the rainfall grid. A piezometer was used to monitor the water pressure and help maintain uniform rainfall intensity throughout the duration of each simulation. Precise flow control and operating pressure was achieved using a needle valve installed in-line between the pump and the piezometer.

The use of an unbounded plot frame, as opposed to a bounded plot frame, was chosen for multiple reasons including (1) minimizing the potential disturbance of the test plot resulting from pounding a 4-sided, single-unit metal plot frame into the test slope, and (2) allowing testing to be performed on slopes covered with riprap, which would be impracticable with the use of a bounded plot. The 48-inch wide runoff apron was constructed of 45-mil pond liner and sheet metal and made wide enough to capture runoff generated by the 42.5-inch wide plot formed by the rainfall simulator grid. A 4-inch strip of pond liner was used to contour to the slope and seal the runoff lip, preventing runoff from flowing underneath the apron. Long nails spaced approximately 2 inches on center were used to secure the pond liner to the slope. Sheet metal was used to form the collection flume that was attached to the pond liner. Depending on site specific conditions, soil underneath the runoff apron was sometimes excavated to provide adequate space for sample bottles to collect runoff and to allow for a steeper apron slope, in order to minimize sediment deposition within the apron.



Figure 3.2. Typical rainfall simulator setup

### 3.3.2 Evaluation and Calibration

Prior to using the rainfall simulator for field testing, numerous calibration tests were performed in the laboratory to determine the simulated rainfall characteristics, the relationship between the piezometer water level and measured rainfall intensity, and the spatial variability of rainfall.

#### 3.3.2.2 Simulated Rainfall Drop Size

The average drop diameter discharged from the drip emitters was determined by collecting a measured number of drops from a single drip button and recording the volume. This procedure was repeated numerous times for different individual drip emitters during each rainfall simulation.

Assuming a spherical drop formation, the drop diameter was estimated using the number of drops and volume measurements determined previously, which was comparable to a method used in a rainfall simulator study performed by Abudi, Carmi, & Berliner (2012). The average drop diameter was determined to be 4.6 mm. Although large in size relative to the median drop diameter of 2.5 mm

measured for high intensity rainfall reported by Laws & Parsons (1943), the drop size is within the drop size distribution found in high intensity natural rainfall (Chow et al., 1988).

### 3.3.2.3 Simulated Rainfall Impact Velocity and Kinetic Energy

The estimation of the simulated raindrop impact velocity (7.1 m/s) was based on the relationships between velocity, fall height and drop diameter developed by van Boxel (1998) and shown in Figure 2.4. Terminal velocities for the simulated raindrop size (9.1 m/s) were computed using *Equation 2.36*. Considering the average simulator fall height (~ 3.0 m), average drop diameter (4.6 mm) and the relationships and equations mentioned above, it was estimated that the simulated rain drops reached approximately 78% of their terminal velocity before contacting the ground surface. However, the kinetic energy content or kinetic energy per unit rainfall depth for this larger diameter raindrop at the described fall height and resulting fall velocity ( $\sim 25.1 \text{ J mm}^{-1}\text{-m}^{-2}$ ), was equivalent to approximately 90% of the energy contents of a more typical natural median raindrop size of 2.5 mm falling at terminal velocity ( $\sim 28.1 \text{ J mm}^{-1}\text{-m}^{-2}$ ). These approximations of kinetic energy contents were determined using *Equation 2.36* and *Equation 2.37*. Additionally, the rainfall simulator kinetic energy content was within the range of the rainfall intensity-kinetic energy relationships (shown in Figure 2.5) developed by van Dijk, Bruijnzeel, & Rosewell (2002) and described in Section 2.8.2.

Another measure of raindrop impact energy was kinetic energy per unit time basis, termed as raindrop power. Considering the combined fall height, drop size, impact velocity, targeted rainfall intensity of 3.60 in/hr and the use of *Equation 2.38*, the simulator produced an estimated raindrop power of approximately  $2,290 \text{ J/m}^2\text{-hr}$ . This resulting raindrop power was well within the range (10 to  $3,000 \text{ J/m}^2\text{-hr}$ ) measured for natural rainfall (Madden et al., 1998; van Dijk et al., 2002).

### 3.3.2.4 Rainfall Simulator Piezometer Head-Rainfall Intensity Calibration Curve

Numerous calibration tests were performed on the rainfall simulator to develop a relationship between the height of the water column in the piezometer and the resulting intensity of the rainfall simulator. During these calibration tests, water volumes were collected from 5 random drip buttons over a period of time. These volumes were averaged and intensities were calculated considering the total number of drip buttons and grid size of the rainfall simulator. This procedure was repeated many

times for different piezometer water levels and different fall heights. The data were collected, graphed and fitted with a trend line to determine a relationship between head difference (difference between height of water in piezometer and rainfall grid height) and rainfall intensity (see Figure 3.3). The purpose of developing this relationship was so uniform rainfall intensity could be maintained in the field by monitoring the water level in the piezometer throughout the duration of the rainfall simulations.

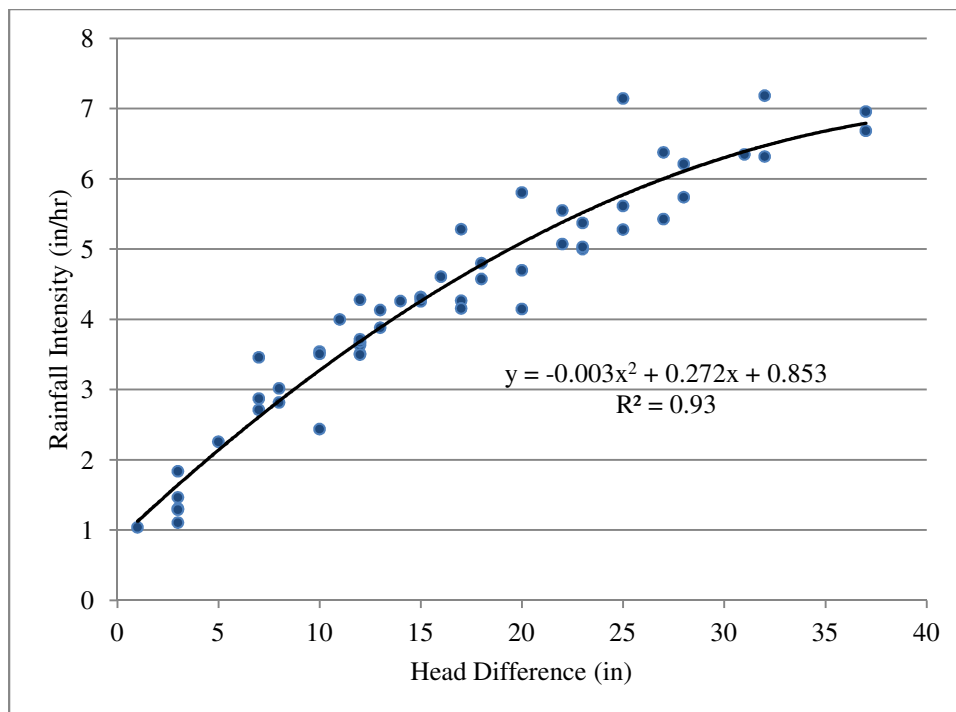


Figure 3.3. Rainfall simulator piezometer head-rainfall intensity curve

### 3.3.2.5 Uniformity

The average distribution uniformity coefficient of the rainfall simulator was calculated through multiple lab tests in order to determine the spatial variability of the simulated rainfall throughout the plot. Six 4-liter containers with 7-inch diameter openings were placed in random locations within the plot area. These containers captured the simulated rainfall over a 6 minute period. Collected water volumes were determined for each container and uniformity coefficients were calculated. This procedure was repeated for a total of 5 runs. Using *Equation 2.39*, an average distribution uniformity coefficient of approximately 88.4% was calculated (Christiansen, 1942).

Generally, acceptable uniformity coefficients for rainfall simulations are greater than 80%, as noted in Section 2.8.5.

### 3.3.3 Field Testing Procedure

As mentioned previously in Section 3.2, a total of 25 rainfall simulations were performed (see Figure 3.4). At each site, at least 2 simulations were performed with the purpose of developing a statistical basis for analyzing the results. A general overview of the site was performed to determine the location of the plot and potential setup issues. Once a plot location was selected, the rainfall simulator was setup over the desired plot area and leveled. The front legs of the rainfall simulator were lengthened by extending the rebar out of the hollow aluminum legs in order to level the rainfall grid. The runoff apron was installed next at the lower edge of the plot. Careful evaluation of the slope and position of the rainfall simulator was performed to ensure runoff would be completely captured in the runoff apron and that no rainfall would fall directly into the runoff apron. The slope was surveyed to determine slope gradient and various characteristics of the plot were noted including percent cover (surface and canopy), cover type (vegetation, rock, mulch and/or litter), and depth of mulch and/or litter. Additionally, cone penetrometer depth to refusal measurements were taken at four locations adjacent to the plot to measure soil strength using a portable soil compaction tester (Dickey John, model no. 155850003AS1). Depth to refusal is an input required in the RCAT. Table 3.2 summarizes the direct field measurements obtained from each rainfall simulation site which were later used as inputs into the various soil erosion prediction models. Prior to the start of each rainfall simulation, a soil sample was taken from just outside the plot to determine antecedent soil moisture, soil texture and particle size distribution. Field test sites were photo documented before and after the rainfall simulations. An acrylic sheet or tarp was temporarily placed over the plot to direct initial rainfall away from the plot area until the desired rainfall intensity was achieved; then, the cover was removed and the simulation officially began.

A simulated storm with a targeted rainfall intensity of 3.60 in/hr and duration of 60 minutes was delivered to each plot. This rainfall intensity was achieved by using the head-intensity relationship described in Section 3.3.2.4 and by maintaining the height of the water column in the

piezometer. This targeted rainfall intensity was representative of a 100-yr, 15-min design storm, based on NOAA Atlas 14 point precipitation estimates, for the Nevada portion of the Lake Tahoe Basin considering various locations along NDOT roadways (i.e., SR 431, SR 28 and US 50). Although it may be considered extreme, the rainfall intensity and duration used was similar to the high intensity (typically based on the 100-yr, 15-min design storms) and long simulation durations used during previous rainfall simulation studies performed in the Lake Tahoe Basin (see Table 2.1 in Section 2.9). Some examples include: (1) 2.36 in/hr and 60 minutes by Grismer & Hogan (2004, 2005a, 2005b), (2) 4.70 in/hr and 45 minutes by Drake et al. (2010); and (3) 3.39 in/hr and 60 minutes by Foltz et al. (2010). During each simulation, two rainfall intensity readings were taken from random drip emitters using a stop-watch and a graduated cylinder at 10-minute intervals. These values were averaged over the entire simulation to estimate rainfall intensity over the 60-minute duration.

Timed grab samples of the runoff were collected at 3-minute intervals throughout the simulation from the collection point at the outlet of the runoff apron, resulting in a total of 20 sample bottles for a 60-minute simulation. These samples were analyzed in the lab to generate hydrographs and sedigraphs (sediment discharge vs. time) and ultimately quantify the amount of soil loss during the simulation. At the end of each simulation, residual sediment deposited on the runoff apron was also collected.



Figure 3.4. Rainfall simulation site photographs

Table 3.2. Summary of rainfall simulation plot characteristics

Site ID	Rainfall Simulation ID	Avg. Rainfall Intensity (in/hr)	Duration (min)	Total Rainfall Depth (in)	Slope (%)	Vegetation Cover (%)	Canopy Cover (%)	Canopy Height (ft)	Rock Cover (%)	Total Surface Cover (%)	Mulch/Litter Depth (in)	Average CP DTR (in)
7	RS 7-1	3.27	60	3.27	64.0	8	2	1	0	8	0.25	11
	RS 7-2	3.31	60	3.31	53.3	10	0		2	12	0.25	5
8	RS 8-1	3.61	60	3.61	42.7	25	0		5	30	0.00	6
	RS 8-2	3.05	60	3.05	43.7	45	5	1	15	60	0.50	5
13	RS 13-1	3.26	60	3.26	20.7	85	0		2	87	0.75	2
	RS 13-2	3.05	60	3.05	24.7	85	45	2	5	90	1.00	2
14	RS 14-1	3.96	60	3.96	60.8	90	0		0	90	2.00	3
	RS 14-2	2.70	60	2.70	61.9	50	0		0	50	2.00	5
15	RS 15-1	3.60	60	3.60	50.9	0	0		0	0	0.00	9
	RS 15-2	3.60	60	3.60	64.8	15	0		5	20	3.00	13
16	RS 16-1	3.51	60	3.51	76.3	5	0		0	5	0.50	14
	RS 16-2	3.48	60	3.48	85.4	15	0		0	15	2.00	23
18	RS 18-1	3.16	60	3.16	58.4	0	0		0	0	0.00	13
	RS 18-2	3.37	60	3.37	60.6	3	0		0	3	1.00	22
20	RS 20-1	3.52	60	3.52	45.1	0	0		3	3	0.00	21
	<sup>2</sup> RS 20-2	3.76	52	3.26	54.1	5	0		5	10	0.00	13
22	RS 22-1	3.72	60	3.72	79.4	0	0		2	2	0.00	6
	RS 22-2	3.76	60	3.76	82.2	0	0		0	0	0.00	5
	RS 22-3	3.88	60	3.88	77.2	0	0		0	0	0.00	6
25	RS 25-1	3.32	60	3.32	80.5	3	0		95	98	0.50	12
	RS 25-2	3.32	60	3.32	67.1	20	0		0	20	1.50	8
27	RS 27-1	4.32	60	4.32	49.7	10	0		75	85	1.00	5
	RS 27-2	3.96	60	3.96	35.0	10	0		80	90	1.00	6
28	RS 28-1	3.54	60	3.54	48.2	3	0		1	4	0.50	27
	RS 28-2	3.29	60	3.29	54.2	3	3	1	1	4	0.50	25

<sup>1</sup> CP DTR denotes cone penetrometer depth to refusal

<sup>2</sup> Simulation RS 20-2 ended after 52 minutes due to the collapse of the simulator frame resulting from a wind gust generated from a passing semi-truck.

### **3.4 Dry Ravel Sediment Traps**

The NDOT Hydraulics Section expressed an interest in quantifying the amount of sediment contributed by dry raveling from various NDOT slopes. Dry ravel is a term that describes the transport of sediment in the absence of rainfall by means of bouncing, sliding, or rolling of sediment particles down a slope (Gabet, 2003). This erosion process was discussed in detail in Section 2.2.1. The design and procedure used for dry ravel measurements was similar to the method outlined by Gabet (2003).

#### **3.4.1 Design and Construction**

Sediment traps were constructed to collect dry ravel and estimate a sediment loss rate, on mass per area basis, over a period of time. A total of 8 sediment traps were constructed for this research project. The 2.5-foot wide sediment traps were constructed using rain gutter, roof flashing, flashing tape and sheet metal.

#### **3.4.2 Field Testing Procedure**

The sediment traps were installed in July 2013 at 8 specific locations where pedestrian disturbance was considered unlikely. These traps were installed at the base of the slope, parallel to the contour lines (see Figure 3.5). The lip of each trap was installed flush with the ground and secured to the slope using three long nails. A long stake was driven in behind each trap to provide additional stability. To minimize the visibility of sediment traps from the roadway and pullout areas, traps were placed behind rocks or vegetation when possible. Soil samples were obtained from the site to determine particle size distribution and soil texture. The slope was surveyed to determine slope gradient and observations of upslope percent cover and cover type were recorded. Additionally, horizontal coordinates of the sediment traps were recorded using GPS survey equipment. One sediment trap, DR 4, was disturbed by pedestrians. Therefore, the trap was relocated to a nearby location with a nearly identical soil type, slope and vegetative cover. Additionally, dry ravel trap DR 5 was removed in mid-September after an automobile accident near the entrance to Sand Harbor.

After installing the sediment traps, the traps were intended to be left in place until the end of October or when snow began to fall within the Tahoe Basin. Dry ravel sediment traps were not monitored during the winter season (November to April) since dry ravel is not thought to be significant due to the

presence of snow and increased soil moisture (Anderson et al., 1959; Gabet, 2003; Krammes, 1965). The goal was to collect the sediment within the sediment traps before the onset of rainfall. The likelihood of rainfall at each site was determined by visual observations and from data obtained from nearby rainfall gages. Any rainfall that occurred before the sediment traps were cleaned out was noted on the collection data sheets. After each collection period, the duration since the previous sample collection was also recorded. Dry ravel field test sites were photo documented before and after cleaning out the trap.

Using GIS spatial measuring tools and aerial imagery, the slope length upslope of each sediment trap was determined. This length measurement was multiplied by the width of the sediment trap (2.5 feet) to estimate the contributing upslope area. The collected sediment mass was divided by the upstream area and the amount of elapsed time between sample collection to estimate the amount of soil loss per area with time, similar to the procedure reported by Gabet (2003) for determining dry ravel sediment mass flux from hill slope transects near Santa Barbara, California.

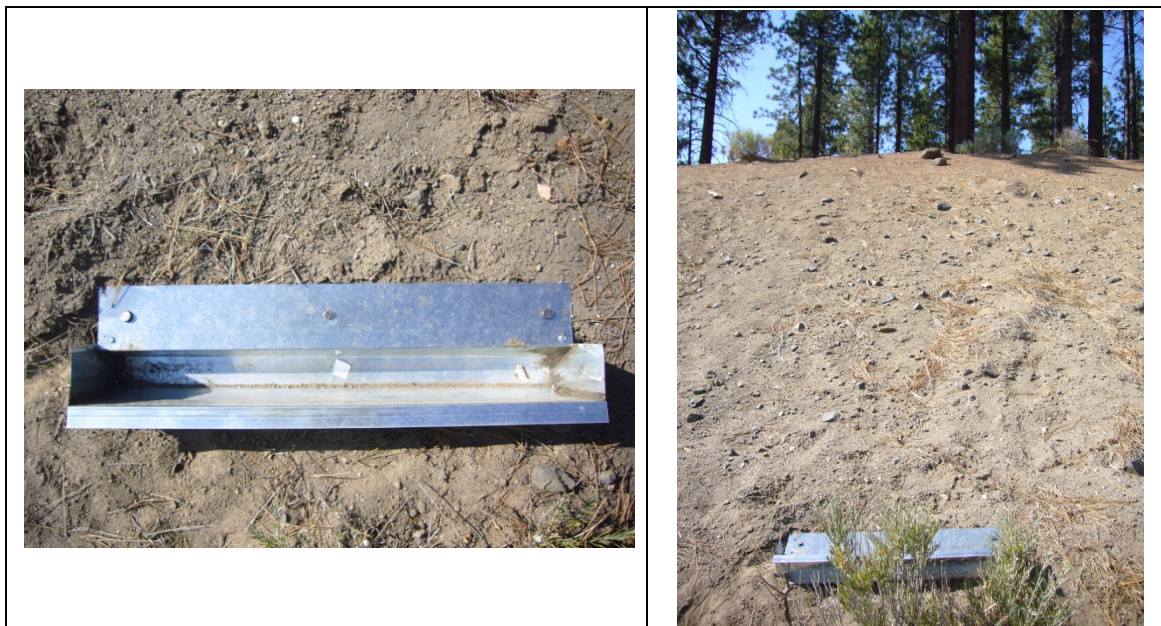


Figure 3.5. Dry ravel sediment trap installation

### 3.5 Particle Size Analysis and Soil Characterization

The data collected during field testing was analyzed using a combination of particle size distribution methods, depending on sample size and the field testing type. The three types of PSD testing methods included: vacuum filtration method (Figure 3.6) per ASTM D3977 - 97 (2013), sieve and

hydrometer method (Figure 3.7) per ASTM D422 - 63 (2007), and laser-diffraction method (Figure 3.8) per ASTM C1070 - 01 (2014). Additionally, the percent organic matter content was determined by weight loss on ignition per ASTM D2974 - 13 (2008).



Figure 3.6. Vacuum filtration

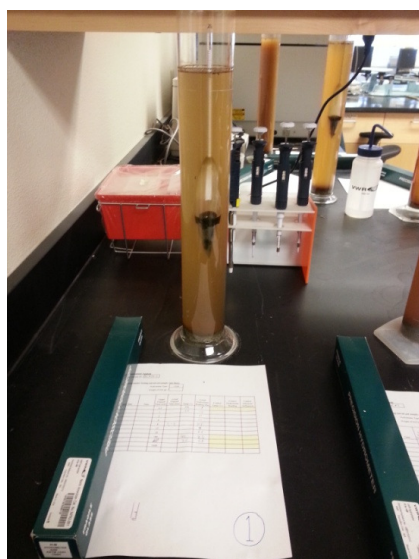


Figure 3.7. Hydrometer testing



Figure 3.8. Laser particle size analyzer (DRI)

The vacuum filtration method uses filter paper with a specific pore diameter size (16 micron filter paper used for this research), a funnel, and a 500-mL Erlenmeyer beaker to separate a targeted particle size from a runoff sample. The runoff sample is passed through the filtrate using vacuum suction and the filter paper is weighed to determine the mass of particles smaller than the pore opening size. The hydrometer

method is used to determine the PSD of particles smaller than the available mechanical sieve sizes and typically requires 50 g of sediment sample size. The method determines PSD by using a hydrometer to measure the specific density of the soil-water suspension and Stokes' Law to determine the velocity that a particle settles in suspension (Eshel et al., 2004). The laser diffraction method is typically limited to small sediment sample sizes (< 1 g) and measures the angle of diffraction of a beam of light passed through a soil-water suspension. The method uses the principle that the angle of diffraction is inversely proportional to the particle size to determine the PSD of the soil sample (Ferro & Mirabile, 2009).

### **3.5.1 Site Soil Samples**

Near surface (6 to 8 inches in depth), homogeneous soil samples were collected at each of the testing locations (dry ravel and rainfall simulation sites) using a spade, scoop or shovel. Prior to collection, the sampling area was cleared of any surface debris (e.g., rocks, mulch, litter, vegetation, etc.). The soil material was immediately transferred to a labeled sample container and the lid was tightly secured in order to preserve the sample for subsequent lab testing. Soil samples collected near the simulation plots were weighed, oven dried at 103 °C for at least 24 hours, and then weighed again to determine the antecedent soil moisture at each plot prior to performing rainfall simulations. Additionally, these soil samples and the soil samples collected near the dry ravel sediment trap locations were analyzed using a combination of sieve and hydrometer analyses methods to determine the percent FSP, and classify soil texture based on the USDA soil textural classification system described in Section 2.11.1. Percent organic matter, modified silt, and very fine sand were also determined for rainfall simulation site soils for use in determining site specific soil parameters used in the RUSLE and WEPP/TBSM soil erosion prediction models. Based on the results of the PSD analyses, Table 3.3 and Table 3.4 summarize the site specific soils characteristics for the rainfall simulation and dry ravel sites, respectively. The tables compare the results to the soils data published in the Washoe County South and Tahoe NRCS soil surveys (USDA-NRCS, 1979 and 2007) based on the soil map unit for the testing locations. The parent material of the soils (e.g., granitic, volcanic, mixed or alluvial), required for the RCAT and TBSM methods, was determined using the soil map units and the descriptions published in the Tahoe NRCS soil survey (NRCS, 2007).

Table 3.3. Rainfall simulation site soil characteristics

Site ID	Rainfall Simulation ID	<sup>1</sup> NRCS Soil Survey Data						<sup>2</sup> Site-Specific Soils Data								
		Soil Map Unit	Soil Parent Material	USDA Soil Texture	Particle Size Distribution (%)			USDA Soil Texture	<sup>3</sup> Particle Size Distribution (%)						<sup>4</sup> OM (%)	
					Sand	Silt	Clay		FSP	Gravel	Sand	Silt	Clay	VFS		MS
7	RS 7-1	9405	Granitic	Loamy sand	79	18	3	Sandy loam	16	32	66	20	14	13	33	1.8
	RS 7-2	9405	Granitic	Loamy sand	79	18	3	Sandy loam	14	16	74	15	11	11	23	1.9
8	RS 8-1	9404	Granitic	Loamy sand	79	18	3	Loamy sand	10	25	76	21	3	22	33	2.8
	RS 8-2	9404	Granitic	Loamy sand	79	18	3	Loamy sand	12	29	77	14	9	16	20	2.2
13	RS 13-1	7141	Mixed	Sandy loam	71	19	9	Sandy loam	15	30	73	19	9	12	27	3.5
	RS 13-2	7141	Mixed	Sandy loam	71	19	9	Sandy loam	13	19	76	15	9	16	24	10.2
14	RS 14-1	7151	Volcanic	Sandy loam	51	36	13	Sandy loam	24	24	55	33	12	6	49	2.5
	RS 14-2	7151	Volcanic	Sandy loam	51	36	13	Sandy loam	15	32	65	26	9	12	41	2.5
15	RS 15-1	7422	Granitic	Loamy sand	85	12	3	Loamy sand	9	12	86	9	4	8	13	0.5
	RS 15-2	7422	Granitic	Loamy sand	85	12	3	Loamy sand	7	30	87	8	5	12	12	0.9
16	RS 16-1	7422	Granitic	Loamy sand	85	12	3	Loamy sand	13	14	80	11	9	16	17	1.9
	RS 16-2	7422	Granitic	Loamy sand	85	12	3	Loamy sand	15	10	79	12	9	16	18	1.3
18	RS 18-1	7422	Granitic	Loamy sand	85	12	3	Loamy sand	11	4	84	12	4	14	16	0.5
	RS 18-2	7422	Granitic	Loamy sand	85	12	3	Loamy sand	10	14	84	10	6	12	16	0.5
20	RS 20-1	7111	Volcanic	Sandy loam	55	29	16	Sand	7	27	88	7	5	11	10	1.1
	RS 20-2	7111	Volcanic	Sandy loam	55	29	16	Sandy loam	17	21	76	12	13	16	16	1.5
22	RS 22-1	7111	Volcanic	Sandy loam	55	29	16	Sandy Loam	19	18	69	24	8	11	33	0.6
	RS 22-2	7111	Volcanic	Sandy loam	55	29	16	Sandy loam	20	13	67	24	9	11	37	0.8
	RS 22-3	7111	Volcanic	Sandy loam	55	29	16	Sandy loam	21	15	67	20	13	8	29	1.0
25	RS 25-1	7413	Granitic	Loamy sand	85	12	3	Loamy sand	10	21	83	9	7	16	14	6.2
	RS 25-2	7413	Granitic	Loamy sand	85	12	3	Loamy sand	8	34	85	11	4	14	15	0.6
27	RS 27-1	7142	Mixed	Sandy loam	71	19	9	Sandy loam	13	18	75	19	6	24	31	3.0
	RS 27-2	7142	Mixed	Sandy loam	71	19	9	Sandy loam	19	19	61	29	10	21	48	1.7
28	RS 28-1	7452	Granitic	Sand	89	7	5	Loamy sand	11	20	85	7	8	14	9	1.4
	RS 28-2	7452	Granitic	Sand	89	7	5	Loamy sand	9	17	86	11	3	12	14	2.1

<sup>1</sup> Soil characteristics from NRCS Soil Survey CA693. <sup>2</sup> Soil characteristics determined from sieve analysis and hydrometer testing of field soil samples. <sup>3</sup> Gravel and FSP is % by mass of the raw sample, other fractions are % by mass of the <2 mm component. The United States Department of Agriculture (USDA) Textural Classification System defines particle sizes as follows: gravel (> 2 mm), sand (< 2 mm, > 0.05 mm), silt (> 0.002 mm, < 0.05 mm), clay (< 0.002 mm), VFS (very fine sand, > 0.05 mm, < 0.10 mm) and MS (modified silt, > 0.002 mm, < 0.10 mm). <sup>4</sup>OM denotes organic matter.

Table 3.4. Dry ravel site soil characteristics

Site ID	Field Testing Type/ID	<sup>1</sup> NRCS Soil Survey Data						<sup>2</sup> Site-Specific Soils Data					
		Soil Map Unit	Soil Parent Material	USDA Soil Texture	Particle Size Distribution (%)			USDA Soil Texture	<sup>3</sup> Particle Size Distribution (%)				
					Sand	Silt	Clay		FSP	Gravel	Sand	Silt	Clay
1	DR 1	1100	Granitic	Loamy sand	85	13	3	Loamy sand	6	55	85	8	7
8	DR 2	9404	Granitic	Loamy sand	79	18	3	Loamy sand	10	25	76	21	3
15	DR 3	7422	Granitic	Loamy sand	85	12	3	Loamy sand	7	30	87	8	5
	DR 4	7422	Granitic	Loamy sand	85	12	3	Sand	6	24	89	9	2
22	DR 8	7111	Volcanic	Sandy loam	55	29	16	Sandy loam	21	15	67	20	13
23	DR 7	7111	Volcanic	Sandy loam	55	29	16	Sandy loam	13	18	75	17	7
28	DR 5	7452	Granitic	Sand	89	7	5	Sand	7	20	88	7	4
29	DR 6	7422	Granitic	Loamy sand	85	12	3	Loamy sand	6	54	87	6	7

<sup>1</sup> Soil characteristics from NRCS Soil Survey CA693 with the exception of Site 1 (NV628). <sup>2</sup> Soil characteristics determined from sieve analysis and hydrometer testing of field soil samples. <sup>3</sup> Gravel and FSP is % by mass of the raw sample, other fractions are % by mass of the <2 mm component. The United States Department of Agriculture (USDA) Textural Classification System defines particles sizes as follows: gravel (> 2 mm), sand (< 2 mm, > 0.05 mm), silt (> 0.002 mm, < 0.05 mm), and clay (< 0.002 mm)

### 3.5.2 Rainfall Simulation Runoff Sediment

Runoff samples, collected during each rainfall simulation, were taken to the laboratory for filtration analyses. Samples were vacuum filtered through Whatman #43 (16 microns) glass fiber filter papers. A beaker containing the filter paper with sediment (> 16 microns in size) and a beaker containing the runoff passing through the filter (< 16 microns) were oven dried at 103 °C for at least 24 hours and then weighed to determine the total sediment, fine sediment and runoff volume associated with the runoff sample. It was observed that for simulations which generated large quantities of sediment, the filtration method yielded inconsistent results for the amounts of FSP since sediment clogged the pores in the filter papers, thus preventing fine sediment from passing through. Therefore, split samples from each rainfall simulation were sent to the Desert Research Institute (DRI) for PSD analyses using a laser diffraction particle size analyzer (Micrometrics, Saturn DigiSizer 5200) as an alternative method. This method was chosen over classical sedimentation methods (e.g., hydrometer and pipette methods) due to the relatively small size of the samples, typically less than 10 grams. The laser diffraction analysis was ultimately used to determine the mass of FSP in the rainfall simulation runoff.

As mentioned in Section 3.3.3, sediment residuals remained on the runoff apron at the end of each simulation. Due to the larger sizes of these residual samples and project budget constraints, the hydrometer method was selected to determine the mass fraction of FSP. Residuals were oven dried at 103 °C for at least 24 hours and then weighed to determine the total sediment prior to performing hydrometer testing.

The total quantity of soil transported during each simulation was calculated based on the sum of two components: (1) the soil contained in the runoff samples and (2) the soil composing the residuals on the runoff apron. To generate comprehensive sedigraph ordinates (collected runoff sediment discharge rate plus deposited sediment discharge rate from the runoff apron), the deposited sediment was assumed to accumulate linearly over the time of the simulation and added to the runoff sedigraph using the following equation, as presented by Naslas et al. (1994) for the same purpose:

$$TS_t = (RS_t / RS) AS + RS_t \quad \text{Equation 3.1}$$

where  $TS_t$  = total sediment discharge rate (g/hr) at time  $t$

$RS_t$  = runoff sediment discharge rate (g/hr) at time  $t$

$RS$  = cumulative runoff sediment (g) at time  $t$

$AS$  = cumulative sediment deposited on runoff apron (g)

FSP sedigraphs were also developed by multiplying the total soil loss sedigraph ordinates by the composite percent FSP determined from the results of laser diffraction (runoff sediment) and hydrometer (residual sediment) PSD testing. The runoff hydrograph and sedigraph for RS 7-1 are shown in Figure 3.9 and Figure 3.10, respectively.

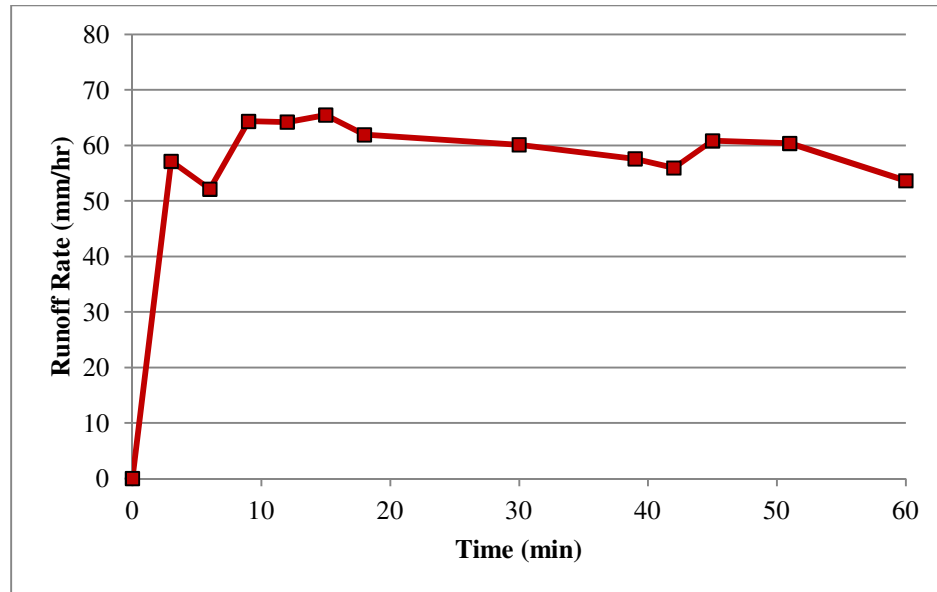


Figure 3.9. Runoff hydrograph (RS 7-1)

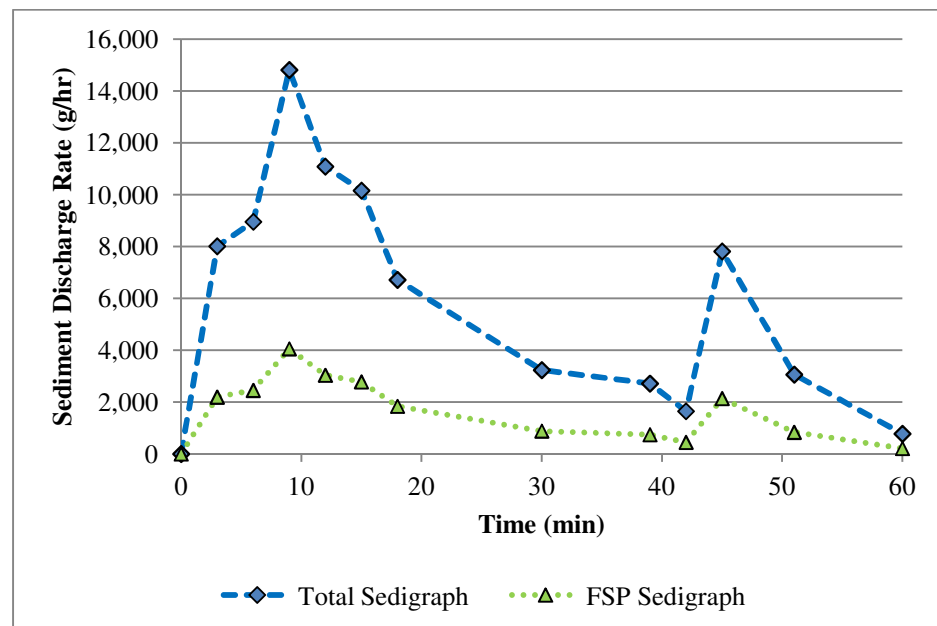


Figure 3.10. Sedigraph (RS 7-1)

### 3.5.3 Collected Dry Ravel

After each dry ravel collection period, the collected sediment was oven dried at 103 °C for at least 24 hours and then weighed to determine the total sediment mass. PSD analyses were performed on the collected dry ravel using sieve analyses and hydrometer methods to determine the percentage of FSP.

### 3.6 Selected Soil Erosion Models

Based on the literature review performed on various soil erosion prediction technologies discussed in Chapter 2, the following soil loss methods were considered the most suitable for estimating the quantity of sediment generated from highway cut and fill slopes within the Lake Tahoe Basin and selected for further evaluation in this study:

- Revised Universal Soil Loss Equation (RUSLE)
- Road Cut and Fill Slope Sediment Loading Assessment Tool (RCAT)
- Tahoe Basin Sediment Model (TBSM) by means of the Water Erosion Prediction Project (WEPP) methodology

These models were selected primarily by considering their applicability to estimating soil loss from uniform hill slopes (RUSLE, RCAT and TBSM), customization for the Tahoe Basin (RCAT and TBSM/WEPP), past use for estimating soil loss on NDOT projects in the Tahoe Basin (RUSLE), and the well-established, historical reliability and acceptance of the models (RUSLE and TBSM/WEPP).

### 3.7 Sensitivity Analysis of Soil Erosion Models

Sensitivity analysis provides a quantitative method for assessing the relative importance of each model input parameter on influencing model results (Nearing, Deer-Ascough, & Laflen, 1990). After evaluating numerous sensitivity indices, a simple index was used to evaluate the parameter sensitivity of each model based on the results of a sensitivity study performed by Pannell (1997), which reported that the sensitivity coefficient proposed by Hoffman & Gardner (1983) performed best. This normalized sensitivity index (SI) allows for parameter comparison between different models and is expressed by the following equation (Pannell, 1997):

$$SI = (O_{max} - O_{min})/O_{max} \quad \text{Equation 3.2}$$

where  $O_{max}$  = average annual soil loss (lb/ac/yr) when the evaluated parameter equals its maximum value

$O_{min}$  = average annual soil loss (lb/ac/yr) from the minimum parameter value

This one-at-a-time sensitivity analysis addresses parameter sensitivity while keeping all other parameters constant (Hamby, 1994). The following represent limitations to the selected sensitivity index (Nearing et al., 1990):

1. For non-linear response models, the linear structure of the sensitivity parameter limits the ability of the index to capture sensitivity variation over the entire range of the parameter.
2. The sensitivity parameter is univariate (varies one parameter-at-a-time), therefore, potential interactions between multiple parameters is not reflected.

### 3.7.1 Model Sensitivity Parameters

The base, minimum and maximum input parameters used for the sensitivity analysis of each model are summarized in Table 3.5. The parameter ranges specified reflect the realistic range of values for cut and fill slopes in the Lake Tahoe Basin. For example, soil erodibility factors ( $K$ ) on the Nevada side of the Lake Tahoe Basin range from 0.02 to 0.43 (USDA- NRCS, 2007); therefore, these values were used as the minimum and maximum, respectively. Due to significant differences in the hydrologic parameters required for each model (e.g., rainfall erosivity factor (RUSLE), average annual precipitation depth (RCAT) and sophisticated climate parameters (TBSM), described in Section 2.6), the sensitivity to climate parameters was not determined in this analysis. Therefore, the sensitivity analysis reflects the influence of site specific conditions on soil loss. The single climate parameter used for the sensitivity analysis represents the appropriate hydrologic parameter associated with the location near U.S. Highway 50 on the east shore of Lake Tahoe (39.10 degrees North, 119.90 degrees West). This location corresponds to the following climate parameters:

- RUSLE: rainfall erosivity factor ( $R$ ) = 48, determined using the NRCS RUSLE2 National Database (NRCS, 2008)
- RCAT: average annual precipitation depth = 29.8 inches, determined using the precipitation depth from Met Grid cell 1161 (PLRM, 2009)
- TBSM: created custom climate file generated by modifying the Marlette Lake, NV SNOTEL site climate file using data generated by PRISM for the specified location (Elliot et al., 2013)

All of the TBSM simulations were performed using the “bare” cover vegetation condition, as this treatment appeared most applicable to the sparsely covered slopes common in NDOT right-of-way. For the TBSM, the sensitivity to various cover conditions (riprap, vegetation, etc.) was evaluated by varying the percent total cover while using the “bare” cover vegetation treatment as the basis. The sensitivity to the various TBSM treatment/vegetation categories was not evaluated in this research.

Table 3.5. Erosion model parameters for sensitivity analyses

Model	Category	Parameter	Units	Base	Minimum	Maximum
RUSLE	Topographic	Slope	%	43	1	85
		Slope Length	ft	50	3	100
	Soil	Soil Erodibility Factor	unitless	0.23	0.02	0.43
	Cover	Canopy Cover	%	50	0	100
		Surface Cover	%	50	0	100
RCAT	Topographic	Slope	%	43	1	85
	Soil	Soil Type	unitless	Granitic	Granitic	Volcanic
		Cone Penetrometer DTR	in	14	1	27
	Cover	Total Cover	%	50	0	100
		Mulch and Litter Depth	in	5	0	10
TBSM	Topographic	Slope	%	50	1	100
		Slope Length	ft	50	3	100
	Soil	Soil Type	unitless	Volcanic	Granitic	Volcanic
		Rock in Soil	%	25	0	50
	Cover	Total Cover	%	50	0	100

### 3.8 Soil Erosion Modeling Approach

The evaluation of the various soil erosion models was performed by comparing the sediment yield (total and fine sediment) observed for each rainfall simulation to the estimated sediment yield, for these same slopes, using the various soil loss models. Since rainfall simulations were based on specific design storms, the models must be run based on single storm event inputs, rather than on an annual event basis. This was accomplished for the RCAT by using the procedure and example presented by Drake et al. (2010) for modeling the 20-year, 1-hour storm event. The TBSM only produces average annual sediment estimates; therefore, event-based TBSM modeling was performed through the full WEPP model downloaded from the USDA-ARS website, where event simulations could be evaluated. Tahoe-specific WEPP inputs from the TBSM interface were input into the full WEPP model. Although RUSLE typically predicts average annual erosion, event-based predictions are possible using the procedures for calculating

individual design storm rainfall erosivity values provided in various RUSLE handbooks (Galetovic et al., 1998; Renard et al., 1997).

The following section explains the model parameters used in the erosion prediction models and also describes specific modeling procedures and techniques (Drake et al., 2010) used to perform single-event predictions and generate soil loss estimates. The site-specific topographic and cover condition measurements used for model inputs are summarized in Table 3.2 and the site-specific soil measurements used for model inputs are summarized in Table 3.3.

### **3.8.1 Revised Universal Soil Loss Equation (RUSLE)**

Values of rainfall erosivity ( $R$ ) were calculated for each rainfall simulation using the measured rainfall data (intensity and applied rainfall depth) and the equations described in Section 2.6.1.1. The maximum 30-minute rainfall intensity ( $I_{30}$ ) used in *Equation 2.5* was set equal to the average intensity, since intensity was essentially uniform throughout each simulation.

This study evaluated two versions of the RUSLE to determine the predictive accuracy between erosion estimates using (1) the assigned soil erodibility ( $K$ ) values from the NRCS soil survey, referred to as RUSLE (KNRCS); and (2)  $K$  values determined from measured site-specific soils data (soil texture and organic matter, see Table 3.3) using the soil-erodibility nomograph/equation (*Equation 2.6*), referred to as RUSLE (KNOMO). The calculated site-specific soil erodibility values ( $K_{NOMO}$ ) used for the RUSLE site-specific model are shown in Table 3.6, located at the end of this section. Included in Table 3.6, for comparative purposes, are the  $K$  values ( $K_{NRCS}$ ) obtained from the NRCS soil survey used for the RUSLE (KNRCS) model predictions.

The topographic factors ( $LS$ ) were calculated based on the field measured data for each plot and the use of the equations described in Section 2.6.1.3. In calculating the slope-length factor ( $L$ ) for cut slopes, a high ratio of rill to interrill erosion was assumed due to the highly disturbed nature and significant slope steepness associated with the typical cut slopes tested in this research. For fill slopes, a high ratio of rill to interrill erosion was also assumed due to the unconsolidated state of the slope and vulnerability to rill erosion, despite the short run length.

The cover-management factor ( $C$ ) was determined for the rainfall simulation sites based on: (1) the observed percent cover (surface and canopy) and canopy height; (2) assumptions regarding the susceptibility of rill to interrill erosion, soil moisture conditions, and prior land-use; and (3) measured values from similar erosion studies performed in the Tahoe Basin. The surface cover ( $SC$ ) subfactor was calculated using *Equation 2.15*. The percent surface cover was determined from field measurements and the empirical coefficient ( $b$ ) of 0.050 was used to reflect highly disturbed soils where rilling is a dominant process. Surface roughness ( $R_u$ ) measurements were not performed in the field; however, values obtained from previous erosion studies in Lake Tahoe were used. In rainfall simulation studies performed by Grismer & Hogan (2004 and 2005) on Lake Tahoe cut slopes, surface roughness values for volcanic and granitic soils averaged approximately 0.39 inches, thus this value was used to model the slopes. The canopy cover ( $CC$ ) subfactor was calculated from percent canopy cover and fall height using *Equation 2.14*. The prior land use ( $PLU$ ) subfactor, which accounts for soil consolidation, was set equal to 0.8 for fill slopes and 0.5 for cut slopes, based on guidance provided by Galetovic et al. (1998). Typically, the  $PLU$  values are lower for cut slopes, as the soil is considered to be more consolidated and resistant to erosion. Conversely, for fill slopes, the soil has been loosened and the soil-aggregation size has been reduced, resulting in higher  $PLU$  values (Galetovic et al., 1998; Renard et al., 2010). The soil moisture ( $SM$ ) subfactor was set to 1.0 for all simulations based on guidance from Renard et al. (2010). Lastly, the support practice ( $P$ ) factor was set equal to 1.0 as no conservation treatments were applied at any of the sites.

RUSLE does not compute the particle size distribution of the runoff sediment; therefore, the percent FSP of the total soil loss was estimated based on a procedure discussed in the *PLRM Applications Guide* (PLRM, 2010a) to estimate FSP. This procedure references the particle size distribution data published in the Tahoe NRCS soil survey (NRCS, 2007) and estimates the percent FSP as the sum of one half of the sum of the percent silt (2 to 50 microns) and the percent clay (< 2 microns). For the evaluation of the KNOMO version of RUSLE, the percent FSP used for determining FSP yields was set equal to the FSP determined from PSD analyses of the bulk soil sample and shown in Table 3.3.

### 3.8.2 Road Cut and Fill Slope Sediment Loading Assessment Tool (RCAT)

As discussed in Section 2.6.5, the RCAT requires the following user inputs: area, precipitation depth, slope, soil type (granitic or volcanic), percent total cover, cone penetrometer DTR, and mulch/litter depth. The majority of these input parameters, with the exception of soil type and precipitation depth, were measured in the field, using the RCAT field assessment guidelines (Drake & McCullough, 2010), and directly inputted into the RCAT. The parent material of the soils used in the RCAT was determined using the designated soil map unit for the rainfall simulation site and the descriptions published in the Tahoe NRCS soil survey (NRCS, 2007). Soils described as “mixed” in the soil survey were inputted into the RCAT as volcanic, as these soils reflected mostly the characteristics of volcanic soils rather than granitic soils. The precipitation depth was determined by multiplying the measured average rainfall intensity by the duration of the rainfall simulation.

### 3.8.3 Tahoe Basin Sediment Model (TBSM)

The TBSM online interface estimates average annual runoff and erosion; however, single-event simulations were required for the purposes of evaluating the model. Therefore, the TBSM Tahoe-specific parameter databases were imported into the WEPP erosion model for event simulation predictions following the recommendations of W. J. Elliot and D. Traeumer (2014).

This study evaluated two versions of the TBSM/WEPP to determine the predictive accuracy between erosion estimates using: (1) the parent material/soil texture based soil parameters from the TBSM database, referred to as TBSM (PB); and (2) estimated soil parameters based on site-specific soils data, referred to as TBSM (SS). For the TBSM (PB) version, the selection of the appropriate soil texture from the TBSM database was based on the parent material information provided in the Tahoe NRCS soil survey (NRCS, 2007). The default value for percent rock in soil of 25 percent was used for all simulations for the TBSM (PB) version. For the TBSM (SS) version, effective hydraulic conductivity ( $K_e$ ), interrill erodibility ( $K_i$ ), rill erodibility ( $K_r$ ), and critical hydraulic shear stress ( $\tau_c$ ) were estimated based on the site-specific soils data (PSD and organic matter, see Table 3.3), and the use of equations described in Section 2.6.3.5. Since the cation exchange capacity ( $CEC$ ) of the soil samples was not determined, the default values from the TBSM database, dependent on the estimated soil parent material (e.g., 2.0 meq/100 g for granitic soils

and 7.0 meq/100 g for volcanic soils), were used in calculating the site-specific parameters. The calculated site-specific soil parameters used for the TBSM/WEPP site-specific model are summarized in Table 3.6. These empirically-calculated site-specific baseline values of  $K_e$ ,  $K_i$ ,  $K_r$ , and  $\tau_c$  were reduced internally during the WEPP simulation based on the percent rock in the soil input and the percent surface cover. The value for percent rock in soil for this version was based on the percent gravel values shown in Table 3.3. These calculated and measured values were used to modify the default values in the existing TBSM database for a particular soil texture in order to create a site-specific soils file for each rainfall simulation. For reference, the default  $K_e$ ,  $K_i$ ,  $K_r$ , and  $\tau_c$  values used for granitic and volcanic soils in the TBSM are listed in the footnotes of Table 3.6.

Slope gradient and horizontal slope length inputs were determined from field measurements for each site. Rainfall information was inputted using the single storm mode in WEPP, which required inputs of storm amount, storm duration, maximum intensity and percent duration to peak intensity. Maximum intensity was set equal to the average rainfall intensity of the site, since the intensity was essentially uniform over the duration of each simulation. The percent duration to peak intensity was set equal to 1 for all simulations to reflect that the peak intensity was achieved immediately upon the start of the simulation.

The vegetation/management files for each rainfall simulation were created in WEPP based on guidance from W. J. Elliot and D. Traeumer (2014). The TBSM “bare” management file was used as the basis for which modifications were made to fit the simulation site conditions. The following three cover values were modified in the WEPP/TBSM management file to represent the conditions of the site: (1) interrill, (2) rill and (3) canopy percent cover. These values were modified according to the observations from the site survey. Interrill and rill cover were set equal to each other and represented the ground surface cover at the site. This procedure is equivalent to changing the percent cover value in the TBSM online interface. All other plant/management parameters remained equal to the default values in the TBSM “bare” management file.

The percent of FSP was determined using the runoff sediment characteristics from the WEPP output text file and the methods presented in the TBSM User’s Manual for determining the fraction of delivered sediment finer than a specified particular particle size (Elliot et al., 2013).

Table 3.6. RUSLE and TBSM/WEPP site-specific soil parameters

Site ID	Rainfall Simulation ID	Soil Texture	RUSLE		TBSM/WEPP			
			$K_{NRCS}$	$K_{NOMO}$	$K_e$ (mm/hr)	$K_i$ (kg s m <sup>-4</sup> )	$K_r$ (s/m)	$\tau_c$ (Pa)
7	RS 7-1	Sandy loam	0.05	0.29	22.90	5.29E+06	0.00746	2.78
	RS 7-2	Sandy loam	0.05	0.24	26.67	4.89E+06	0.00646	2.74
8	RS 8-1	Loamy sand	0.05	0.30	27.45	7.00E+06	0.00886	1.59
	RS 8-2	Loamy sand	0.05	0.21	27.97	5.73E+06	0.00738	2.36
13	RS 13-1	Sandy loam	0.10	0.14	21.63	4.99E+06	0.00557	2.54
	RS 13-2	Sandy loam	0.10	0.03	23.46	5.86E+06	0.00687	2.31
14	RS 14-1	Sandy loam	0.10	0.31	14.11	3.95E+06	0.00427	3.08
	RS 14-2	Sandy loam	0.10	0.27	18.03	5.08E+06	0.00604	2.57
15	RS 15-1	Loamy sand	0.10	0.09	32.71	4.26E+06	0.01859	2.50
	RS 15-2	Loamy sand	0.10	0.08	33.10	4.99E+06	0.01290	2.31
16	RS 16-1	Loamy sand	0.10	0.10	29.57	5.86E+06	0.00801	2.29
	RS 16-2	Loamy sand	0.10	0.11	28.97	5.73E+06	0.01005	2.35
18	RS 18-1	Loamy sand	0.10	0.11	31.73	5.47E+06	0.02049	2.10
	RS 18-2	Loamy sand	0.10	0.10	31.35	5.10E+06	0.01998	2.36
20	RS 20-1	Sand	0.37	0.14	29.39	4.75E+06	0.01012	2.40
	RS 20-2	Sandy loam	0.37	0.17	23.06	5.77E+06	0.00936	2.58
22	RS 22-1	Sandy loam	0.37	0.30	19.95	4.88E+06	0.01830	2.51
	RS 22-2	Sandy loam	0.37	0.33	18.94	4.76E+06	0.01387	2.63
	RS 22-3	Sandy loam	0.37	0.26	19.01	4.36E+06	0.01055	3.03
25	RS 25-1	Loamy sand	0.17	0.15	31.16	5.83E+06	0.00681	2.21
	RS 25-2	Loamy sand	0.17	0.21	32.22	5.48E+06	0.01991	2.11
27	RS 27-1	Sandy loam	0.10	0.18	22.67	7.31E+06	0.00927	1.67
	RS 27-2	Sandy loam	0.10	0.31	16.31	6.84E+06	0.01018	2.11
28	RS 28-1	Loamy sand	0.05	0.03	32.29	5.50E+06	0.00912	2.33
	RS 28-2	Loamy sand	0.05	0.06	32.81	5.08E+06	0.00645	2.14

See Table 3.3 for site-specific soils data used to calculate soil parameters. See Section 2.6.1.2 and Section 2.6.3.5 for RUSLE and TBSM/WEPP soil parameter equations, respectively. The default values for  $K_e$ ,  $K_i$ ,  $K_r$ , and  $\tau_c$  used for the granitic and volcanic soil types in the TBSM are the following (Elliot et al., 2013): for granitic soil types ( $K_e = 25.0$  mm/hr,  $K_i = 3.0E+05$  kg s m<sup>-4</sup>,  $K_r = 0.001$  s/m, and  $\tau_c = 4.0$  Pa), for volcanic soil types ( $K_e = 20.0$  mm/hr,  $K_i = 7.5E+05$  kg s m<sup>-4</sup>,  $K_r = 0.008$  s/m, and  $\tau_c = 1.5$  Pa).

### 3.9 Statistical Analyses

This section describes the statistical methods used to (1) evaluate potential correlations between each of the rainfall simulation plot/dry ravel slope characteristics and the erosion and runoff parameters, and (2) assess the prediction accuracy of each soil erosion model.

#### 3.9.1 Regression Correlation Comparison Techniques

Linear and nonlinear regressions were used to statistically analyze the relationships between independent and dependent variables. This statistical analysis evaluated the correlation between the individual plot characteristics (independent variables) and the runoff/erosion parameters (dependent

variables). This evaluation of measured relationships was used to determine significant correlations and compare to the parameter sensitivity of the various erosion models described in Section 3.7. Parameters were considered to be significantly correlated if the p-value ( $p$ ) from the regression analyses was less than 0.05 (i.e. above the 95% confidence interval), thus indicating that the independent parameter is significant in changing the response of the dependent variable. The relative strength of the significant correlations was determined from the magnitude of the coefficient of determination ( $R^2$ ). Multivariate regression analyses were also used to evaluate the correlation between combinations of plot characteristics and runoff/erosion parameters. The results of the multivariate regression analyses were primarily used to compare and confirm the results of the single-factor regression analyses, as development of statistical predictive equations was beyond the scope of the project.

### 3.9.2 Model Evaluation Techniques

The model efficiency values were used to objectively compare the soil loss predictions from the RUSLE, TBSM and RCAT methodologies with the field measured soil losses determined from the rainfall simulations. The model efficiency ( $R^2_{eff}$ ) is defined as (Nash & Sutcliffe, 1970):

$$R^2_{eff} = 1 - \frac{\sum_{i=1}^n (Q_{mi} - Q_{ci})^2}{\sum_{i=1}^n (Q_{mi} - Q_m)^2} \quad \text{Equation 3.3}$$

where  $R^2_{eff}$  = efficiency of the model

$Q_{mi}$  = measured value of event  $i$

$Q_{ci}$  = model computed value of event  $i$

$Q_m$  = mean of the measured values

$R^2_{eff}$  compares the measured values to a 1:1 line representing a scenario where measured values equal model computed values. Nash-Sutcliffe model efficiency values can range from  $-\infty$  to 1, indicating the following: (1)  $R^2_{eff} = 1$  represents a relationship where predicted values match measured values perfectly; (2)  $R^2_{eff} = 0$  signifies that the mean value of the observed data is as accurate as the model predictions; and (3)  $R^2_{eff} < 0$  indicated that the measured mean is more accurate than the model predictions. Therefore, a  $R^2_{eff}$  closer to 1 suggests a model with more accurate predictions (Spaeth et al., 2003). The model efficiency value has been employed to evaluate numerous soil erosion models in previous studies, as discussed in Section 2.7.

Model predicted values were also evaluated to determine the percentage of values that fell within the 95% confidence intervals (*CI*) developed from replicated erosion plots. Soil erosion measurements are highly variable, even from replicated plots. Therefore, Laflen et al. (2004) used replicated erosion plots to establish the *CI* as a function of the measured erosion value. These *CI* values were used to evaluate whether model predictions fell within the typical percentile bounds observed from the field replicated plots. The reasoning behind this statistical approach was that an erosion model should not be expected to perform better than the measured variation between replicated plots. The confidence interval about a measured value is calculated by the following equation (Laflen et al., 2004):

$$CI_{95} = 1.43 M^{0.694} \quad \text{Equation 3.4}$$

where  $CI_{95}$  = 95% confidence interval (tons/ha)

$M$  = measured soil erosion (tons/ha)

The lower and upper bounds ( $LB$  and  $UB$ , in tons/ha) for the  $CI_{95}$  are determined by:

$$LB = M - CI_{95} \quad \text{Equation 3.5}$$

$$UB = M + CI_{95} \quad \text{Equation 3.6}$$

## Chapter 4

**RESULTS AND DISCUSSION****4.1 Overview**

This chapter summarizes the results of the model parameter sensitivity analyses, bulk soil PSD analyses, rainfall simulations, and dry ravel monitoring, as well as the statistical analyses used to identify significant correlations between the physical characteristics of the test sites and the measured runoff/erosion parameters. Additionally, the soil losses predicted by the RCAT, TBSM/WEPP, and RUSLE erosion models are compared to the measured soil losses from the rainfall simulations to assess model performance; limitations of these models and potential modifications to improve the predictive performance of each model are also discussed.

**4.2 Soil Erosion Model Sensitivity Analyses**

As described in Section 3.7, sensitivity analyses were performed on the various topographic, cover and soil parameters used in the soil loss models to determine the response of the dependent parameters (e.g., total and FSP soil losses) for each model using a sensitivity index (SI) presented by Hoffman & Gardner (1983). The results of the sensitivity analyses, organized by model parameter and sensitivity rank, are summarized in Table 4.1. Negative *SI* values indicated that an increase/decrease in the independent parameter caused the opposite trend to occur in the response parameter. However, when determining relative sensitivity, the absolute values of *SI* were considered; therefore, greater absolute *SI* values signified greater parameter sensitivity to the model outputs.

Table 4.1. Erosion model sensitivity analyses

Response Parameter	Rank	RCAT		TBSM		RUSLE	
		Independent Parameter	SI	Independent Parameter	SI	Independent Parameter	SI
Total Soil Loss	1	Slope	0.899	Surface Cover	-1.000	Surface Cover	-0.993
	2	Surface Cover	-0.803	Slope	1.000	Slope	0.983
	3	ML Depth	-0.803	Slope Length	0.953	Soil Erodibility	0.953
	4	CP DTR	-0.570	Rock in Soil	0.806	Slope Length	0.931
	5	Soil Type	0.207	Soil Type	0.100	Canopy Cover	-0.905
FSP Soil Loss	1	Slope	0.899	Surface Cover	-1.000	RUSLE does not predict FSP soil loss	
	2	Surface Cover	-0.875	Slope	1.000		
	3	ML Depth	-0.875	Slope Length	0.952		
	4	CP DTR	-0.570	Rock in Soil	0.805		
	5	Soil Type	0.547	Soil Type	0.747		

RCAT ML depth denotes the average mulch and litter depth

RCAT CP DTR denotes the average cone penetrometer depth to refusal

Surface cover and slope, the two most sensitive parameters in the TBSM and RUSLE models, were found to be nearly identical in their magnitude of significance. RCAT was found to be most sensitive to slope, followed by surface cover and mulch and litter depth, which had identical *SI* values. As shown in *Equation 2.32*, RCAT multiplies the mulch and litter depth by the percentage of surface cover to obtain a surface cover index which is used to determine the impacts of coverage on reducing erosion. The dependence of the RCAT model on mulch and litter coverage for sediment reduction presents a problem for riprap lined slopes and other cover treatments which do not include significant mulch and litter coverage. Riprap lined slopes are prevalent in the NDOT right-of-way and are considered to be quite effective in reducing erosion. Since RCAT does not consider riprap as a type of surface cover on these slopes, the RCAT surface cover index equals zero despite the significant surface coverage by the rock; therefore, riprap essentially receives little or no credit in reducing erosion on slopes. The various types of surface coverage (e.g., mulch, litter, rock, and vegetation) are considered relatively equal in effectiveness in both the RUSLE and the TBSM models, as surface cover is defined as any form of non-erodible cover protecting the ground surface (Renard et al., 1997).

Of the three models evaluated, the RCAT was the only model which does not incorporate the slope length into erosion predictions. The RCAT documentation states that RCAT predictions should be fairly accurate for slopes less than 3 meters (~10 feet) in length where rill formation is unlikely, but may under predict bare slopes where rilling commonly occurs (Drake & McCullough, 2010). The exclusion of slope length in the RCAT model may be a limitation, as many cut slopes, particularly within the NDOT right-of-way, exceed the 10 foot threshold for rill erodibility.

The cone penetrometer DTR was found to be a moderately significant parameter in influencing erosion results for the RCAT; however, the other two erosion models evaluated do not incorporate this as a parameter. The amount of infiltration and runoff experienced by the slopes in the TBSM and RUSLE is primarily dependent on the soil texture, organic matter content and/or the amount of rock in the soil.

As expected, the amount of FSP in the soil loss was found to be most dependent on soil type in both the RCAT and TBSM models, as noted by the significant change in the soil type parameter *SI* values

between the total soil loss and FSP soil loss results, while other parameters' *SI* values remained nearly constant.

#### 4.3 Evaluation of Bulk Soil Characteristics

The particle size distribution and texture of the soil were determined for each testing location (rainfall simulation and dry ravel monitoring sites) to estimate the availability of particle sizes for erosion, attempt to establish relationships between the bulk soil PSDs and the runoff and dry ravel PSDs, and compare site-specific soil characteristics to the characteristics reported in the NRCS soil survey. Generally, the soil texture classifications, determined using the USDA Textural Classification System described in Section 2.11.1, from the NRCS soil survey, matched the classifications determined from analyses of the site-specific soil samples, as shown in Table 3.3 and Table 3.4. The textures of soils from the granitic origin were typically sand or loamy sand, while the volcanic and mixed soils were predominantly sandy loam. However, five of the eight soil textures from the tested fill slope locations (RS 7-1 and 7-2, RS 20-1, and RS 28-1 and 28-2) were classified differently than the NRCS soil survey. This misclassification was likely due to the unknown origin of the fill materials (native or imported) and possibly the presence of pulverized road sand transported from the road surface. Although parent materials were used to group soils in past Tahoe erosion research (Grismer et al., 2008; Grismer & Hogan, 2004, 2005a, 2005b) and often used to categorize soil types in Tahoe-specific soil erosion models, the inclusion of "foreign" or mixed material found in fill slopes in this research complicates using the parent material and soil texture terms interchangeably for these types of slopes. Since nearly all the site-specific cut slope soil samples were classified similarly to the NRCS assigned soil texture, with the minor exception of DR 4 (loamy sand vs. sand), both soil texture and parent material were used to describe these "native" cut slopes.

Linear regressions were performed to determine the correlations between the estimated fractions of sand, silt, and clay from the NRCS soil survey and the corresponding site-specific fractions. Including both cut and fill slopes, all comparisons resulted in significant correlations ( $p$ -values ( $p$ ) < 0.01) with coefficients of determination ( $R^2$ ) ranging from 0.24 (clay) to 0.53 (sand and silt). When only cut slopes were considered, the correlation strengthened significantly as the  $R^2$  values increased by nearly 0.20 for all size fractions. As expected, the correlations for the fill slope soils were not significant. This statistical

comparison revealed that the NRCS soil survey estimated PSDs for the cut slope testing locations quite well. However, the insignificant correlations for the fill slope soils reflected the unique nature of fill slopes relative to cut slopes.

Table 4.2 summarizes the average bulk soil PSDs for all testing locations. Excluding the fill slope locations, the volcanic and mixed soils exhibited finer soil textures than the granitic soils, as denoted by the larger proportion of silt, clay, and FSP fractions. The average bulk soil FSP fractions were 10%, 15%, and 19% for the granitic, mixed, and volcanic cut slope soils, respectively. This observation supports the findings of Grismer & Hogan (2004, 2005a, 2005b) and Grismer et al. (2008), who reported that the bulk soil particle sizes of granitic soils were nearly twice the size of volcanic soils. The average FSP fractions for the fill slope locations ranged from 8% (sands and loamy sands) to 16% (sandy loams). As expected, the organic matter content in the soils was relatively small (< 3%) for most rainfall simulation sites (see Table 3.3 in Chapter 3), with the exception of the densely vegetated plots at site 13 (RS 13-1 and RS 13-2) and the riprap lined slope at site 25 (RS 25-1).

Table 4.2. Summary of bulk soil characteristics

Slope Type	Parent Material	Soil Texture	n	<sup>1</sup> Mean Particle Size Distribution, $\mu$ (%) (Std. Deviation, $\sigma$ )			
				Sand	Silt	Clay	FSP
Cut	Granitic	Sand and Loamy Sands	14	83 (4)	12 (4)	6 (2)	10 (3)
	Mixed	Sandy Loams	4	71 (7)	20 (6)	8 (2)	15 (3)
	Volcanic	Sandy Loams	7	66 (6)	24 (5)	10 (2)	19 (4)
Fill	-	Sand and Loamy Sands	5	87 (1)	8 (2)	5 (2)	8 (2)
	-	Sandy Loams	3	72 (5)	15 (4)	12 (1)	16 (1)

Soil characteristics determined from sieve analyses, hydrometer testing, and laser diffraction PSD analyses of collected erosion samples.

<sup>1</sup> FSP is % by mass of the raw sample, other fractions are % by mass of the < 2 mm component. The United States Department of Agriculture (USDA) Textural Classification System defines particle sizes as follows: sand (< 2 mm, > 0.05 mm), silt (> 0.002 mm, < 0.05 mm), and clay (< 0.002 mm).

#### 4.4 Rainfall Simulation Evaluation

The runoff hydrographs (see Figure 3.9) revealed that runoff at most sites was generated within the initial 3 minutes of the simulations followed by relatively steady-state runoff over the remaining duration of the simulations, which is considered typical of small-plot rainfall simulations performed on

disturbed areas (Copeland, 2009; Foltz et al., 2010, 2011). Additionally, the sedigraphs (see Figure 3.10) for most sites exhibited a peak sediment discharge rate followed by decreasing sediment discharge rates. This is also considered typical of disturbed areas where loose soil material at the surface is quickly transported by initial flows (Foltz et al., 2011).

Table 4.3 summarizes the runoff and erosion observed during the rainfall simulations. Additional details regarding testing locations, plot characteristics, bulk soil characteristics and rainfall simulation properties were described in Chapter 3.

Table 4.3. Summary of runoff and erosion measurements during rainfall simulations

RS ID	Slope Type	Soil Texture	Runoff Coefficient	Total Sediment (g)	Total Equivalent Soil Loss ( $\text{g m}^{-2} \text{mm}^{-1}$ )	Soil Loss FSP (%)	FSP (g)	FSP Equivalent Soil Loss ( $\text{g m}^{-2} \text{mm}^{-1}$ )
RS 7-1	Fill	Sandy loam	0.70	5,435	47.26	27	1,489	12.95
RS 7-2	Fill	Sandy loam	0.69	8,390	72.07	38	3,193	27.43
RS 8-1	Cut	Loamy sand	0.30	571	4.50	19	108	0.85
RS 8-2	Cut	Loamy sand	0.07	288	2.68	7	20	0.19
RS 13-1	Cut	Sandy loam	0.04	239	2.08	18	43	0.37
RS 13-2	Cut	Sandy loam	0.00	4	0.03	17	1	0.01
RS 14-1	Cut	Sandy loam	0.13	59	0.43	33	20	0.14
RS 14-2	Cut	Sandy loam	0.15	284	2.99	29	82	0.86
RS 15-1	Cut	Loamy sand	0.01	536	4.23	8	45	0.36
RS 15-2	Cut	Loamy sand	0.08	690	5.45	14	93	0.74
RS 16-1	Cut	Loamy sand	0.10	1,726	13.98	9	154	1.25
RS 16-2	Cut	Loamy sand	0.02	1,183	9.67	8	97	0.79
RS 18-1	Cut	Loamy sand	0.02	594	5.35	6	35	0.32
RS 18-2	Cut	Loamy sand	0.01	942	7.95	9	81	0.68
RS 20-1	Fill	Sand	0.21	1,816	14.67	19	350	2.83
RS 20-2	Fill	Sandy loam	0.05	864	7.54	12	107	0.94
RS 22-1	Cut	Sandy loam	0.73	17,163	131.18	33	5,749	43.94
RS 22-2	Cut	Sandy loam	0.37	3,030	22.91	26	797	6.02
RS 22-3	Cut	Sandy loam	0.50	4,307	31.56	31	1,347	9.87
RS 25-1	Cut	Loamy sand	0.01	13	0.11	9	1	0.01
RS 25-2	Cut	Loamy sand	0.00	366	3.14	6	21	0.18
RS 27-1	Cut	Sandy loam	0.15	828	5.45	20	169	1.11
RS 27-2	Cut	Sandy loam	0.27	82	0.59	37	30	0.22
RS 28-1	Fill	Loamy sand	0.66	1,354	10.87	26	354	2.85
RS 28-2	Fill	Loamy sand	0.43	1,149	9.93	19	213	1.84

Although at least two rainfall simulations were performed at each site, not all simulations at a site were necessarily replicated test plots. For instance, RS 25-1 and RS 25-2 were simulations performed on a riprap-lined slope and a relatively bare slope, respectively. These slopes were selected in an attempt to directly quantify the reduction in erosion achieved due to the riprap slope treatment, which resulted in a

96% reduction in total sediment and a 95% reduction in FSP. For replicated plots, the coefficient of variation (*CV*) was calculated to determine the spatial variability of runoff and soil loss between similar plots. The soil loss *CV* values were calculated using the soil loss per unit rainfall applied (“equivalent soil loss”), in order to normalize soil loss values for comparative purposes. Using linear regression techniques, the equivalent soil losses were compared to the actual collected soil masses, resulting in a significant correlation ( $p < 0.0001$ ,  $R^2 = 0.99$ ). Therefore, the two values essentially describe the same phenomenon, thus reflecting the low variability in applied rainfall intensity between the various rainfall simulations. The average *CV* values for the replicated plots were 57% and 44% for runoff and total soil loss, respectively. The total soil loss *CV* value was higher than the 20% to 36% reported by Foltz et al. (2011) in studying erosion from unpaved, forest access roads in the Tahoe Basin. However, the *CV* value for total soil loss was near the range of 45% to 49% predicted for erosion measurements from typical replicated rainfall simulation plots (Foltz et al., 2011; Laflen et al., 2004), thus revealing the high spatial variability associated with rainfall-runoff erosion measurements.

For general discussion purposes, Table 4.4 summarizes the averages, standard deviations, and ranges of measured runoff and erosion parameters for all rainfall simulations, organized by soil texture. As noted in some previous Tahoe erosion research (Grismer & Hogan, 2005a), the magnitude of runoff and erosion depends considerably on the soil characteristics of the hill slope. The slopes composed of sandy loams (primarily of volcanic descent) typically generated greater amounts of runoff and erosion than the slopes composed of sand and loamy sands (primarily of granitic descent). Additionally, as expected based on the bulk soil PSD analysis (see Section 4.3) and previous Tahoe erosion research (Grismer et al., 2008; Grismer & Hogan, 2005a), the slopes with sandy loams exhibited greater soil loss FSP fractions than the slopes with sand and loamy sands. The combination of higher mass erosion rates and soil loss FSP fractions associated with the sandy loams, resulted in significantly greater FSP sediment yields relative to the sand and loamy sands. This observation suggests that the volcanic and mixed soils (sandy loams) represent the most critical slopes, with regard to slope stabilization practices for NDOT in order to reduce FSP contributions into Lake Tahoe.

Table 4.4. Summary of runoff and erosion parameters for rainfall simulations

		Mean Measured Runoff and Erosion Parameters, $\mu$ (Std. Deviation, $\sigma$ ) (Range)			
Soil Texture	n	Runoff	Total	Soil Loss	FSP
		Coefficient	Equivalent Soil Loss ( $\text{g m}^{-2} \text{mm}^{-1}$ )	FSP (%)	Equivalent Soil Loss ( $\text{g m}^{-2} \text{mm}^{-1}$ )
Sand and Loamy Sands	13	0.15 (0.20) (0.00 - 0.66)	7.1 (4.5) (0.1 - 14.7)	12 (6) (6 - 26)	1.0 (1.0) (0.0 - 2.8)
Sandy Loams	12	0.32 (0.28) (0.01 - 0.73)	38.2 (39.9) (0.0 - 131.2)	27 (8) (12 - 38)	8.7 (13.8) (0.0 - 43.9)

The aforementioned comparisons group the simulation plots solely based on soil texture and neglect any influences that various physical characteristics of the simulation plots (e.g., slope and surface cover) may have had on runoff and erosion. The magnitude of erosion and runoff also depends on other site parameters, besides soil texture, as determined through regression correlation analyses and discussed in Subsections 4.4.1 and 4.4.2. However, the selection process for simulation plots was intended to encompass a broad spectrum of plot characteristics (e.g., soil textures, cut and fill slopes, slope gradients, percent cover and coverage types); therefore, the distribution of values in Table 4.4 provides basic comparisons and some estimates of the possible upper and lower limits of erosion and runoff which might be expected during a high intensity storm event.

The regression (linear and nonlinear) analyses presented in the following subsections will provide some insight into the significant correlations between the individual physical characteristics of the simulation plots (independent variables) and the runoff and erosion parameters (dependent variables) in a step-wise fashion. Multiple linear regressions were also used to evaluate the potential correlation between combinations of plot characteristics and the dependent runoff and erosion parameters. The multiple linear regressions were primarily used for comparing to the results of the single-factor regression analyses, as the development of statistical predictive equations was beyond the scope of the research. The dependent variables evaluated included runoff coefficient, percent soil loss of FSP, and equivalent total and FSP soil losses; the independent variables consisted of the soil type, topographic features, and cover characteristics measured at each rainfall simulation plot as described in Chapter 3. Parameters were considered to be significantly correlated if they were equal or greater to the 95% confidence level ( $p < 0.05$ ) in a regression

analysis. The relative strength of the significant correlations was determined from the magnitude of the coefficient of determination ( $R^2$ ).

Linear regression methods were also used to determine if there was any influence among multiple characteristics of the simulation plots simultaneously. These analyses revealed strong correlations between bulk soil organic matter and surface cover ( $R^2 = 0.47, p < 0.001$ ), particularly the amount of vegetation ( $R^2 = 0.32, p < 0.01$ ) and canopy cover ( $R^2 = 0.65, p < 0.001$ ) present at the simulation plots. In general, the organic matter content of the soil, determined using lab testing methods described in Section 3.5, increased as the amount of vegetative cover increased.

Additionally, correlations were observed between cone penetrometer DTR measurements and soil texture, as illustrated in Figure 4.1.

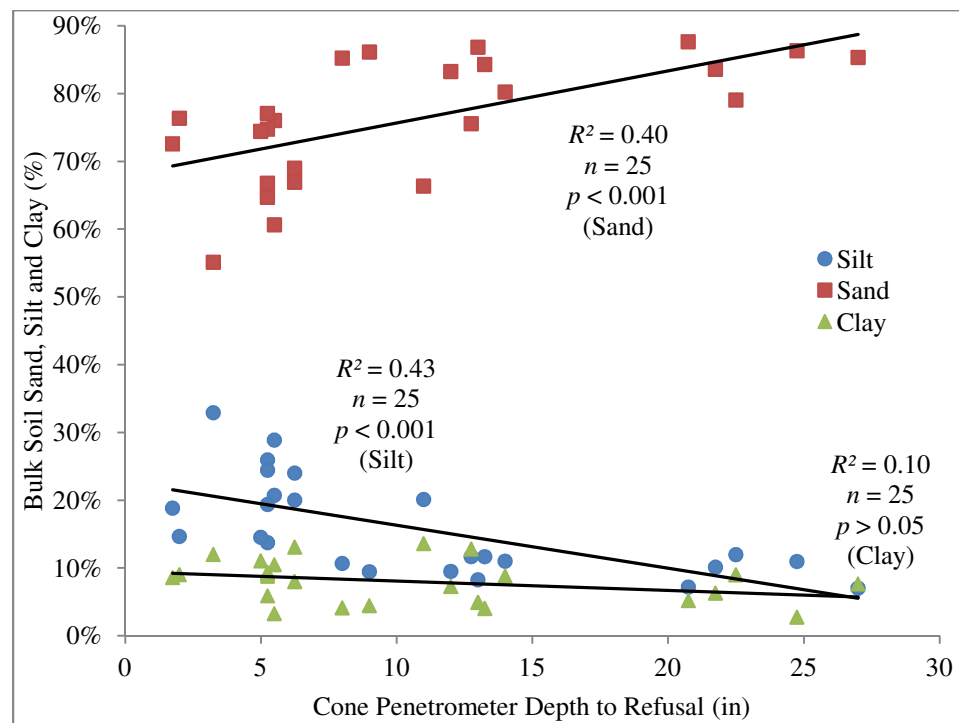


Figure 4.1. Variation of percent sand, silt and clay with cone penetrometer depth to refusal

The significant linear (sand and silt content) relationships suggested that the cone penetrometer may be an effective surrogate tool for rapidly assessing soil texture in the field, which could serve particularly useful in determining the soil texture of the imported material typically used in fill slopes, as discussed in Section 4.3. Measurements of cone penetrometer DTR for the sandy loam slopes ranged from 2 to 13 inches ( $n = 12, \mu = 6, \sigma = 3$ ), while the sand and loamy sand slopes varied from 5 to 27 inches ( $n = 13, \mu = 15, \sigma = 7$ ).

Therefore, the sandy loams revealed significantly less variation in cone penetrometer DTR measurements relative to the sand and loamy sand soil textures.

Vegetative cover and slope gradient were also significantly correlated ( $R^2 = 0.25$ ,  $p < 0.01$ ), as vegetative cover tended to decrease with increasing slope gradient. This observation is consistent with the difficulties associated with establishing vegetation on steep slopes, a widespread issue limiting revegetation efforts along the NDOT corridor within the Lake Tahoe Basin.

As mentioned previously, the primary focus of the research was to evaluate the effectiveness of the various soil erosion models for predicting soil losses for slopes having a wide variety of characteristics (e.g., cut and fill slopes, slope gradients, cover conditions, and soil types), thus leading to complexities when attempting to establish significant relationships and the need to segregate the full dataset into subgroups for meaningful statistical analyses. The fill slopes appeared to exhibit more noticeable variations in the measured runoff and erosion parameters, in comparison to the cut slopes. Therefore, correlation analyses that included both cut and fill slopes typically resulted in less significant correlations than the segregated groups including only cut slopes. Additionally, regression results for the fill slope dataset alone yielded virtually no significant correlations, likely a result of the minimal variation in physical plot characteristics between the tested fill slopes and the relatively small sample size (6 total rainfall simulations).

#### **4.4.1 Rainfall Simulation Runoff Assessment**

Soil moisture content was determined prior to each rainfall simulation to determine if antecedent moisture content potentially influenced the runoff and erosion results. These values ranged from 0.4 to 5.5 percent and a linear regression analysis revealed no correlation between antecedent soil moisture and the corresponding runoff coefficients. The runoff coefficients were determined by dividing the volume of runoff collected during the simulation, as determined from the runoff hydrographs described in Section 3.5.2, by the volume of rainfall applied to the simulation plot, as determined by multiplying the average rainfall intensity by the plot area and duration of the rainfall simulation. Most sites produced runoff coefficients within the range of 0 to 30 percent with the exception of the bare, extremely steep, sandy loam cut slopes at site 22 (RS 22-1, 22-2, and 22-3) and the moderately steep fill slopes at sites 7 (RS 7-1 and 7-

2) and 28 (RS 28-1 and 28-2). Based on visual observations during the rainfall simulations, these slopes appeared to experience soil crusting, defined as a condition when a soil develops a surface crust when initially exposed to rainfall, resulting in a drastic reduction in infiltration capacity (Abudi et al., 2012). This condition typically develops for soils with high silt content in semi-arid regions or on smoother surfaces (Abudi et al., 2012; Battany & Grismer, 2000b). The volcanic soils at site 22 possessed relatively high silt contents (> 20%), possibly contributing to soil crusting and the subsequent increase in runoff observed. Although surface roughness was not measured in the field, fill slopes would generally be expected to exhibit smoother slopes due to the constructed nature and high compaction levels generally associated with these slopes, possibly leading to the crust-forming response and requiring further consideration in future research. The linear relationship between the silt content of the bulk soil and the runoff coefficient, as shown in Figure 4.2, revealed the significant impact of soil texture on runoff and the unique runoff characteristics associated with the fill slopes.

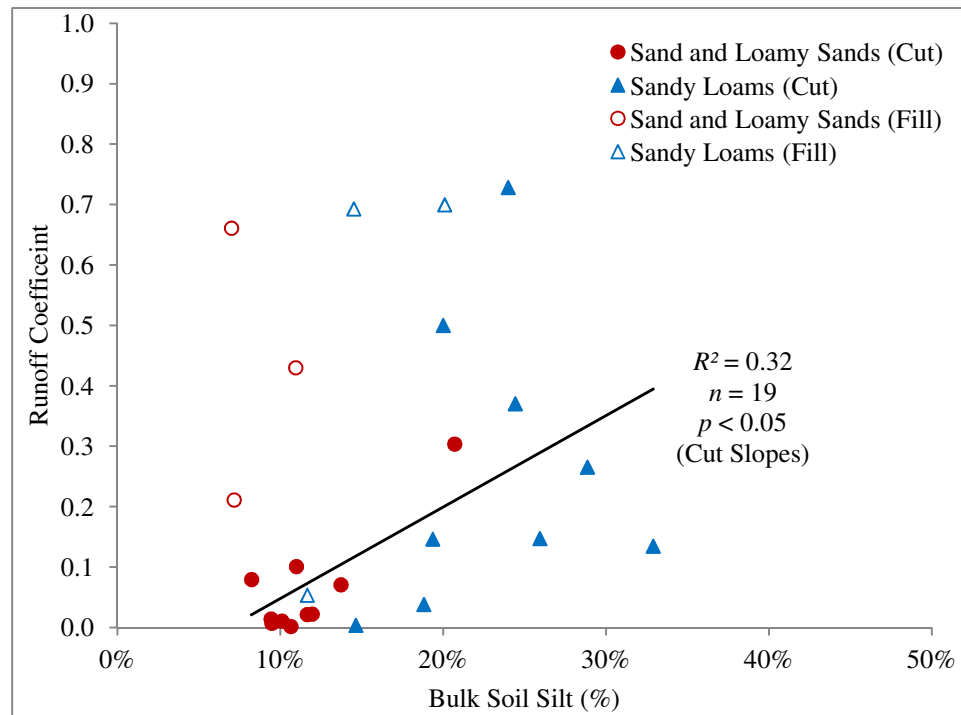


Figure 4.2. Variation of runoff coefficient with percent silt in bulk soil

As shown in Figure 4.2, the fill slopes, particularly for the sand and loamy sand soil textures, typically resulted in abnormally high runoff coefficients relative to the silt content of the soil, suggesting the influence of surface crusting for these slopes. By separating the cut and fill slope simulation sites, the influence of crusting was thought to be primarily confined to the fill slope locations. When considering only the cut slope dataset, significant correlations were observed between runoff and most of the bulk soil fractions (sand, silt and FSP); however, the silt fraction resulted in the most significant correlation, as runoff generally increased with increasing silt content (see Figure 4.2). Following further segregation of the cut slope dataset by soil texture, the strength of the correlation between percent silt and runoff increased by approximately 0.40 for the sand and loamy sand textures ( $R^2 = 0.73$ ,  $p < 0.01$ ). However, the sandy loams, interestingly, exhibited no significant correlations for this relationship, thus suggesting that other factors influence runoff for these soil textures.

For the sandy loam slopes, surface cover ( $R^2 = 0.51$ ), slope gradient ( $R^2 = 0.52$ , log-linear relationship), and organic matter content ( $R^2 = 0.75$ , log-linear relationship) resulted in more significant correlations with runoff, as the runoff coefficient increased with increasing slope and decreasing surface cover and organic matter content. Figure 4.3, Figure 4.4 and Figure 4.5 illustrate the relationship between the runoff coefficient and the surface cover, slope gradient and the organic matter content of the bulk soil, respectively, for the cut slope dataset.

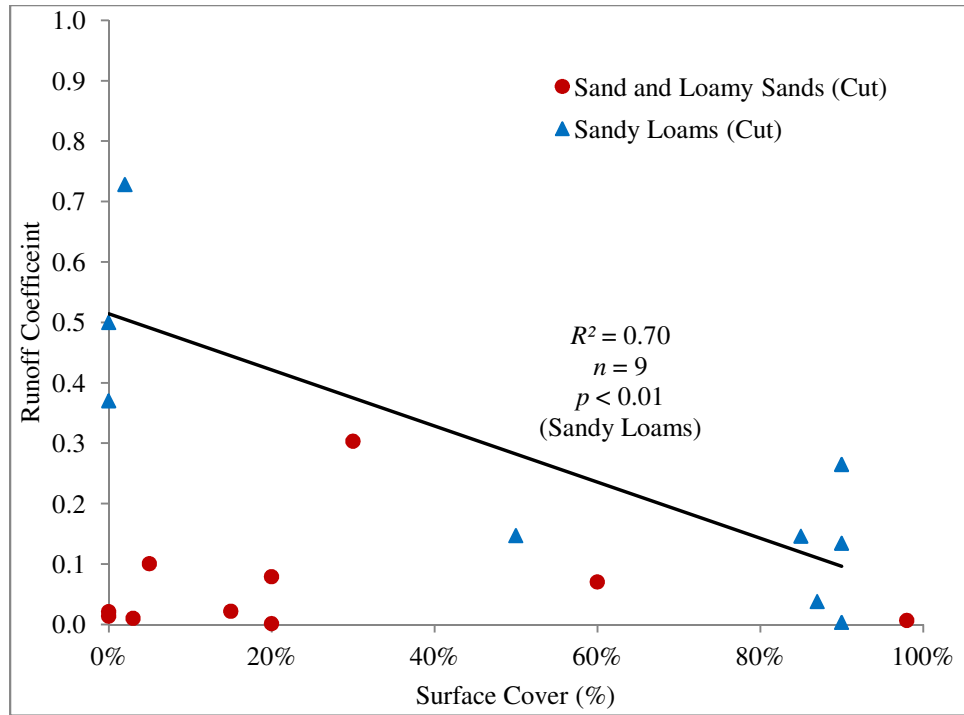


Figure 4.3. Variation of runoff coefficient with surface cover for cut slopes

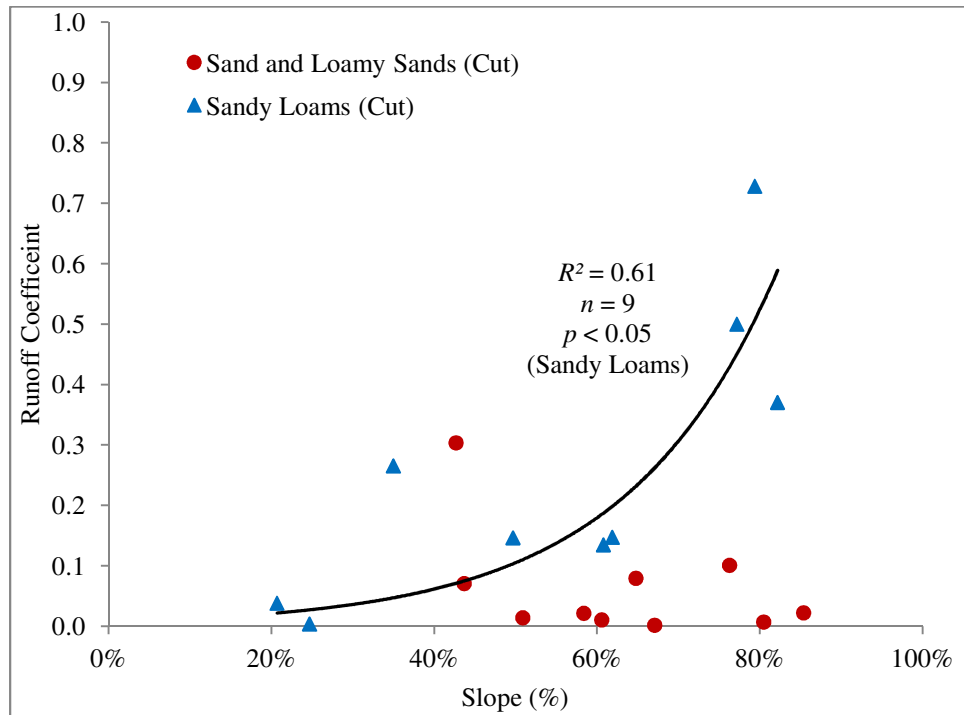


Figure 4.4. Variation of runoff coefficient with slope gradient for cut slopes

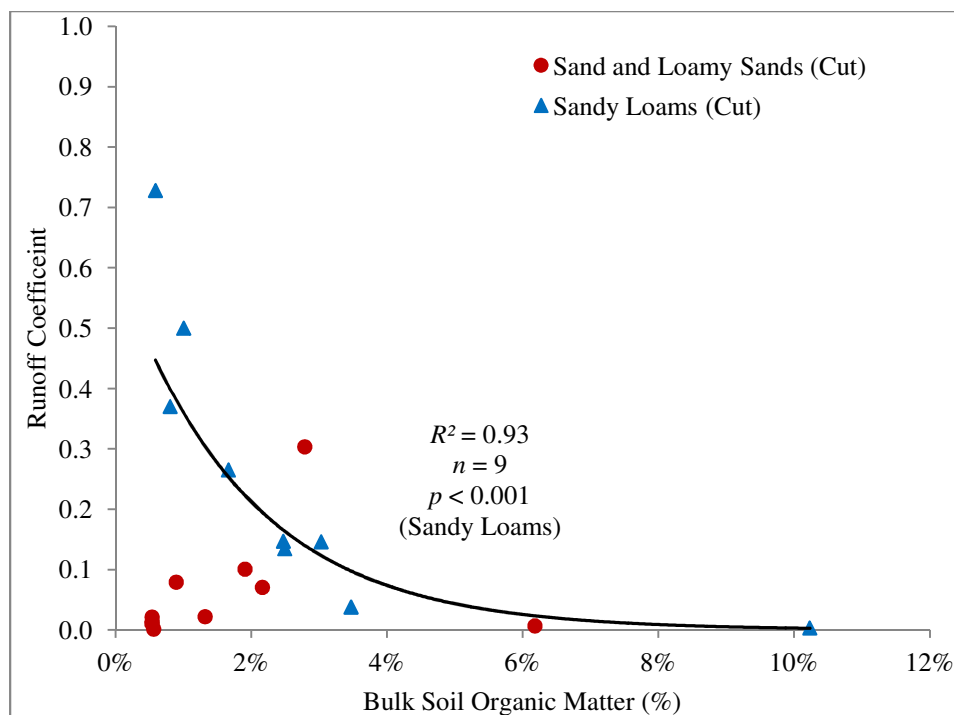


Figure 4.5. Variation of runoff coefficient with percent organic matter in bulk soil for cut slopes

As shown in Figure 4.3, Figure 4.4 and Figure 4.5, the regression coefficients for surface cover, organic matter content, and slope gradient increased by nearly 0.10 to 0.20 when considering only the sandy loam cut slope dataset, suggesting that other factors (e.g., surface roughness and compaction levels), similar to the sand and loamy sand fill slopes, influenced the runoff for the sandy loam fill slopes. Based on the significant relationships identified by regression analyses, runoff for the sandy loam cut slopes appeared to be most dependent on the organic matter content of the bulk soil, followed by the surface cover and slope gradient. Conversely, the runoff from the sand and loamy sand slopes appeared to be primarily soil texture dependent and relatively unaffected by surface cover, organic matter content, and slope gradient conditions, suggesting that the greater infiltration capacity associated with these soils, resulting from higher sand and lower silt and clay fractions, dominated the runoff process. In assessing bare cut slopes in the Tahoe Basin, Grismer et al. (2008) reported similar observations between granitic (sand and loamy sands) and volcanic (loamy sand) soils, finding that slope influenced runoff for volcanic soils, while granitic soils appeared unaffected by variations in slope gradient.

#### 4.4.2 Rainfall Simulation Erosion Assessment

In terms of erosion, increasing surface cover and organic matter content appeared to exert the greatest influence on reducing total soil loss when analyzing the entire dataset. These significant nonlinear correlations, based on the log transform of the total equivalent soil loss values, resulted in  $R^2$  values of 0.63 ( $p < 0.001$ ) and 0.56 ( $p < 0.001$ ) for the surface cover and organic matter content, respectively. Based on the coefficient of determination,  $R^2$ , the strength of the correlations increased by nearly 0.10-0.20 for surface cover (see Figure 4.6) and nearly 0.05 for organic matter content (see Figure 4.7) when segregating the dataset by soil texture, thus implying a dependence on soil texture.

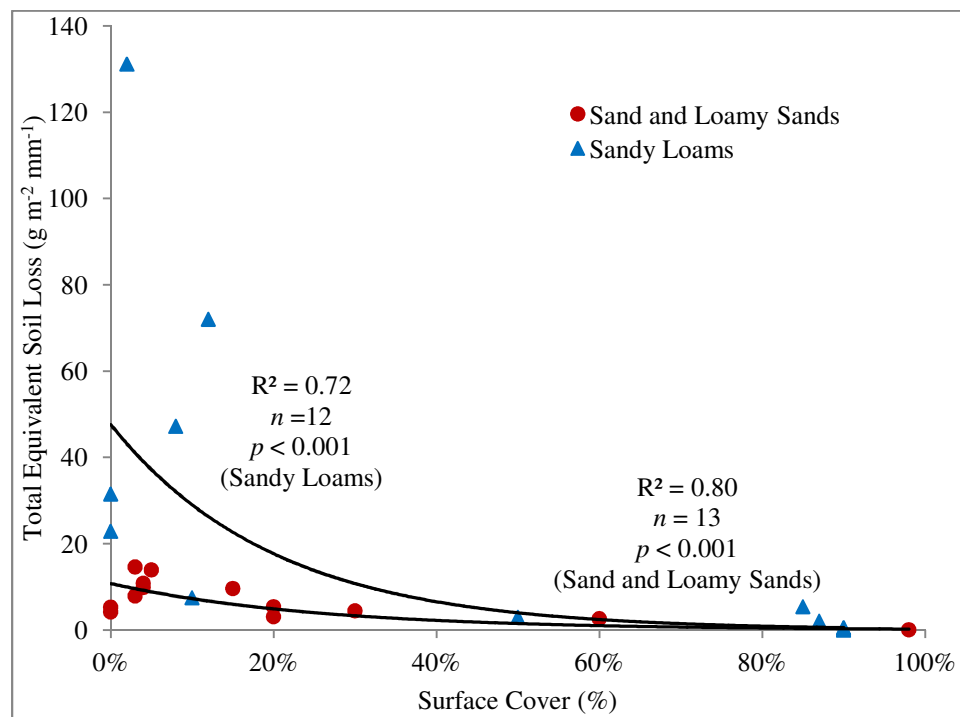


Figure 4.6. Variation of total equivalent soil loss with surface cover

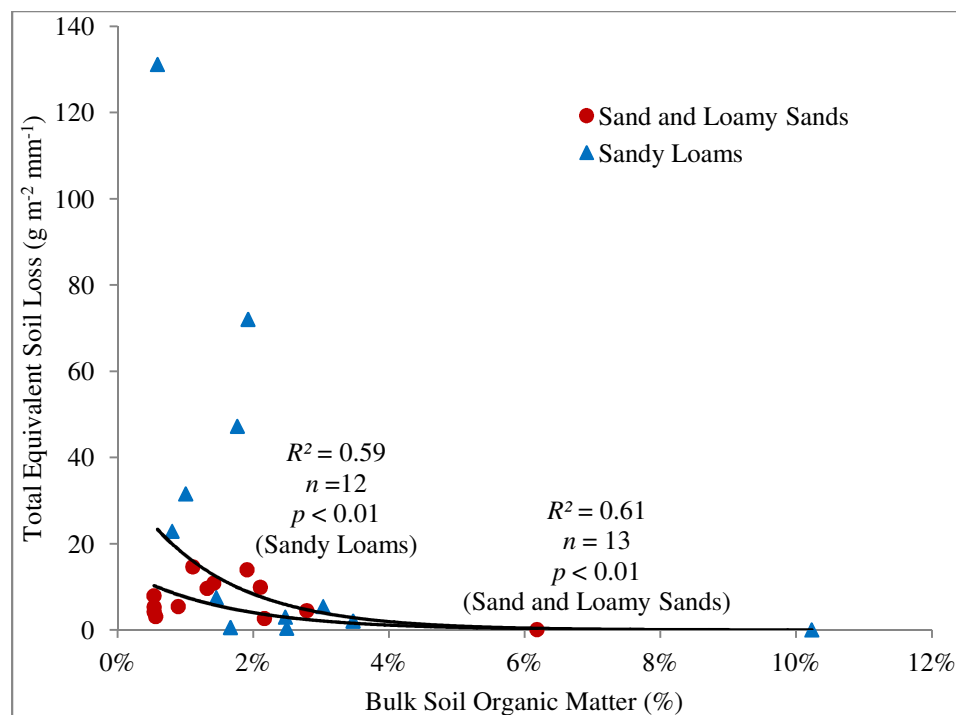


Figure 4.7. Variation of total equivalent soil loss with percent organic matter in bulk soil

Surface cover is generally considered the single most important factor in reducing erosion (Renard et al., 2010) and is typically designated as the most significant parameter in soil erosion models (see model sensitivity analysis in Section 4.2). Based on the nonlinear regression coefficients and exponents for the total equivalent soil loss versus surface cover analyses shown in Figure 4.6, the sandy loam slopes generated two to four times greater mass erosion than that from sand and loamy sand slopes. These findings support the observations reported by Grismer & Hogan (2005a, 2005b) where total sediment yields from volcanic slopes (sandy loams) were three to four times greater than granitic slopes (sand and loamy sands) for Tahoe Basin cut slopes of all treatment types. In general, soil losses for all soil textures significantly increased when surface cover was less than approximately 20%.

Additionally, soil organic matter content is a significant input in determining the soil erodibility parameters in both the RUSLE and TBSM/WEPP soil erosion prediction models (Renard et al., 1997; USDA-ARS, 1995b). The results of the rainfall simulations shown in Figure 4.7 suggest that as the bulk organic content of the soils tested exceeded about 2% or 3%, the observed soil losses declined notably. The significance of organic matter content on reducing erosion intuitively suggests that the presence of surface coverage due to mulch and litter further reduces erosion. The presence of mulch and litter typically

coincided with surface cover of any form, including riprap covered slopes, where mulch and litter usually accumulated in between void spaces in the riprap, therefore creating difficulties in determining which type of surface cover contributed greatest to erosion reductions. Based on linear and nonlinear regression techniques, the thickness of the mulch and litter layer yielded insignificant correlations with erosion, although this relationship warrants further assessment by focusing specifically on slopes covered with varying layer thicknesses of mulch and litter.

Although surface cover in direct contact with the ground surface is considered most effective in reducing erosion (Renard et al., 1997), canopy cover also appeared to reduce erosion, resulting in significant nonlinear correlations ( $R^2 = 0.30$ ,  $p < 0.01$ ) for the entire dataset. Canopy cover acts to dissipate some of the impact energy of raindrops prior to striking the ground surface (Renard et al., 2010). The presence of canopy cover at RS 13-2 further reduced erosion and runoff when compared to a similar slope (RS 13-1) devoid of canopy cover, resulting in a nearly 98% reduction in erosion and a 90% reduction in runoff. However, RS 13-2 also contained three times the amount of organic matter content of RS 13-1 (10% to 3%), likely a byproduct of the abundance of canopy directly above the plot surface. Therefore, considering the organic matter content disparity and the small sample size (only one of the simulations contained considerable canopy cover), the significance of this relationship warrants further assessment.

When considering the entire dataset, soil losses generally increased with increasing slope gradient; however, the strength of the nonlinear regression correlation proved relatively weak ( $R^2 = 0.17$ ,  $p < 0.05$ ) in comparison to the impacts of surface cover and organic matter content on reducing erosion. Based on the coefficient of determination,  $R^2$ , the strength of the correlations related to surface cover increased by nearly 0.10 after removing the fill slopes from the dataset. After further segregating the cut slope dataset by soil texture, the sandy loam cut slopes exhibited a significant correlation with slope gradient, as shown in Figure 4.8. In general, soil losses for sandy loams dramatically increased as slope gradient exceeded about 60%, which also corresponds to the typical angle of repose for non-cohesive soils (Coduto, 2001).

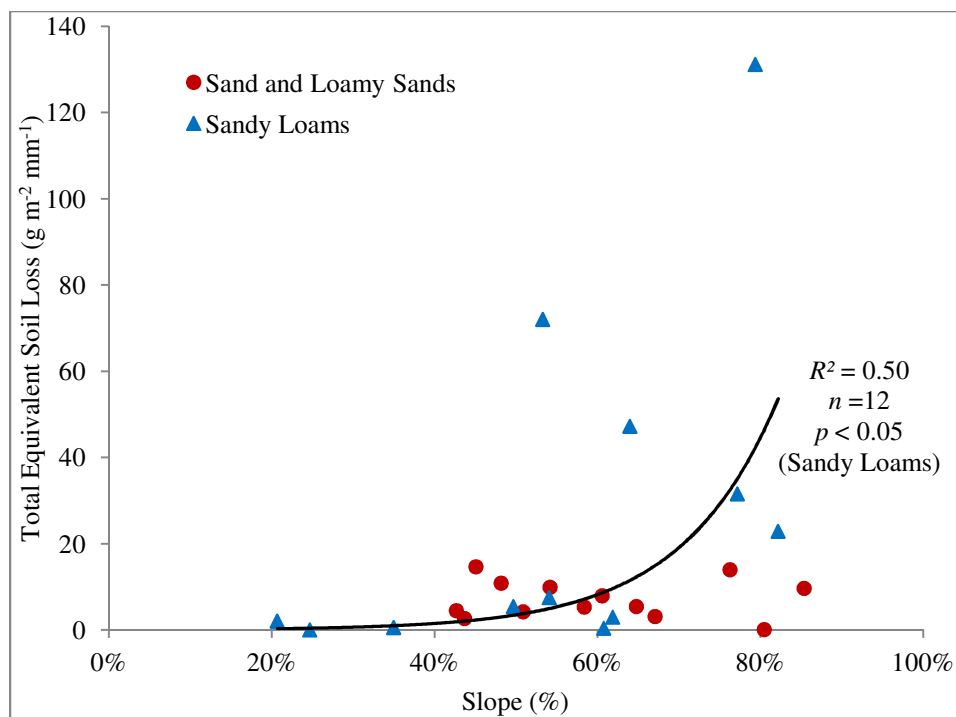


Figure 4.8. Variation of total equivalent soil loss with slope gradient

The sand and loamy sand slopes revealed no significant correlations between slope and total soil loss, perhaps suggesting that the higher sand content and increased infiltration capacity associated with these soil textures, as well as the influence of cover conditions, governs over any impacts from slope gradient.

#### 4.4.2.2 Rainfall Simulation FSP Erosion Assessment

In order to address the most critical aspect of this research and the primary focus of Tahoe Basin water quality improvement efforts, linear regression methods focused on identifying significant correlations between the independent parameters and the FSP fraction of the erosion and ultimately the magnitude of FSP mass erosion from highway cut and fill slopes. Using the 1:1 line to compare the percent FSP in the bulk soil samples to the percent FSP in the eroded soil, as shown in Figure 4.9, sands and loamy sands typically yielded lower FSP fractions than the bulk soil (with the exception of fill slopes), while sandy loams typically generated higher fractions of FSP in the eroded soil. Fill slopes with sand and loamy sand tended to produce greater ratios of soil loss FSP fractions to bulk soil FSP fractions when compared to the cut slope relationships.

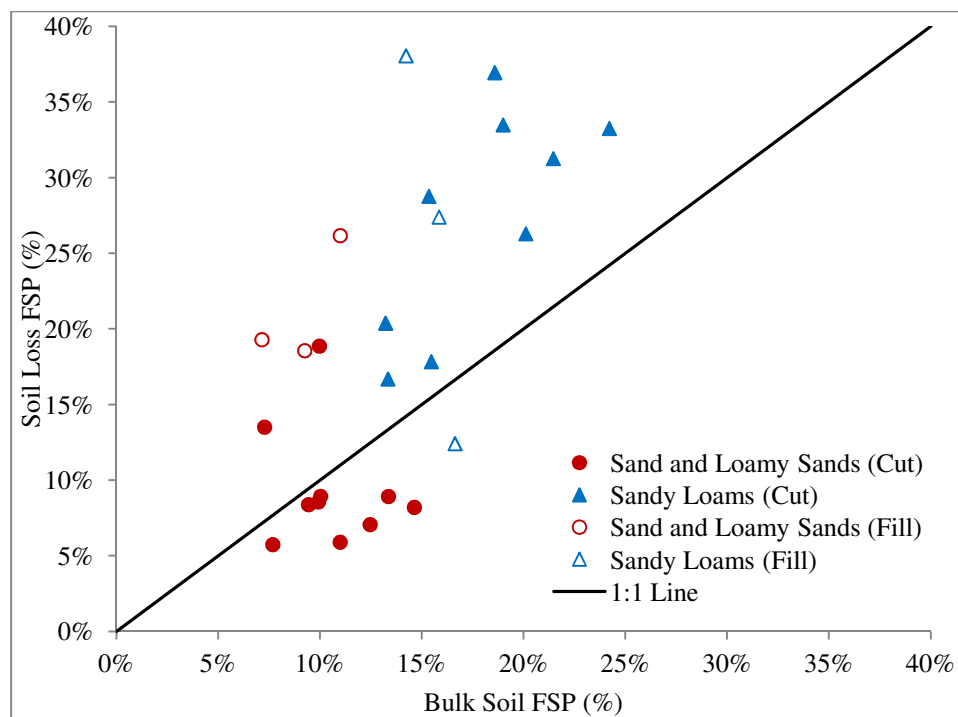


Figure 4.9. Variation of FSP in runoff with FSP in bulk soil

When considering the entire dataset, the percent FSP in the eroded soil was primarily dependent on soil texture, as expected, based on significant linear correlations ( $p < 0.05$ ) and relatively large coefficients of determination for the sand ( $R^2 = 0.52$ ), silt ( $R^2 = 0.48$ ), clay ( $R^2 = 0.26$ ), and FSP ( $R^2 = 0.42$ ) fractions of the bulk soil samples. The strength of the correlations significantly increased when only the cut slope dataset was considered, as  $R^2$  values increased between 0.10 and 0.35 for all size fractions, suggesting that other factors (e.g., surface roughness and soil compaction) may be influencing the runoff, erosion, and soil loss PSDs for the fill slopes, as mentioned previously. In particular, the silt fraction in the bulk soil for the cut slope dataset was significantly correlated ( $R^2 = 0.83$ ,  $p < 0.001$ ), as shown in Figure 4.10, suggesting that the silt content in the bulk soil represents the best predictor for determining the FSP content in the soil loss for cut slopes, even more so than the actual FSP content in the bulk soil. The variation in the soil loss FSP for the majority of the sand and loamy sand slopes was minimal, as most rainfall simulations for these slopes generated 6% to 10% soil loss FSP.

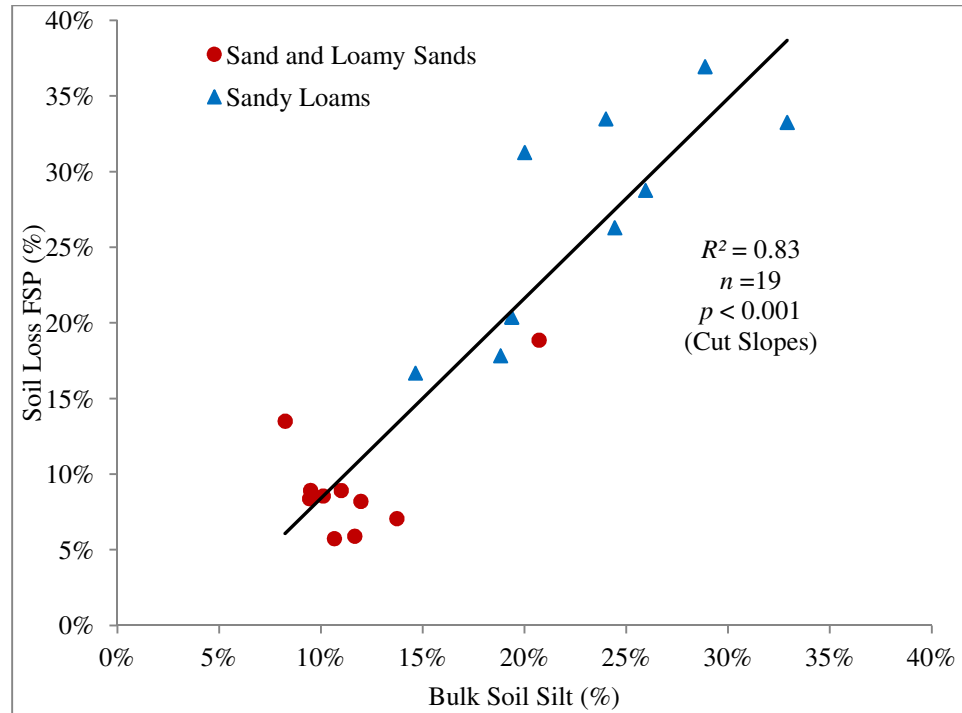


Figure 4.10. Variation of FSP in soil loss with silt content of bulk soil for cut slopes

Additionally, linear regression correlation analyses between the runoff coefficient and the percentage of FSP in the eroded soil resulted in a significant correlation between the two parameters ( $p < 0.0001$ ,  $R^2 = 0.55$ ) for all soil textures and slope types (cut and fill). Therefore, more runoff consistently yielded higher percentages of FSP. Figure 4.11 shows this correlation between the runoff coefficient and the percentage of soil loss FSP, including  $R^2$  and  $p$  values segregated by soil texture.

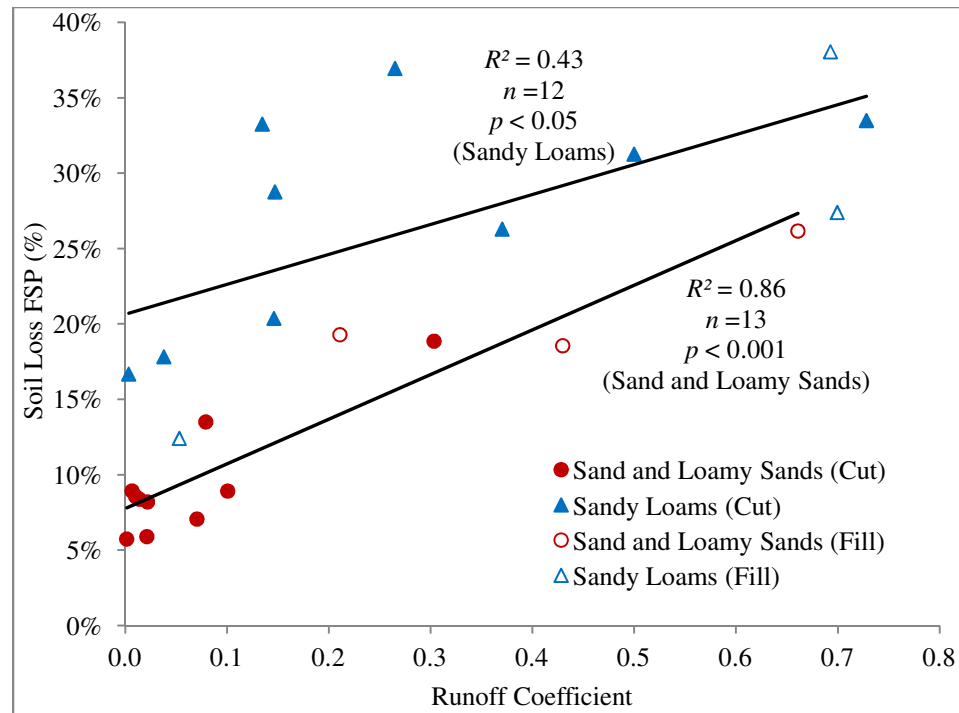


Figure 4.11. Variation of FSP in soil loss with runoff coefficient

The correlations shown in Figure 4.10 and Figure 4.11 imply that the FSP fraction in the soil loss not only depends on the availability of the fines in the bulk soil, but also on the magnitude of runoff and infiltration for a given soil type and soil condition (e.g., compaction and surface roughness). Soils with higher silt content typically exhibited increased erosion and runoff rates, likely due to the availability of easily mobilized fine sediment and the susceptibility to surface crusting (see Subsection 4.4.1). Conversely, soils with higher clay content exhibited increased resistance to detachment due to cohesive interparticle forces (Dennett, Sturm, Amirtharajah, & Mahmood, 1998). Furthermore, soils with higher sand content typically exhibited higher infiltration and lower runoff rates than soils with higher silt content (NRCS, 2003). This possibly explains why the ratio of the percent FSP in the bulk soil between the volcanic soils (sandy loams) and the granitic soils (sands and loamy sands) was nearly 2:1, while the soil loss FSP between the two parent material/soil textures was nearly 3:1 (see Table 4.4). In general, the volcanic soils possessed greater amounts of fine particles and also typically generated more erosive runoff than the granitic soils, primarily due to the lower sand and higher silt fractions, thus resulting in greater sediment transport of FSP.

The lack of significant correlations between soil loss FSP fraction and slope gradient, even for the bare cut slope dataset, differed from the findings reported by Grismer et al. (2008). That study,

summarized in Section 2.9, evaluated 17 bare plots with various soil types (granitic and volcanic) and slope gradients (15% to 55%). The authors reported significant correlations between slope gradient and soil loss PSDs for bare cut slopes in the Tahoe Basin, as steeper slopes tended to yield finer PSDs in the eroded soil.

Similar to the regression analysis for total soil loss, surface cover and organic matter content resulted in the most significant correlations with FSP soil loss, indicating that FSP soil losses decreased as both surface cover and organic matter content increased. For surface cover, the log transforms of the FSP soil loss values resulted in a nonlinear correlation with an  $R^2$  of 0.46 ( $p < 0.001$ ). As shown in Figure 4.12, the strength of the correlations increased when separating the dataset into subgroups based on soil texture. The results suggested that as surface cover exceeds about 20%, FSP soil losses were dramatically reduced. Considering the regression coefficient and exponents, the sandy loams (volcanic soils) yielded four to ten times greater FSP soil losses than the sand and loamy sands (granitic soils). This was a result of the greater mass erosion rates for the sandy loams, as well as the finer particle composition associated with these soils, relative to the sand and loamy sand soil texture.

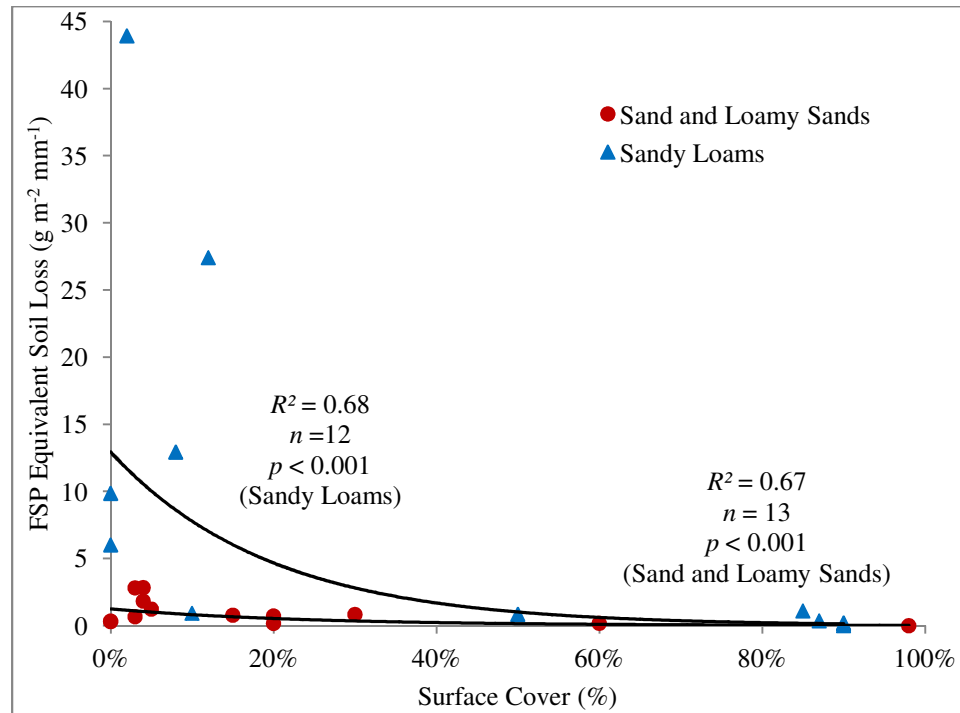


Figure 4.12. Variation of FSP in soil loss with surface cover

In conclusion, the FSP fraction in the eroded soil was found to be primarily dependent on soil texture. However, the overall amount of FSP was primarily dependent on surface cover with a lesser dependence on soil texture. Despite the higher erosion and runoff rates generally associated with the fill slopes, relative to the cut slopes, these slopes were thought to generally be less susceptible to sediment transport considerations and connectivity to Lake Tahoe. Fill slope runoff and erosion was typically a sheet flow phenomena which dispersed over natural terrain, while cut slope runoff/erosion usually concentrated in roadside conveyance drainage channels, ultimately leading to storm drains, culverts, and drainage ways that discharge into Lake Tahoe.

#### **4.4.3 Comparison of Results for Lake Tahoe Rainfall Simulation and Erosion Studies**

The total soil losses from the rainfall simulations were compared to erosion results from previous rainfall simulation-based erosion studies performed in the Tahoe Basin (see Section 2.9 for erosion study plot condition descriptions and Table 2.1 for simulated rainfall characteristics). The erosion studies used various plot sizes, rainfall intensities and simulation durations; therefore, reported soil loss values were adjusted for comparative purposes by dividing the total sediment yield (soil loss per unit area) by the applied rainfall depth to determine an “Equivalent Soil Loss”. This “normalization” procedure was similar to the method used by Battany & Grismer (2000b) to compare Napa Valley rainfall simulations to vineyard rainfall erosion studies in Europe. Table 4.5 summarizes the mean and range of equivalent soil loss values from past erosion studies.

Table 4.5. Comparison of erosion measurements from Lake Tahoe Basin erosion studies

Reference	Plot Condition	Soil Texture	Field Slope (%)	Mean Total Equivalent Soil Loss, $\mu$ (Range) ( $\text{g m}^{-2} \text{mm}^{-1}$ )
Munn (1974)	Bare and cover	Loamy sand and sandy loam	0 -60	10.2 (1.7 – 21.6)
Guerrant et al. (1991)	Bare and cover	Loamy sand	<15, 15-30, >30	15.2 (1.4 – 60.2)
Naslas et al. (1994)	Bare and cover	Loamy sand and sandy loam	<15, 15-30, >30	7.7 (0.1 – 22.0)
Grismer & Hogan (2004)	Bare and cover (cut slopes)	Sand, loamy sand and sandy loam	48 - 72	0.3 (0.0 – 1.7)
Grismer & Hogan (2005a)	Bare (cut slopes)	Sand, loamy sand and sandy loam	22 - 78	2.0 (0.0 – 6.2)
Grismer & Hogan (2005b)	Bare and cover (cut slopes)	Loamy sand and sandy loam	30 - 70	0.4 (0.0 – 4.5)
Foltz et al. (2010)	Bare (forest roads)	Sand and loamy sand	2 - 10	17.3 (8.1 – 27.5)
This Study	Bare and cover (cut and fill slopes)	Sand, loamy sand and sandy loam	21 - 85	16.7 (0.0 – 131.2)

The equivalent soil losses measured during this research ranged from 0.0 to 131.2  $\text{g m}^{-2} \text{mm}^{-1}$  ( $n = 25$ ,  $\mu = 16.7$ ,  $\sigma = 29.0$ ), resulting in a greater distribution of erosion measurements than those determined in previous erosion studies, particularly the upper limit of 131.2  $\text{g m}^{-2} \text{mm}^{-1}$ , which was approximately two times greater than the next highest value of 60.2  $\text{g m}^{-2} \text{mm}^{-1}$  reported by Guerrant et al. (1991). This large variability reflects the highly disturbed and erosive nature of the highway cut and fill slopes, as well as the wide range of slope gradients (21% – 85%), soil textures (sand, loamy sands and sandy loams), and cover conditions (0% – 98%), which were evaluated during this study. Other factors possibly leading to the difference in results include the following:

1. This erosion research employed a longer, unbounded plot length of > 4 feet, while other studies typically employed bounded plots with run lengths of less than 3 feet (see Table 2.1). The steep, bare nature of several of the tested slopes, in combination with slightly longer run lengths, potentially led to the development of rilling. Rill erosion is caused by small, concentrated ephemeral flow paths that may lead to significant amounts of erosion. Rill erosion typically develops on steep slopes with longer run lengths (> 15 feet). However, rill erosion is possible on extremely disturbed and steep slopes over shorter run lengths (Cerda, 1999; Renard et al., 1997).

Rilling appeared evident, particularly on the steep, bare slopes at test sites 7 and 22. Figure 4.13 shows evidence of rilling on a steep cut slope in the same vicinity along U.S. Highway 50 in the Lake Tahoe Basin after a summer thunderstorm event in August 2014.



Figure 4.13. Rilling of cut slope along U.S. Highway 50

2. The results from the previous erosion studies using rainfall simulations were not adjusted for differences in rainfall kinetic energy. This research used a rainfall kinetic energy of approximately  $25.1 \text{ J mm}^{-1}\text{-m}^{-2}$ , which equated to nearly 90% of the energy content of a typical high-intensity natural storm event (Laws & Parsons, 1943; van Dijk et al., 2002). The rainfall kinetic energies reported in comparable studies ranged from 30% to 70% of natural rainfall kinetic energy. The relationship between storm energy and the influence on soil erosion is well documented and, as discussed in Section 2.8.2, soil erosion is considered to be directly proportional to the total storm energy (van Dijk et al., 2002; Wischmeier & Smith, 1965, 1978).
3. The runoff apron used to collect sediment during the rainfall simulations collected both sediment entrained in the runoff, as well as sediment resulting from rainfall splash erosion. The latter is often neglected in other rainfall simulation-oriented erosion studies due to the presence of splash guards that prevent the mixture of splash and runoff erosion (Grismer & Hogan, 2004, 2005a, 2005b). Additionally, many of the previous erosion studies in the Lake Tahoe Basin did not

clarify whether sediment remaining on the runoff apron/trough after the end of the simulation was included in quantifying the amount of erosion from the plot. As mentioned previously, the sediment remaining on the runoff apron during this study was collected and included as eroded sediment regardless of whether the origin was interrill, rill, or splash erosion, as all forms contributed to erosion.

Despite the wide distribution of results, the average equivalent soil loss value, considering all rainfall simulations, equaled  $16.7 \text{ g m}^{-2} \text{ mm}^{-1}$ , which was within the typical ranges reported in other studies. The erosion studies by Grismer & Hogan (2004, 2005a, 2005b) were expected to be the most comparable of the rainfall simulation based erosion studies, as those research efforts focused solely on highly disturbed slopes (ski runs and roadway cut slopes) within the Tahoe Basin. However, the range of erosion results from those studies, including the results from the bare, steep cut slope dataset (Grismer & Hogan, 2005a), were significantly lower than comparable studies. The range of equivalent soil loss values from bare slopes ( $\leq 20\%$  surface cover) from the current research project ranged from 3.1 to  $131.2 \text{ g m}^{-2} \text{ mm}^{-1}$  ( $n = 16$ ,  $\mu = 24.9$ ,  $\sigma = 33.9$ ), which greatly exceeded the limits of the comparable study by Grismer & Hogan (2005a) shown in Table 4.5. Notably, the collected data from the erosion studies performed by Grismer & Hogan (2004, 2005a, 2005b) served as the primary dataset used for the development of statistical relationships used to predict sediment yields in both the RCAT and the TBSM (Drake et al., 2010; Elliot et al., 2013). Again, both of these models tended to under-predict the amount of soil losses compared to the predictions from the RUSLE model. This is discussed further in Section 4.6.

#### **4.5 Evaluation of Dry Ravel Monitoring**

Table 4.6 summarizes the results of the dry ravel monitoring, including the physical characteristics of the test plots (e.g., slope type, slope gradient, surface cover and soil texture), the collected sediment yields, and the percent FSP. Additional details regarding testing locations and bulk soil characteristics were described in Chapter 3. In an effort to distinguish contributions of erosion due to dry ravel from erosion due to rainfall-runoff, the reported sediment yields due to dry ravel only included the mass of sediment collected during dry periods, as determined from visual observations and hourly precipitation data

from nearby rain gages. The collection periods included in this analysis occurred between July 10, 2013 and August 15, 2013, a dry period of 36 days.

Table 4.6. Summary of dry ravel monitoring

DR ID	Slope Type	Soil Texture	Slope (%)	Total Surface Cover (%)	Mean Measured Dry Ravel Erosion Parameters, $\mu$ (Std. Deviation, $\sigma$ )		
					Total Sediment Yield ( $\text{kg m}^{-2} \text{ yr}^{-1}$ )	Dry Ravel FSP (%)	FSP Sediment Yield ( $\text{kg m}^{-2} \text{ yr}^{-1}$ )
DR 1	Cut	Loamy Sand	52	10	0.377 (0.279)	4	0.016 (0.011)
DR 2	Cut	Loamy Sand	32	50	0.029 (0.008)	8	0.002 (0.001)
DR 3	Cut	Loamy Sand	57	25	0.119 (0.131)	12	0.013 (0.016)
DR 4	Cut	Sand	61	15	0.193 (0.220)	4	0.007 (0.007)
DR 5	Fill	Sand	40	10	1.314 (0.064)	9	0.119 (0.006)
DR 6	Fill	Loamy Sand	77	85	0.110 (0.081)	3	0.002 (0.002)
DR 7	Cut	Sandy Loam	48	10	0.105 (0.080)	15	0.016 (0.012)
DR 8	Cut	Sandy Loam	83	15	32.432 (13.713)	11	3.567 (1.508)

As mentioned in Section 3.4.2, the sediment yields due to dry ravel were normalized for comparative purposes by dividing the collected mass by the contributing area of the hill slope, a procedure used in previous dry ravel studies (Anderson et al., 1959; Krammes, 1965; Lamb, Scheingross, Amidon, Swanson, & Limaye, 2011). General observations of the locations of the sediment traps used during dry ravel monitoring and the surrounding hill slopes revealed evidence of numerous dry ravel cones at the base of the hill slopes, as shown in Figure 4.14, particularly near the sediment traps located at DR 1, DR 4, and DR 8.



Figure 4.14. Dry ravel deposition cones along U.S. Highway 50

Additionally, on July 10, 2013, the installation date of dry ravel sediment trap DR 8, NDOT maintenance crews were observed cleaning out large amounts of sediment accumulation from roadside ditches near the site along US Highway 50 near Glenbrook, NV, presumably a result of the significant amounts of dry ravel along this corridor (see Figure 4.14).

Single and multiple linear regressions were performed to determine the most significant correlations between the physical characteristics of the slopes (independent parameters) and the dry ravel erosion parameters (dependent parameters). These analyses revealed that slope was the most highly correlated parameter ( $R^2 = 0.38$ ), although the correlation was not considered significant ( $p > 0.05$ ). When considering only the dataset for the cut slopes, the strength of the correlation between slope and total dry ravel yields increased ( $R^2 = 0.65$ ,  $p < 0.05$ ), thus suggesting that the unique structure of fill slopes (e.g., soil compaction and surface roughness), relative to cut slopes, influenced the dry ravel characteristics. It was hypothesized that the volcanic soils (loamy sands) may be less prone to dry ravel than the granitic soils (sands and loamy sands) due a slightly lower angle of repose and greater soil cohesion resulting from higher silt and clay content. However, there were no significant correlations between the bulk soil PSDs and the total dry ravel sediment yields, perhaps a result of the limited sample size; thus, the hypothesis was inconclusive.

In an effort to predict sediment yield contributions from dry ravel activities, the limited dataset ( $n = 8$ ) was used to parameterize the nonlinear slope-dependent dry ravel sediment transport equation presented by Gabet (2003) based on field measurements on sandy loam hill slopes in the semi-arid region near Santa Barbara, California. *Equation 2.1* was visually fit and parameterized using the field dataset, yielding values of  $0.025 \text{ kg m}^{-2} \text{ yr}^{-1}$  for  $\kappa$  and 0.83 for  $\mu$ . The use of this equation and the parameterized values to predict dry ravel sediment yields in the Tahoe Basin was limited to slopes with gradients less than or equal to 83% (39.7°). The parameterized equation was limited in that it is only slope dependent and did not consider the potential impacts of slope vegetation and soil type. Lamb et al. (2011) studied dry ravel in the San Gabriel Mountains and noted that vegetation can act as a dam, thus trapping loose sediment along a hill slope and reducing dry ravel yields. This predictive equation for dry ravel and the average values summarized in Table 4.6 reflect yields expected during dry summer months, not annual yield predictions.

Figure 4.15 illustrates the relationship between average dry ravel sediment yield and slope for the various sediment trap locations. The error bars represent the range of sediment yield values for different collection periods and the shaded region represents the critical angle of repose region for the sand, loamy sand, and sandy loam soil textures of the Tahoe Basin (Coduto, 2001; Gabet, 2003; Lamb et al., 2011). The line shown in Figure 4.15 represents the parameterized *Equation 2.1* presented by Gabet (2003). Due to the wide variability in dry ravel measurements, the data was plotted on log-log scale for viewing purposes.

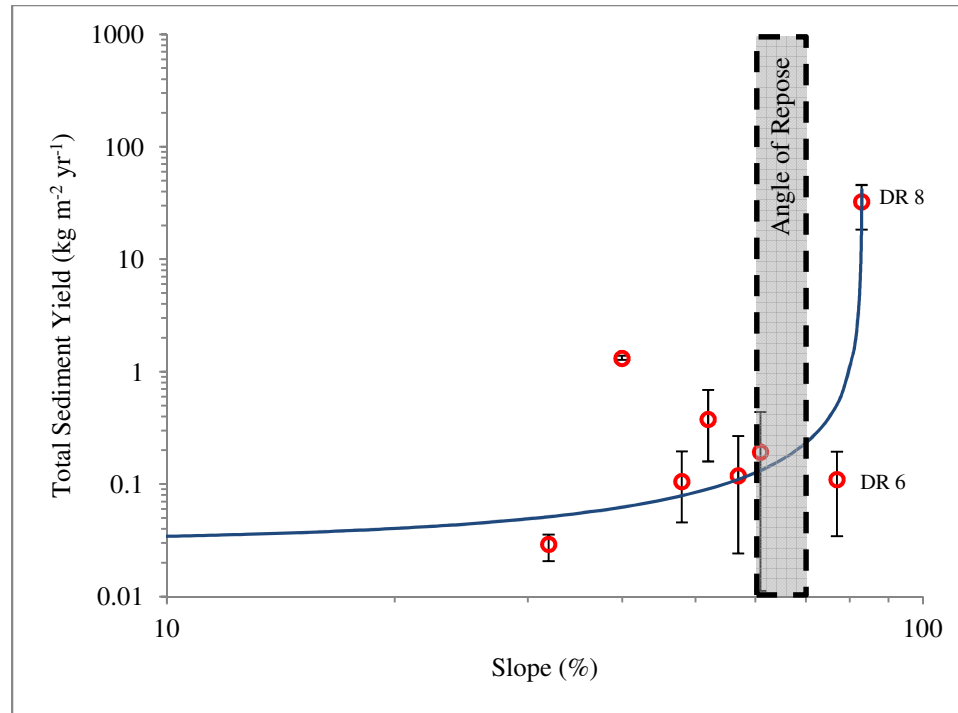


Figure 4.15. Variation of sediment yield from dry ravel with ground slope

An initial review of Figure 4.15 reveals high variability in the measured sediment yields, particularly for DR 8, which was significantly greater than the remainder of the measured values. However, previous dry ravel erosion studies in semi-arid regions noted similar drastic increases, resembling an exponential trend, in sediment yields originating from hill slopes with slopes exceeding 30° to 35° (60% to 70%), a threshold corresponding to the typical angle of repose for non-cohesive soils (Anderson et al., 1959; Gabet, 2003; Krammes, 1965; Lamb et al., 2011). The sediment trap at DR 6 was located at the base of a fill slope with a slope gradient that exceeded the angle of repose (see Figure 4.15). However, the compacted nature of the fill slopes and significant coverage by pine needle litter (estimated 85% slope coverage) potentially resulted in the low dry ravel yields, despite the significant steepness of the slope.

The average FSP fractions of the collected dry ravel were 7% ( $\sigma = 4\%$ ) for the granitic soils (sand and loamy sands) and 13% ( $\sigma = 3\%$ ) for the volcanic soils (sandy loams), respectively. This nearly 2:1 FSP fraction ratio between the volcanic and the granitic soils corresponded with the relationships observed in the bulk soil sample PSD analyses discussed in Section 4.3. When comparing the percentage of FSP collected in the dry ravel samples to the percentage of FSP collected in the bulk soil samples, as shown in Figure 4.16, there appeared to be a correlation as most values were near the 1:1 slope line; this suggested that the PSD of the bulk soil was similar to that collected from dry ravel sediment traps. The most significant deviation from this trend was DR 8, which was also the steepest slope tested, perhaps suggesting that larger sediment and rock fragments are more vulnerable to transport as dry ravel on steep slopes than finer sediment particles due to gravitational forces.

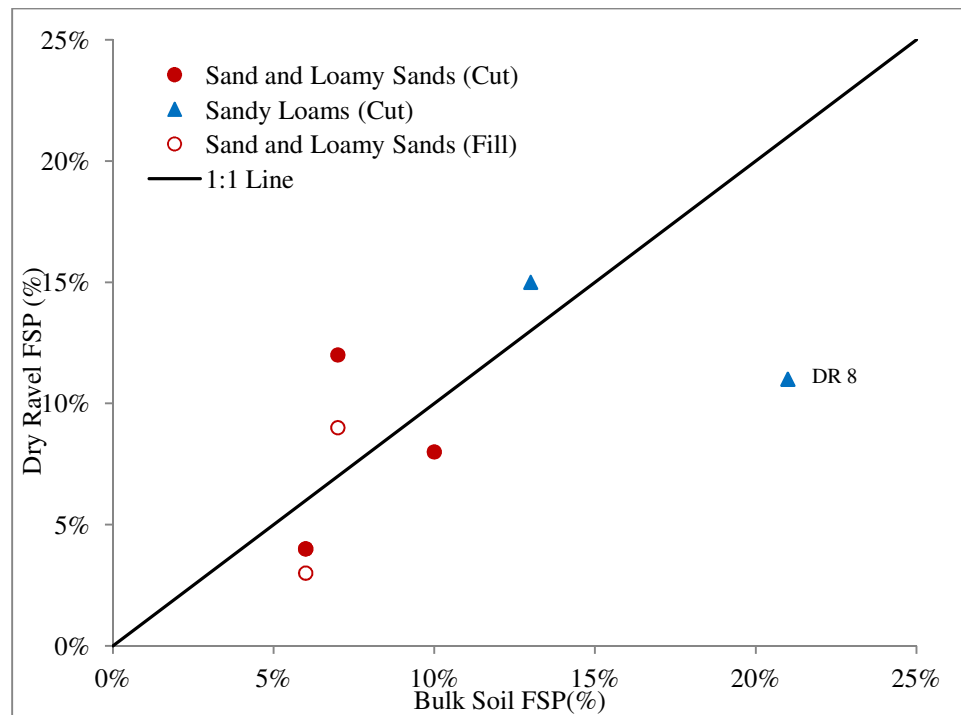


Figure 4.16. Variation of FSP in the collected dry ravel with FSP in bulk soil

As expected, the ratio of the FSP fraction of the dry ravel and the FSP fraction of the bulk soil (nearly 1:1, see Figure 4.16), was different than the ratio of the FSP fraction of the rainfall simulation erosion and the FSP fraction of the bulk soil (1:5:1, see Figure 4.9), thus reflecting the nature of the rainfall and runoff to detach and transport a greater proportion of the finer sediment.

#### 4.6 Soil Erosion Model Performance and Potential Improvements

The overall performance of each of the selected soil erosion models was assessed using: (1) the Nash-Sutcliffe model efficiency ( $R^2_{eff}$ ); and (2) the lower and upper bounds ( $LB$  and  $UB$ ) of the 95 percent confidence interval ( $CI$ ) about the measured erosion values. The  $R^2_{eff}$  values may range from  $-\infty$  to 1.0. An  $R^2_{eff}$  value of 1 describes a model that perfectly matched the observed data, a value of 0.0 indicates that the mean of the observed values were predicted as well as the model, while a value below 0.0 suggests that the mean of the observed value was a better predictor than the model (Nash & Sutcliffe, 1970; Spaeth et al., 2003). The model efficiency value has been employed to evaluate numerous soil erosion models in previous studies, particularly the WEPP and RUSLE models (Laflen, Flanagan, & Engel, 2004; Larsen & MacDonald, 2007; Spaeth et al., 2003; Tiwari et al., 2000). Considering the high spatial variability associated with soil erosion, Laflen et al. (2004) used replicated erosion plots to establish the  $CI$  as a function of the observed erosion. These  $CI$  values were used to evaluate whether model predictions fell within the typical percentile bounds observed from the field replicated plots. Further explanation of these statistical model evaluation tools was described in Section 3.9.2.

As mentioned in Section 3.8, the RUSLE and TBSM/WEPP models were evaluated using two scenarios. The first scenario used the soils data obtained from the NRCS soil survey database, “RUSLE (KNRCS)”, and the default parameters for the parent material/soil texture- obtained from the TBSM Tahoe database, “TBSM (PB)”, to estimate soil loss. The second scenario used site-specific soil properties (PSDs, organic matter content) to calculate site-specific soils parameters using empirical equations, to predict soil loss within the RUSLE, “RUSLE (KNOMO)”, and the TBSM/WEPP, “TBSM (SS)” models. Soil parameter equations, based on site-specific soil properties, were not provided in the RCAT documentation; therefore, only one version of the RCAT was evaluated.

Table 4.7 summarizes the results of the model predictions and comparisons to the observed values, as well as highlights the models which most accurately estimated soil losses (total and FSP) for each rainfall simulation. Figure 4.17 and Figure 4.18 illustrate the predicted total and FSP soil losses, respectively, for each rainfall simulation versus the observed values. Due to the large range of observed and predicted values, the values were plotted on a log-log scale to better display the results.

Table 4.7. Summary of observed and predicted soil loss from rainfall simulation plots

Rainfall Simulation ID	Observed Total Soil Loss (g)	Observed FSP Soil Loss (g)	<sup>1</sup> Predicted Total Soil Loss (g)					<sup>2</sup> Predicted FSP Soil Loss (g)				
			RCAT	TBSM (PB)	TBSM (SS)	RUSLE (KNRCS)	RUSLE (KNOMO)	RCAT	TBSM (PB)	TBSM (SS)	RUSLE (KNRCS)	RUSLE (KNOMO)
RS 7-1	5,435	1,489	16	227	956	666	<b>3,928</b>	6	9	229	70	<b>623</b>
RS 7-2	8,390	3,193	20	177	573	525	<b>2,482</b>	7	7	122	55	<b>353</b>
RS 8-1	571	108	15	41	<b>364</b>	157	932	5	2	16	16	<b>93</b>
RS 8-2	288	20	13	3	78	25	<b>108</b>	4	1	<b>22</b>	3	13
RS 13-1	239	43	22	21	<b>90</b>	12	16	12	5	<b>26</b>	2	2
RS 13-2	4	1	20	13	79	<b>6</b>	<b>2</b>	11	3	23	<b>1</b>	<b>1</b>
RS 14-1	59	20	70	<b>51</b>	160	25	78	32	11	50	6	<b>19</b>
RS 14-2	284	82	70	79	101	80	<b>212</b>	32	15	23	20	<b>33</b>
RS 15-1	536	45	13	284	<b>605</b>	1,446	1,318	5	12	<b>63</b>	108	124
RS 15-2	690	93	17	201	<b>757</b>	621	486	6	8	<b>75</b>	47	35
RS 16-1	1,726	154	31	381	930	<b>1,306</b>	1,281	11	15	<b>170</b>	98	171
RS 16-2	1,183	97	31	300	631	829	<b>916</b>	11	12	<b>119</b>	62	134
RS 18-1	594	35	15	254	<b>563</b>	1,185	1,352	5	<b>10</b>	61	89	149
RS 18-2	942	81	16	294	<b>714</b>	1,192	1,246	6	12	96	<b>89</b>	124
RS 20-1	1,816	350	12	578	868	6,242	<b>2,380</b>	5	105	89	1,401	<b>170</b>
RS 20-2	864	107	16	542	<b>839</b>	4,196	1,900	7	<b>96</b>	192	942	316
RS 22-1	17,163	5,749	207	878	1,101	<b>6,389</b>	5,181	93	152	197	<b>1,434</b>	971
RS 22-2	3,030	797	209	932	<b>1,048</b>	7,291	6,454	94	162	212	1,637	<b>1,299</b>
RS 22-3	4,307	1,347	216	973	1,176	7,571	<b>5,256</b>	97	170	288	1,700	<b>1,128</b>
RS 25-1	13	1	29	<b>4</b>	78	23	<b>21</b>	10	<b>1</b>	18	2	2
RS 25-2	366	21	43	<b>170</b>	602	910	1,105	<b>15</b>	7	55	67	85
RS 27-1	828	169	76	68	<b>265</b>	35	61	34	15	<b>56</b>	5	8
RS 27-2	82	30	31	39	251	19	<b>59</b>	<b>14</b>	9	71	3	11
RS 28-1	1,354	354	13	236	631	<b>841</b>	478	4	10	<b>106</b>	48	53
RS 28-2	1,149	213	12	193	400	747	<b>883</b>	4	8	38	42	<b>82</b>

<sup>1</sup> Bold values indicate that the model column best predicted total soil loss for the corresponding rainfall simulation

<sup>2</sup> Bold values indicate that the model column best predicted FSP soil loss for the corresponding rainfall simulation

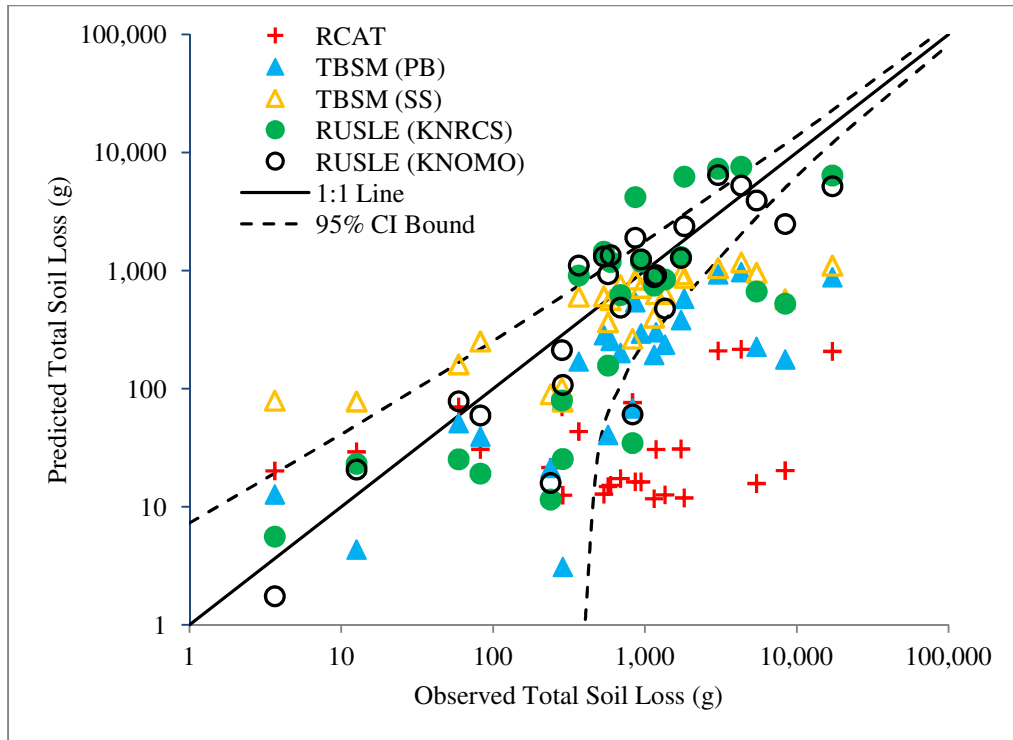


Figure 4.17. Comparison of predicted total soil losses with observed total soil losses

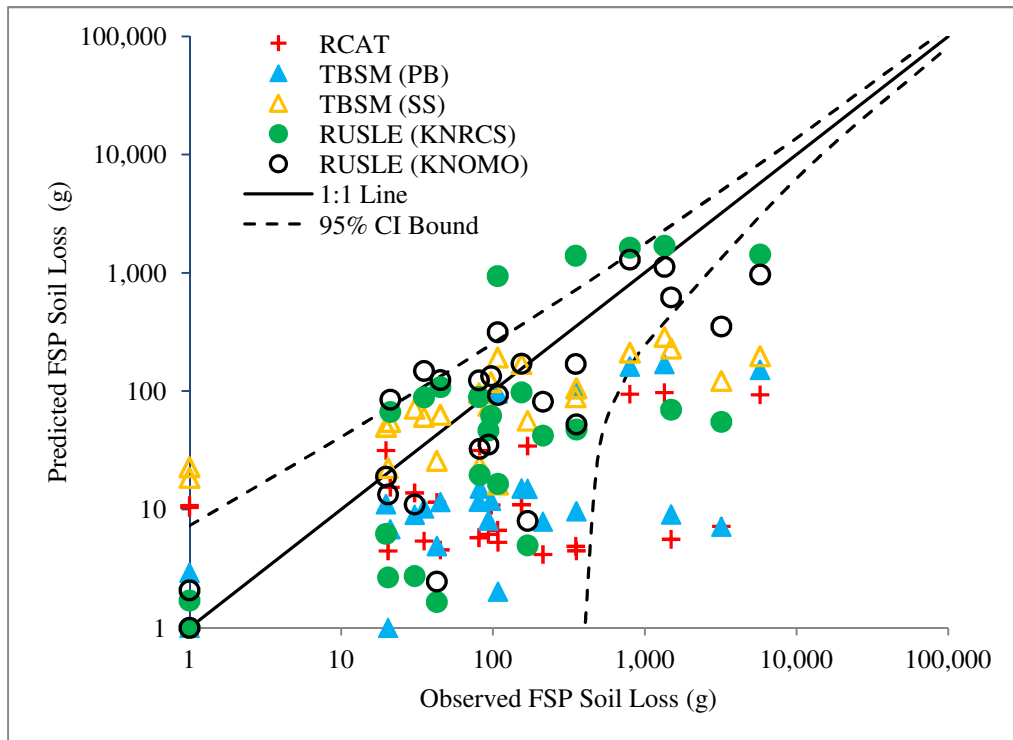


Figure 4.18. Comparison of predicted FSP soil losses with observed FSP soil losses

In reviewing the predictive accuracy of all the models for each rainfall simulation, as denoted by the bold values in Table 4.7, the RUSLE (KNOMO) model most accurately predicted 44% and 40% of the rainfall simulations for total and FSP soil loss, respectively. The TBSM (SS) model also performed well, relative to other models, predicting 36% and 32% of the rainfall simulations most accurately for total and FSP soil loss, respectively. Conversely, the RCAT performed best for only 8% of the rainfall simulations for predicting FSP soil loss and none of the rainfall simulations for predicting total soil loss. The TBSM (SS) model tended to over-predict the smaller sediment yields and under-predict the larger sediment yields for both the total and FSP soil loss. For predicting total and FSP soil loss, both RUSLE models typically under-predicted the smaller sediment yields and the very largest sediment yields, but generally over-predicted the moderate sediment yields. These basic observations follow the common tendency of erosion models to over-predict the smaller sediment yields and under-predict the larger sediment yields (Lafren et al., 2004). The accuracy of model predictions and the tendencies of the models to over- or under-predict soil losses are graphically shown in Figure 4.17 and Figure 4.18. The solid line represents the 1:1 line or the line designating a perfect match between the predicted and the observed values; therefore, data points closer to the 1:1 line indicated more accurate predictions. Data points located above the 1:1 line indicated that the model over-predicted and data points located below the 1:1 line signified that the model under-predicted soil losses. The dashed lines in Figure 4.17 and Figure 4.18 represent the 95% CI upper and lower limits; therefore, data points located outside these limits indicated that the model predictions were outside the typical percentile bounds observed from the field replicated plots (see Section 3.9.2), thus highlighting inaccuracies of the models.

When comparing only the three model predictions that were generated without inputting site-specific soil parameters (e.g., RCAT, TBSM (PB) and RUSLE (KNRCS)) amongst each other, the RUSLE (KNRCS) outperformed the others by most accurately predicting 56% and 48% of the rainfall simulations for both total and FSP soil loss, respectively, followed by the TBSM (PB) (40% total soil loss and 28% FSP soil loss), and lastly by the RCAT (4% total soil loss and 24% FSP soil loss). The TBSM (PB) and RCAT models tended to substantially under-predict both total and FSP soil loss across all ranges of sediment

yields, as illustrated by the majority of data points located below the 1:1 line in Figure 4.17 and Figure 4.18.

The results of the  $R^2Eff$  and 95% CI statistical analyses of the models are summarized in Table 4.8. The statistical results were subdivided into 3 categories based on slope type (all slopes, cut slopes only, and fill slopes only) to determine how model results changed depending on the type of slope analyzed.

Table 4.8. Soil erosion model performance evaluation statistics

Measurement	Model	Slope Type					
		All		Cut		Fill	
		$R^2Eff$	% Inside 95% CI	$R^2Eff$	% Inside 95% CI	$R^2Eff$	% Inside 95% CI
Total Soil Loss	RCAT	-0.29	28%	-0.17	39%	-1.27	0%
	TBSM (PB)	-0.16	56%	-0.04	67%	-1.10	33%
	TBSM (SS)	-0.08	68%	0.00	72%	-0.77	67%
	RUSLE (KNRCS)	0.20	52%	0.46	67%	-1.47	17%
	RUSLE (KNOMO)	0.40	68%	0.42	76%	0.16	67%
FSP Soil Loss	RCAT	-0.18	72%	-0.09	74%	-0.73	67%
	TBSM (PB)	-0.15	76%	-0.06	89%	-0.72	33%
	TBSM (SS)	-0.09	80%	-0.03	84%	-0.53	67%
	RUSLE (KNRCS)	0.16	84%	0.38	89%	-0.89	67%
	RUSLE (KNOMO)	0.19	76%	0.26	79%	-0.23	67%

In reviewing the results of the  $R^2Eff$  statistical evaluation for both total and FSP soil losses for all the rainfall simulations, the correlations between the observed and predicted values for the RCAT, TBSM (PB) and TBSM (SS) resulted in  $R^2Eff$  values less than 0.0, indicating that the mean of the observed values was a better predictor of sediment yield than the model estimates. The two versions of the RUSLE models most accurately predicted sediment yields for total soil loss based on the  $R^2Eff$  values of 0.20 and 0.40 for the RUSLE (KNRCS) and RUSLE (KNOMO) models, respectively. Additionally, the RUSLE performed best in estimating FSP soil loss, resulting in  $R^2Eff$  values of 0.16 and 0.19 for the RUSLE (KNRCS) and RUSLE (KNOMO) models, respectively. The RUSLE does not predict the PSDs of eroded soil; however, a simplified method, described in Section 3.8.1, was used to estimate the FSP fraction based on the fractions of silt and clay present in the bulk soil.

All of the  $R^2Eff$  values for each model improved after eliminating the fill slopes from the dataset, suggesting the difficulty in predicting soil erosion on fill slopes when using the NRCS soil surveys to

identify soil textures and/or parent materials for these non-native slopes. As expected for the fill slope only dataset, the performance of the models using the site-specific soil parameter data, RUSLE (KNOMO) and TBSM (SS), significantly outperformed all of the parameter based models. Although the  $R^2Eff$  values from this study are fairly low relative to the perfect fit value of 1, they are comparable to other erosion studies that evaluated the accuracy of both the RUSLE and WEPP models. Spaeth et al. (2003) evaluated the USLE and RUSLE using rainfall simulation data on a diverse set of rangeland vegetation types and reported  $R^2Eff$  values of -8.99 for the USLE and 0.17 for the RUSLE. Larsen & MacDonald (2007) compared the sediment yield predictions from the RUSLE and Disturbed WEPP models versus collected data from wildfire areas in the Colorado Front Range Mountains. This study reported  $R^2Eff$  values of 0.06 and 0.19 for the RUSLE and the WEPP models, respectively.

From a practical standpoint and a perspective that considers the clarity of Lake Tahoe, the inaccuracies of model predictions at the lower end are less significant than the predictive errors of the models for the larger sediment yields. The dataset was subdivided into two categories, based on the median of the observed values for FSP soil loss of 97 grams: (1) rainfall simulations with observed FSP soil losses less than 97 g; and (2) those with soil losses greater than 97 g. For the dataset with FSP soil losses less than 97 g, the TBSM (SS) model performed best with an  $R^2Eff$  value of 0.08 for the FSP soil loss predictions. The RUSLE (KNOMO) model performed best ( $R^2Eff$  value of -0.01) for the dataset including the rainfall simulations with observed FSP soil losses greater than 97 g.

Using the 95% *CI* values to evaluate the performance of each model (see Table 4.8), the RUSLE and the TBSM models consistently produced greater percentages of predictions (total and FSP soil losses) that were within the 95% *CI* of the observed values, when compared to the RCAT model predictions. Only 28% of the total soil losses predicted using RCAT were within the 95% confidence intervals, which was significantly lower than the other models. In considering the predicted FSP soil losses, the performance of the RCAT model improved, primarily due to the greater percentages of the soil loss FSP of the RCAT model relative to the other models. The percent FSP of the estimated eroded soil in the RCAT ranged from 20% to 30% for the granitic soils and 40% to 50% for the volcanic soils. Conversely, the percent FSP in runoff for the TBSM (PB) model ranged from 4% to 10% for the granitic soils and 15% to 25% for the

volcanic soils. The percentages of soil loss FSP used for the RUSLE (KNRCS) model estimates ranged from 6% to 11% for the granitic soils and 14% to 25% for the volcanic soils. The TBSM and RUSLE estimates for percent FSP in the soil loss are more comparable to the observed percentages from the rainfall simulations shown in Table 4.3. The large fractions of FSP in the runoff associated with the RCAT greatly increased the FSP soil loss predictions, despite the lower total soil loss predicted by the model, resulting in 72% of the predictions falling within the 95% confidence intervals. Despite the improvement in predicting FSP soil loss relative to the total soil loss predictions, the RCAT still yielded the lowest  $R^2_{Eff}$  value among the various models. The site-specific parameter models, RUSLE (KNOMO) and TBSM (SS), generally performed better than the NRCS parameter based and default parameter models, RUSLE (KNRCS) and TBSM (PB), in predicting values within the 95% *CI*. This improvement in performance was primarily associated with the significantly greater percentage of fill slope erosion predictions within the 95% *CI*, relative to the non site-specific model (e.g., RCAT, TBSM (PB) and RUSLE (KNRCS)) predictions.

The following subsections discuss the general performance of each of the three models evaluated and describe potential modifications to improve predictive accuracy of each model.

#### **4.6.1 Revised Universal Soil Loss Equation (RUSLE)**

Overall, the RUSLE outperformed the two other models which were evaluated when estimating both total and FSP soil losses (see Table 4.8), particularly when comparing predictions for the slopes where the greatest amounts of soil erosion were observed during the rainfall simulations. The use of RUSLE is typically applied to relatively simple hill slopes due to model limitations in estimating deposition and channel erosion within a small watershed (see Section 2.6.1). The strengths of the RUSLE include: (1) prediction of erosion from uniform hill slopes; (2) the simplicity of the model; (3) the ease of applying to various hill slopes throughout the United States by using the properties published in the NRCS soil surveys; and (4) the historical applications and the use of over 10,000 plot years of rainfall data (natural and simulated) to develop the predictive equations (Galetovic et al., 1998). The majority of roadway cut and fill slopes may be classified as uniform, relatively simple hill slopes, where deposition typically occurs at the toe of slopes. Therefore, the RUSLE is considered to be capable of adequately predicting soil losses for these types of slopes in the Lake Tahoe Basin.

When applying the RUSLE within the Lake Tahoe Basin, the primary concerns regarding the predictive accuracy and applicability include: (1) the ability of the climate parameter (rainfall-runoff erosivity factor,  $R$ ) within RUSLE to accurately account for a climate dominated by snow precipitation and snowmelt; (2) the inability of the model to predict the PSD of the soil losses; and (3) the potential difficulties associated with integrating the RUSLE with a continuously simulated model, such as the PLRM. These concerns, as well as other potential model improvements, are discussed in the subsequent section.

#### 4.6.1.2 Model Improvements

The following generally describe some potential modifications to the RUSLE to improve the predictive accuracy of the model.

1. As shown in Table 4.8, when comparing predicted soil losses from the fill slopes to those from the cut slopes, large inaccuracies were observed in all of the models for the predicted erosion (total and FSP) from the fill slopes. However, the RUSLE model appeared to provide more accurate predictions than the TBSM/WEPP and the RCAT. The improvement in the prediction accuracy for the RUSLE was particularly apparent when comparing the site-specific model, RUSLE (KNOMO), to the NRCS soil survey based model, RUSLE (KNRCS). The use of site-specific soils data to calculate model soil parameters greatly improved model predictions for fill slopes, while the model predictions using the NRCS soil survey data resulted in inaccurate estimates of PSDs and ultimately soil erodibility values ( $K$ ) for fill slopes, primarily due to the mixed, non-native nature of the fill slope soil material, as discussed in Section 4.3. To improve PSD estimates and  $K$  values for fill slopes which would lead to better overall predictive performance of the model for these types of slopes, the cone penetrometer tool may prove useful for rapidly determining soil texture for fill slopes, as discussed in Section 4.4 and shown in Figure 4.1. In estimating the organic matter content of the bulk soil for use in ultimately calculating the  $K$  value (see *Equation 2.6*), a predictive equation may be developed based on the soil texture, and the percentage of surface and canopy cover, as these plot characteristics were significantly correlated (see Section 4.4).

2. To account for the increased runoff and erosion associated with fill slopes, presumably a result of surface crusting due to decreased surface roughness (see Section 4.4), surface roughness values in the RUSLE should be adjusted accordingly based on slope type (cut or fill) to improve modeling results. The average surface roughness value reported by Grismer & Hogan (2004 and 2005) for various cut slopes in the Lake Tahoe Basin was 0.39 inches and this value was used for all slope types modeled during this research. For cut slopes, this value appeared to work well for erosion predictions as evidenced by the reasonable  $R^2Eff$  values for the RUSLE model when considering the cut slope dataset summarized in Table 4.8. For fill slopes, this value yielded inaccurate predictions as evidenced by the low  $R^2Eff$  values in Table 4.8. For fill slopes, a surface roughness value of 0.24 inches was recommended for smooth fill slopes, based on guidance from Galetovic et al. (1998), to reflect the smoother, more compact nature of the fill slope soil material. When this lower value of surface roughness was used for the fill slopes in an experimental model run, the resulting  $R^2Eff$  values for the total soil loss improved from 0.16 to 0.26. It is recommended that surface roughness values for multiple NDOT fill slopes in the Lake Tahoe Basin be measured in the field in order to develop a representative value for these slopes. Galetovic et al. (1998) provided guidelines for measuring slope surface roughness in the field.

Additionally the prior land use (*PLU*) subfactor in the RUSLE, which relates to the consolidation state of the soil, could be calibrated to the erosion results of the rainfall simulations to further refine the values and develop a *PLU* factor representing both cut slopes and fill slopes in the Lake Tahoe Basin. Typically, the *PLU* values are lower for cut slopes, as the soil is considered to be more consolidated and resistant to erosion. Conversely, for fill slopes, the soil has been loosened and the soil-aggregation size has been reduced, resulting in higher *PLU* values (Galetovic et al., 1998; Renard et al., 2010). As mentioned in Section 3.8.1, the fill slopes were modeled using a *PLU* set equal to 0.8 and the *PLU* for cut slopes was set equal to 0.5, based on guidance provided by Galetovic et al. (1998).

3. The soil erodibility values (*K*) for the RUSLE (KNOMO) model version were calculated for all slopes based on the bulk soil PSDs, the organic matter content, and the use of *Equation 2.6*. The

$K$  values for the sand and loamy sand soils (predominantly from the granitic origin) averaged 0.13 ( $\sigma = 0.07$ ) and the sandy loam soils (predominantly from the volcanic origin) averaged 0.24 ( $\sigma = 0.09$ ). The calculated  $K$  values for each slope simulation were shown in Table 3.6. The use of these site-specific  $K$  values resulted in better model performance, as shown in Table 4.8. These values could be further supplemented with additional soil sampling along NDOT roadways or the mentioned average values could be used to simplify the RUSLE calculation process for the Lake Tahoe Basin, similar to the way the RCAT and TBSM/WEPP models provide default soil parameters for the granitic and volcanic soil textures. However, this simplification could result in less accurate estimations than using the more location specific soils data and RUSLE parameters provided in the NRCS soil survey.

4. Since the RUSLE did not include predictions of PSDs in the soil loss, various methods need to be used to develop reasonable estimates. As mentioned in Section 3.8.1, the *PLRM Applications Guide* (PLRM, 2010a) provided a procedure for estimating soil loss FSP based on the silt and clay fractions provided by the NRCS soil survey. A regression correlation analyses revealed that this procedure provided reasonable estimates of soil loss FSP for the cut slopes, as indicated by the high  $R^2$  (0.83) and low  $p$ -value ( $p < 0.0001$ ). As mentioned in Subsection 4.4.2.2 and shown in Figure 4.10, the silt content of the bulk soil for the cut slopes was strongly correlated to the percent of soil loss FSP ( $R^2 = 0.83$ ,  $p < 0.001$ ). The linear regression equation resulting from this relationship may also be used to predict the soil loss FSP fractions for cut slopes, as follows:

$$FSP = 1.3 SILT - 4.8 \quad \text{Equation 4.1}$$

where  $FSP$  = percent fine sediment particles (< 16 microns) in the eroded soil

$SILT$  = percent silt content in the bulk soil

Although the correlations between the bulk soil characteristics and soil loss PSDs for the cut slopes dataset was significant, the correlations for the fill slopes were insignificant. The fill slopes appeared to produce greater ratios of soil loss FSP to silt content in the bulk soil than did the cut slopes, as shown in Figure 4.9, likely a result of increased runoff on fill slopes due to less surface roughness and greater soil compaction. When comparing the observed percentage of FSP

in the soil losses for the fill slope dataset to the percentages predicted for these same slopes, using *Equation 4.1*, the average ratio of observed values to predicted values was approximately 2:1 for the sandy loam fill slopes and nearly 4:1 for the sand and loamy sand fill slopes. Therefore, for the limited dataset, the fill slopes tended to produce two to four times the amount of FSP, depending on soil type, as the fraction predicted by *Equation 4.1*; however, this relationship needs to be assessed further.

5. As mentioned in Section 2.6.1.1, the RUSLE does not predict soil erosion from snowmelt events. Precipitation in the form of snowfall and the runoff during snowmelt are the dominant forms of precipitation and runoff in the Lake Tahoe Basin. However, erosion from snowmelt is considered much less significant than erosion from summer thunderstorm events (Ryan & Elliot, 2005). As a result, adjusting the RUSLE rainfall-erosivity factor to account for snowmelt may not be necessary. However, the RUSLE does provide procedures to account for snowmelt erosivity by using empirical relationships to increase the standard annual erosivity values.

The TBSM/WEPP model uses sophisticated climates for model simulations, as discussed in Section 2.6.3.3. These simulations are continuous on a daily time step and predict both runoff and erosion. Although the RUSLE does not specifically predict runoff for a given slope, the RUSLE rainfall-erosivity factor ( $R$ ) does indirectly consider the magnitude of runoff and the impacts of interrill and rill erosion (Renard et al., 1997). For acceptance of the  $R$  factor in the Tahoe Basin, annual  $R$  values could be calculated using 15-minute rainfall data from one of the Lake Tahoe Basin precipitation gages, using the guidelines from the various RUSLE handbooks (Renard et al., 1997; Yoder et al., 2004). These values could be compared to the average annual  $R$  values presented in the NRCS RUSLE2 National Database to determine the accuracy of the NRCS published  $R$  values.

6. Integrating the RUSLE into the PLRM presents a challenge due to the fact that the RUSLE does not predict runoff volumes, a requirement for the PLRM, which uses the characteristic runoff concentrations (CRCs) for each land use, dependent on the characteristics of the land use (e.g., soil type, condition, etc.) to estimate erosion (PLRM, 2010b). To estimate runoff for cut and fill

slopes, future research could determine relationships between storm type (duration and intensity) and runoff to determine specific runoff “thresholds” dependent on the magnitude of the storm, ultimately estimating the annual runoff for a specific slope. Similarly, Larsen & MacDonald (2007) determined that a minimum RUSLE *R* value or amount of precipitation was required to generate overland flow and erosion from certain plots located in the Colorado Front Range. Alternatively, relationships could be generalized using the average runoff coefficient values presented in this research (see Table 4.4) or developing empirical runoff relationships based on the dataset (see Section 4.4.1). The concentrations used for PLRM integration could be estimated based on the annual slope erosion predictions per the RUSLE methodology and the runoff volumes predicted using the estimated runoff coefficients, dependent on soil type and other physical parameters (e.g., slope, surface cover, etc.). However, these values were measured using 100-year rainfall events; therefore, the average annual runoff coefficients would likely be less. This alternative approach would be similar to the method used in the RCAT to estimate average annual runoff volume, which is ultimately required for calibration and integration with the PLRM (Drake et al., 2010). The RCAT assumes a slope dependent annual runoff equation (*Equation 2.33*), based on slope runoff research in the Lake Tahoe Basin (Heyvaert et al., 2008), to estimate runoff volume (Drake et al., 2010). Future research could evaluate runoff coefficients for cut and fill slopes for a variety of simulated storm events and soil moisture conditions to develop range of runoff coefficients.

#### **4.6.2 Tahoe Basin Sediment Model (TBSM)**

Total and FSP soil losses predicted by the TBSM/WEPP models for the rainfall simulation plots were less accurate than the predictions using the RUSLE models, but were more accurate than those from the RCAT model (see Table 4.8). When subdividing the dataset into larger (> 97 g) and smaller (< 97 g) FSP sediment yields, the TBSM (SS) model version performed better than all other models for predicting the smaller sediment yields.

The strength of the TBSM/WEPP methodology exists in the process-based structure and the continuous simulation capabilities of the model, as discussed in Section 2.6.3. While the RUSLE focuses

solely on rainfall-runoff initiated erosion predictions, the TBSM/WEPP estimates erosion from all water-induced erosion mechanisms, including erosion resulting from snowmelt. The inclusion of the snowmelt erosion processes is a significant feature for predicting erosion in climates dominated by snow precipitation and snowmelt, such as the Lake Tahoe Basin. However, the enhanced capabilities of the WEPP also create increased model complexity, in contrast to the relatively simplistic model formats of both the RUSLE and RCAT. The TBSM simplifies the application of WEPP by providing a straightforward, online interface that contains only a limited number of selectable parameters specific to the Lake Tahoe Basin. However, the TBSM model simplification and limitation in user flexibility leads to less accurate erosion predictions in comparison to allowing the modeler to input site-specific (SS) soils data, as shown by the difference in  $R^2_{Eff}$  values between the TBSM (PB) and TBSM (SS) model simulations (see Table 4.8). The TBSM/WEPP model structure and features (see Section 2.6.3) are superior, relative to the RUSLE and RCAT, for modeling sediment yields from small watersheds, due to the ability to account for sediment deposition and channel erosion. However, the methodology used in predicting erosion on simple, uniform hill slopes, such as roadway cut and fill slopes, is similar to the prediction methods used in the RUSLE (Laflen et al., 1991).

#### 4.6.2.2 Model Improvements

The following items generally describe some potential modifications to the TBSM to improve the predictive accuracy of the model.

1. As discussed in Section 4.4, the magnitude of erosion and runoff was largely dependent on the soil texture of the slope. As shown by the improved predictive performance of the site-specific (SS) soil parameter model, “TBSM (SS)”, in comparison to the model using the default parameters for the parent material soil texture obtained from the TBSM Tahoe database, “TBSM (PB)”, erosion predictions could be improved by using more site-specific soils data. Currently, the TBSM Tahoe soils database for granitic soils uses the following PSDs for the granitic soils (sand = 90%, silt = 8%, clay = 2%) and volcanic soils (sand = 65%, silt = 28%, clay = 7%). These default values are comparable to the average values presented in Table 4.2. However, the TBSM could implement an add-on to the model that would allow the user to select the NRCS soil map unit encompassing

the location of the cut or fill slope of interest. Based on the selected soil map unit, the TBSM could then internally populate the NRCS estimated bulk soil PSDs and use the empirical equations presented in Section 2.6.3.5 to calculate the baseline  $K_e$ ,  $K_i$ ,  $K_r$ , and  $\tau_c$  soil parameters for the slope. This model improvement may perhaps lead to more accurate soil loss predictions at the expense of added model complexity.

2. As shown in Table 3.6 and the associated footnotes, the default soil erodibility parameters ( $K_e$ ,  $K_i$ ,  $K_r$ , and  $\tau_c$ ) for both the granitic and volcanic soil types were significantly lower than the calculated values, based on the PSD and the organic matter content of the bulk soil, using the empirical equations provided in the WEPP documentation and presented in Section 2.6.3.5. Modifying the TBSM default soil parameters, based on site-specific soils data and empirical equations, for the TBSM (SS) model simulations improved model performance over the TBSM default model, the TBSM (PB), as shown in Table 4.8. These erodibility parameters greatly influenced runoff and erosion results; therefore, further review is needed to determine the appropriateness of the TBSM default soil parameters for highway cut and fill slope applications. Particular attention should be directed to the value of the rill erodibility parameter,  $K_r$ , as rill erosion was evident during numerous rainfall simulations and apparent on highway slopes in the Lake Tahoe Basin after significant thunderstorms in August 2014 (see Figure 4.13). As mentioned previously, the TBSM model did not perform as well in predicting the largest sediment yields, again suggesting that the  $K_r$  parameter should be reviewed. Calibration techniques to improve these soil parameters should be considered.
3. The runoff and erosion data collected from the 25 rainfall simulations performed during this research provide valuable data that could be used to calibrate the baseline infiltration parameters ( $K_e$ ) and soil erodibility parameters ( $K_i$ ,  $K_r$ , and  $\tau_c$ ) used in the TBSM. These calibration efforts would need to be performed using the full WEPP version. Calibration procedures for the WEPP were detailed by Flanagan et al. (2012). Additionally, Foltz et al. (2010) described calibration techniques using runoff and erosion data collected from rainfall simulations. As mentioned in Section 4.4.3, the primary runoff and erosion dataset used to develop the relationships used in the

TBSM was from the research performed by Grismer & Hogan (2004, 2005a, 2005b). The erosion results reported in these studies were typically lower than comparable studies (see Table 4.5 and discussion in Section 4.4.3). The runoff and erosion data collected during the current research could either supplement the data from Grismer & Hogan (2004, 2005a, 2005b) or be used to develop a new set of calibrated parameters for specific use on highway cut and fill slopes in the Lake Tahoe Basin. Perhaps the TBSM developers could implement new vegetation/treatment classes, one for cut slopes and one for fill slopes, based on these calibration efforts.

4. The inaccuracy of the TBSM in predicting erosion from fill slopes was evident (see Table 4.8). As discussed in Section 4.4, fill slopes consistently exhibited greater amounts of runoff and erosion than comparable cut slopes, presumably due to: (1) surface crusting, as a result of decreased surface roughness; (2) increased soil compaction; and (3) less soil consolidation related with these constructed slopes. Perhaps a new slope treatment/vegetation class could be developed to represent the unique characteristics of fill slopes. Similar to the RUSLE, the default surface roughness in the TBSM/WEPP could be adjusted to better simulate the smoother surfaces typically associated with fill slopes. Additionally, TBSM/WEPP parameters reflecting the consolidation state or compaction level of the soil could be adjusted to provide more accurate predictions.

#### **4.6.3 Road Cut and Fill Slope Sediment Loading Assessment Tool (RCAT)**

The total and FSP soil losses predicted by the RCAT model were the least accurate of all the models evaluated for the cut and fill slopes which were tested during this research project (see Table 4.8). In general, the RCAT tended to significantly under-predict soil losses, particularly for the slopes producing the largest sediment yields. Notably, only 28% of the RCAT predictions for total soil loss fell within the 95% confidence intervals (see Table 4.8), thus highlighting the inaccuracies of the RCAT predictions. The strengths of the RCAT include that: (1) it was developed specifically for roadway cut and fill slope applications within the Lake Tahoe Basin; (2) the regression equations used for predictions were developed from Tahoe-specific rainfall simulations; and (3) it provides methods to integrate with the PLRM. Despite the aforementioned strengths of the RCAT, the model is particularly time and labor intensive in comparison

to the other models which depend primarily on Tahoe-specific parameterized data (TBSM) or estimated soils data from the NRCS soil surveys (RUSLE). Specifically, the RCAT requires the modeler to record field measurements of cone penetrometer DTR and mulch and litter depths (see Section 2.6.5 for details on field assessment procedures). The noted time and labor requirements associated with field measurements, relative to the RUSLE and WEPP/TBSM models, deserve consideration when assessing the predictive performance of the RCAT; ideally, the added complexity and the requirement to perform site-specific field measurements should, in theory, increase the predictive accuracy of the erosion model.

#### 4.6.3.2 Model Improvements

The following items generally describe some potential modifications to the RCAT to improve the predictive accuracy of the model.

1. Slope length is a standard input in most soil erosion models, including both the RUSLE and WEPP/TBSM models. However, the RCAT model excludes slope length as a model input parameter, despite general acceptance that erosion rates, particularly on bare, steep slopes, increase linearly on slopes exceeding approximately 2 to 4 meters (6 to 12 feet) in length (Cerda, 1999; Drake & McCullough, 2010; Renard et al., 1997). The RCAT developers defend that predictions are accurate for smaller slope lengths, less than 3 m (about 9 feet) in length, but potentially under-predict sediment yields on slopes where rill formation is probable (Drake & McCullough, 2010). Although the impacts of slope length on erosion rates were not evaluated during this research project, highway cut and fill slopes within the Lake Tahoe Basin commonly exceed 5 m (about 15 feet) in length and possess slope gradients greater than 70%, thus frequently leading to rill erosion formations during moderately sized summer thunderstorms, as shown in Figure 4.13. Therefore, the exclusion of slope length as a model input is potentially a limitation of the RCAT, particularly for estimates of erosion from the steep, long and often bare slopes common in the Lake Tahoe Basin. The RCAT methodology could incorporate a slope length factor, similar to the RUSLE, to increase erosion rates according to the measured slope length and slope gradient. The RUSLE uses *Equation 2.7*, *Equation 2.8* and *Equation 2.9* to estimate the effects of slope length on erosion rates, depending on the slope gradient and the expected ratio of

rill to interrill erosion on a given slope. For example, erosion predictions for a 60% slope with a moderate ratio of rill to interrill erosion increase by nearly three times when the slope length increases from 4 m (about 12 feet) to 15 m (about 50 feet) (Renard et al., 1997). Using similar methods as the RUSLE, a slope length factor could be applied to RCAT sediment yield predictions to account for increased slope lengths. Notably, RCAT erosion rates were determined from rainfall simulation plots on a 1 m (about 3 feet) run length. Therefore, increases in erosion rates for longer slope lengths could be adjusted according to the baseline of approximately 1 m.

2. As mentioned in the discussion of the model sensitivity analyses in Section 4.2, the RCAT uses *Equation 2.32* to calculate a surface cover index (*SC*), which ultimately determines the impacts of surface coverage on reducing erosion in the model. The higher the *SC* value, the greater the reduction in erosion due to surface cover. The current structure of *Equation 2.32* requires mulch and litter coverage to generate non-zero values for *SC*, thus limiting erosion reductions for slope treatments absent of mulch and litter (e.g., riprap slopes). As discussed in Section 4.4.2, surface coverage in all forms (e.g., riprap, surface and canopy vegetation, and mulch and litter) effectively reduced erosion on the rainfall simulation plots, relative to the bare slope plots (see Figure 4.6). The formulation of *Equation 2.32* could be restructured so that only the percentage of the surface covered by mulch and litter is multiplied by the mulch and litter depth and the remaining surface coverage from other features (e.g., surface and canopy vegetation, riprap or natural rock outcroppings) could be properly considered in determining slope erosion reductions.
3. The RCAT uses a slope dependent equation to estimate the runoff from cut and fill slopes (see *Equation 2.33*), which indirectly impacts the magnitude of erosion from a slope. This equation neglects the impacts of soil texture on runoff. Therefore, the predicted runoff volume from a slope composed of granitic soil (sand and loamy sand) is considered to be equivalent to the runoff from a slope with volcanic soil (sandy loam) for a given slope gradient. Additionally, the maximum runoff coefficient in *Equation 2.33* is limited to 0.15. As shown in Table 4.4 and Figure 4.4, the runoff characteristics from the rainfall simulation plots depended significantly on the soil texture and numerous plots generated runoff coefficients greater than 0.15, particularly the fill slopes.

During this research project, the volcanic slopes (sandy loams) generally produced two to three times greater runoff than the granitic slopes (sand and loamy sands). Perhaps the RCAT developers could modify the method used to predict runoff to also consider soil texture and the type of slope (cut or fill) in order to more accurately predict runoff from these slopes.

4. As mentioned in Section 4.4.3, the dataset used for the development of the RCAT and TBSM models, based on the research findings of Grismer & Hogan (2004, 2005a, 2005b) and Grismer et al. (2008), produced erosion yields significantly lower than comparable studies. The result of these lower erosion measurements may have led to the significantly lower erosion predictions by the RCAT, particularly for the higher sediment yields (see Figure 4.17). Additionally, the runoff coefficients predicted by the RCAT were not significantly correlated with the observed runoff coefficients from the rainfall simulation plots ( $R^2 = 0.03$ ,  $p > 0.40$ ). In order to determine if the inaccuracies in the sediment yield predictions from the RCAT model were the result of the inaccurate predictions of runoff by the RCAT model, a trial run was performed by calibrating the runoff predicted by the RCAT to match the runoff observed during the rainfall simulations. This calibration effort slightly improved the predictive accuracy of the RCAT model, in comparison to the uncalibrated version, as determined from increases in  $R^2Eff$  values by 0.11 and 0.15 for total and FSP soil losses, respectively. However, the calibrated version still significantly under-predicted soil losses thus suggesting that the sediment concentrations, used in the RCAT to multiply by the estimated runoff volume and ultimately predict sediment yields, were the primary reason for the inaccurate predictions of the RCAT model. The runoff and erosion data collected during the current research could potentially supplement the data collected by Grismer & Hogan (2004, 2005a, 2005b) and be used to refine the regression equations and improve the RCAT erosion estimates for highway cut and fill slopes in the Lake Tahoe Basin.

## Chapter 5

### SUMMARY AND CONCLUSIONS

Reducing erosion, particularly FSP contributions from urban stormwater, and identifying erosion sources and key parameters that influence the erosion process is critical to restoring Lake Tahoe's famed clarity. This research project conducted rainfall simulations and installed dry ravel sediment traps on a diverse set of highway cut and fill slopes along the roadways maintained by NDOT within the Lake Tahoe Basin, in order to improve the understanding of the rainfall-runoff and dry ravel erosion processes. In the case of the rainfall simulations, the data was used to identify significant correlations between the physical characteristics of the rainfall simulation plots and the observed runoff and erosion results, quantify the percentage of FSP in the eroded soil, and assess the predictive accuracy of various soil erosion models (i.e., RUSLE, WEPP/TBSM, and RCAT). Prior to this research, little quantitative information existed regarding contributions of dry ravel to erosion and sediment yields within the Lake Tahoe Basin. Therefore, the data collected for dry ravel will improve the understanding of this erosion process, identify slope characteristics that enable dry ravel, as well as quantify the magnitude of dry ravel erosion in the Lake Tahoe Basin. The textural analyses of the bulk soil samples collected at the rainfall simulation and dry ravel sites confirmed that granitic parent material soils were generally classified as sands and loamy sands, while the volcanic parent material soils were typically classified as sandy loams per the USDA textural classification system. On average, the volcanic soils (sandy loams) contained nearly twice the amount of FSP in comparison to the granitic soils (sand and loamy sands).

The results of the rainfall simulations revealed that slopes composed of sandy loams (primarily of volcanic origin) typically generated greater amounts of runoff and erosion than comparable slopes composed of sand and loamy sands (primarily of granitic origin). The fill slopes appeared to exhibit more noticeable and less predictable variations in the measured runoff and erosion parameters, in comparison to the cut slopes. Generally, fill slopes exhibited smoother (i.e., less surface roughness) slopes due to the constructed nature and high compaction levels associated with these slopes, possibly leading to the formation of surface crusting which subsequently increased runoff and erosion. In terms of mass erosion rates, the sandy loam slopes generated two to four times greater mass erosion than that from sand and

loamy sand slopes. Additionally, as expected based on the bulk soil PSD analyses, the slopes with sandy loams exhibited greater soil loss FSP fractions than the slopes with sand and loamy sands. The ratio of the percent FSP in the bulk soil between the volcanic soils (sandy loams) and the granitic soils (sands and loamy sands) was nearly 2:1, while the soil loss FSP between the two parent material/soil textures was nearly 3:1. In general, the volcanic soils possessed greater amounts of fine particles and also typically generated more erosive runoff than the granitic soils, primarily due to the lower sand and higher silt fractions, thus resulting in greater sediment transport of FSP. The sandy loams (volcanic soils) yielded four to ten times greater FSP soil losses than the sand and loamy sands (granitic soils). As discussed, the magnitude of runoff and erosion depends considerably on the soil characteristics of the hill slope. However, of the various physical characteristics of the rainfall simulation plots, surface cover exerted the greatest influence on reducing total soil losses. Notably, surface cover is typically designated as the most significant parameter in soil erosion models. The general observations from the rainfall simulations suggested that the volcanic and mixed soils (sandy loams) represent the most critical slopes with regards to the need for NDOT to implement slope stabilization techniques in order to reduce FSP contributions into Lake Tahoe.

Based on visual observations and the results of this research, dry ravel represents a significant form of erosion in the Lake Tahoe Basin, particularly on bare slopes with slope gradients exceeding approximately 60%. Despite the limited dataset, a nonlinear, slope dependent dry ravel transport equation was parameterized to fit the collected data. This equation may provide reasonable predictions for slopes less than 83%. However, the future installation of additional sediment traps across the Lake Tahoe Basin is recommended in order to improve this transport equation, particularly for slopes greater than 60%. In order to better capture the variation of dry ravel across the slope, future research should install wider traps or multiple sediment traps side by side, in a linear fashion, for a significant length along the toe of slope. This proposed field testing method differs from the single trap installation employed during this research, but should better represent the spatial variation of dry ravel deposition cones across a given slope. The PSD analyses of the collected dry ravel revealed that the amount of fines in the bulk soil was similar to the amount in the dry ravel collected from the sediment traps. Additionally, the dry ravel collected during this

research occurred during the dry summer months when the soil was relatively dry and soil cohesion was lower. Past studies evaluating dry ravel reported a seasonal decline in dry ravel due to increased particle cohesion resulting from greater soil moisture. Future research could potentially install soil moisture probes to determine how dry ravel yields fluctuate throughout the year depending on the soil moisture content of the hill slope.

The RUSLE and TBSM/WEPP models were evaluated using two scenarios. The first scenario used the soil data obtained from the NRCS soil survey database, “RUSLE (KNRCS)”, and the default parameters for the parent material/soil texture- obtained from the TBSM Tahoe database, “TBSM (PB)”, to estimate soil losses. The second scenario used site-specific soil properties (PSDs, organic matter content) to calculate site-specific soils parameters using empirical equations, to predict soil losses within the RUSLE, “RUSLE (KNOMO)”, and the TBSM/WEPP, “TBSM (SS)” models. Soil parameter equations, based on site-specific soil properties, were not provided in the RCAT documentation; therefore, only one version of the RCAT was evaluated.

Considering the predictive accuracy of all the soil loss models with the observed soil losses for each rainfall simulation, the RUSLE (KNOMO) model most accurately predicted total soil losses and FSP soil losses for 44% and 40% of the rainfall simulations, respectively. The TBSM (SS) model also performed relatively well compared to the other models, predicting 36% and 32% of the rainfall simulations most accurately for total and FSP soil losses, respectively. Conversely, the RCAT performed best for only 8% of the rainfall simulations for predicting FSP soil losses and none of the rainfall simulations for predicting total soil losses. The TBSM (SS) model tended to over-predict the smaller sediment yields and under-predict the larger sediment yields for both the total and FSP soil loss. For predicting total and FSP soil loss, both RUSLE models typically under-predicted the smaller sediment yields and the very largest sediment yields, but generally over-predicted the moderate sediment yields. Using the Nash-Sutcliffe model efficiency value ( $R^2Eff$ ) to assess model performance, the two versions of the RUSLE models most accurately predicted sediment yields for total soil losses based on the  $R^2Eff$  values of 0.20 and 0.40 for the RUSLE (KNRCS) and RUSLE (KNOMO) models, respectively. Additionally, the RUSLE performed best in estimating FSP soil losses, resulting in  $R^2Eff$  values of 0.16 and 0.19 for the

RUSLE (KNRCS) and MUSLE (KNOMO) models, respectively. The correlations between the observed and predicted values for the RCAT, TBSM (PB) and TBSM (SS) resulted in  $R^2_{Eff}$  values less than 0.0, indicating that the mean of the observed values was a better predictor of sediment yield than the model estimates. All the models were limited in their ability to accurately predict erosion from fill slopes due to the unique characteristics of these slopes. From a practical standpoint and a perspective that considers the clarity of Lake Tahoe, the inaccuracies of model predictions at the lower end are less significant than the predictive errors of the models for the larger sediment yields. The MUSLE performed most accurately in predicting the largest sediment yields, while the TBSM performed best in predicting the smaller sediment yields. The simulated rainfall used to assess these models was a high intensity, 100-year design storm. Therefore, these models may perform drastically different for other types of storms. Additionally, snow precipitation and snowmelt are dominant processes in the Tahoe Basin and this research did not address erosion from these types of precipitation and runoff events. Future research could potentially address these problems by performing rainfall simulations on these same slopes using smaller design storms (e.g., 20-year, 1-hour design storm) to observe how the models perform for these smaller rainfall events and if similar performance results occur. Additionally, collecting erosion measurements from actual storm events in the Tahoe Basin or over an annual period could provide valuable data on how different storms and precipitation types impact erosion on these highway slopes.

The proposed modifications to the various models to improve the predictive accuracy of models for highway cut and fill slopes in the Tahoe Basin include: (1) improving erosion estimates for fill slopes by determining appropriate adjustments to the surface roughness and soil consolidation factors used in the MUSLE and TBSM; (2) using a cone penetrometer to rapidly estimate soil texture for fill slopes where soil textures assigned by NRCS may not be appropriate; (3) further supplementing model datasets and equations with the data collected during the current research project; (4) using linear regression equations to predict soil loss FSP fractions for cut slopes, based on the silt content of the bulk soil, to assist in converting predicted soil losses in MUSLE into predicted FSP soil losses; (5) expanding the TBSM model interface to allow users to input site-specific soils data from the NRCS soil surveys, as more site-specific soils data generally improved the predictive accuracy of the model; (6) developing more accurate soil

parameters for use in the TBSM by using calibration techniques and the soil, runoff and erosion data collected from the rainfall simulations performed during this research; (7) incorporating a slope length factor into the RCAT; and (8) improving the RCAT estimates of slope runoff by considering the soil texture of the slope, rather than basing runoff predictions solely on slope gradients.

Overall, this research provided valuable erosion and runoff data for highway cut slopes in the Lake Tahoe Basin. This data and the results of this research should help NDOT better identify critical slopes where slope stabilization techniques will be most effective, understand the erosion process (rainfall-runoff and dry ravel erosion) and the magnitude of erosion within their right-of-way. The rainfall simulations and model performance assessment provide insight as to which models may best predict slope erosion resulting from a high-intensity summer thunderstorm. Additionally, the recommended model improvements will hopefully result in better erosion prediction tools for the Lake Tahoe Basin which are capable of more accurately quantifying FSP reductions from slope stabilization practices, identifying appropriate credits through the Lake Clarity Crediting Program and ultimately helping in reducing FSP contributions to Lake Tahoe and restoring the world renowned lake clarity back to historic levels.

## REFERENCES

- Abudi, I., Carmi, G., & Berliner, P. (2012). Rainfall simulator for field runoff studies. *Journal of Hydrology*. doi:10.1016/j.jhydrol.2012.05.056
- Amore, E., Modica, C., Nearing, M. A., & Santoro, V. C. (2004). Scale effect in USLE and WEPP application for soil erosion computation from three Sicilian basins. *Journal of Hydrology*. doi:10.1016/j.jhydrol.2004.01.018
- Anderson, H. W., Coleman, G. B., & Zinke, P. J. (1959). Summer slides and winter scour: dry-wet erosion in southern California mountains. In *Technical Paper 36*. Berkeley, CA: Pacific Southwest Forest and Range Exp. Stn., Forest Service: US Department of Agriculture.
- Ascough II, J. C., Baffaut, C., Nearing, M. A., & Liu, B. Y. (1997). The WEPP watershed model: I. hydrology and erosion. *Transactions of the ASAE*, 40(4), 921–933.
- ASTM C1070 - 01. (2014). Standard test method for determining particle size distribution of alumina or quartz by laser light scattering. West Conshohocken, PA: ASTM International. doi:10.1520/C1070
- ASTM D2974 - 13. (2008). Standard test Methods for moisture, ash, and organic matter of peat and other organic soils. West Conshohocken, PA: ASTM International. doi:10.1520/D2974
- ASTM D3977 - 97. (2013). Standard test methods for determining sediment concentration in water samples. West Conshohocken, PA: ASTM International. doi:10.1520/D3977
- ASTM D422 - 63. (2007). Standard test method for particle-size analysis of soils. West Conshohocken, PA: ASTM International. doi:10.1520/D0422
- Battany, M. C., & Grismer, M. E. (2000a). Development of a portable field rainfall simulator for use in hillside vineyard runoff and erosion studies. *Hydrological Processes*, 14, 1119–1129. Retrieved from [http://onlinelibrary.wiley.com/doi/10.1002/\(SICI\)1099-1085\(20000430\)14:6<1119::AID-HYP8>3.0.CO;2-O/abstract](http://onlinelibrary.wiley.com/doi/10.1002/(SICI)1099-1085(20000430)14:6<1119::AID-HYP8>3.0.CO;2-O/abstract)
- Battany, M. C., & Grismer, M. E. (2000b). Rainfall runoff and erosion in Napa Valley vineyards : effects of slope , cover and surface roughness. *Hydrological Processes*, 14(August 1999), 1289–1304.
- Beard, K. V. (1976). Terminal velocity and shape of cloud and precipitation drops aloft. *Journal of Atmospheric Sciences*, 33, 851–864.
- Beasley, D. B., Huggins, L. F., & Monke, E. J. (1980). ANSWERS: A model for watershed planning. *Transactions of the ASAE- American Society of Agricultural Engineers*.
- Brown, R. B. (2003). *Soil Texture*. University of Florida, Soil and Water Science Department (pp. 1–8). Retrieved from <http://edis.ifas.ufl.edu/pdffiles/SS/SS16900.pdf>
- Cerda, A. (1999). Rain simulators and their application to geomorphology: state of the art. *Cuadernos de Informacion Geografica*, 25, 45–84.
- Chow, V. Te, Maidment, D. R., & Mays, L. W. (1988). *Applied Hydrology*. Water Resources and Environmental Engineering (Vol. 41, p. 572). doi:10.1016/j.soncn.2011.11.001

- Christiansen, J. E. (1942). Irrigation by sprinkling. *Agricultural Experiment Station, University of California, Berkeley, CA. Bulletin 670.*
- Coduto, D. P. (2001). *Foundation design: principles and practices* (2nd ed., p. 883). Upper Saddle River, NJ: Prentice Hall.
- Coordinated Technology Implementation Program (CTIP). (2012). *Roadside revegetation technical guide* (pp. 1–400).
- Copeland, N. S. (2009). Improving Erosion Modeling on Forest Roads in the Lake Tahoe Basin : Small Plot Rainfall Simulations to Determine Saturated Hydraulic Conductivity and Interrill Erodibility Grand Sierra Resort and Casino, 0300(09).
- Dennett, K. E., Sturm, T. W., Amirtharajah, A., & Mahmood, T. (1998). Effects of adsorbed natural organic matter on the erosion of kaolinite sediments. *Water Environment Research*, 70(3), 268–275.
- Dillaha, T. A., Beasley, D. B., & Huggins, L. F. (1982). Using the ANSWERS model to estimate sediment yields on construction sites. *Soil and Water Conservation*, 12(April), 117–120.
- Drake, K., & McCullough, R. A. (2010). *Road Cut and Fill Slope Sediment Loading Assessment Tool: User's Guide, Version 1.0* (pp. 1–30).
- Drake, K., McCullough, R. A., & Grismer, M. (2010). *Road Cut and Fill Slope Sediment Loading Assessment Tool: Project Report*. Retrieved from [http://www.fs.fed.us/psw/partnerships/tahoescience/documents/final\\_rpts/P039RCATFinalProjectReport.pdf](http://www.fs.fed.us/psw/partnerships/tahoescience/documents/final_rpts/P039RCATFinalProjectReport.pdf)
- Elliot, W. J., & Hall, D. E. (2010). Tahoe Basin Sediment Model (TBSM). Moscow, ID: U.S. Department of Agriculture, Forest Service, Rocky Mountain Research Station. Retrieved from <http://forest.moscowfsl.wsu.edu/fswapp>
- Elliot, W. J., Liebenow, A. M., Laflen, J. M., & Kohl, K. D. (1989). *A compendium of soil erosion data from WEPP cropland soil field erodibility experiments 1987 and 1988. NSERL Report No. 3.* Columbus, Ohio.
- Elliot, W. J., Traeumer, D. E., Hall, D. E., & Brooks, E. S. (2013). Tahoe Basin Sediment Project (TBSM) user manual. Fort Collins, CO: United States of Agriculture (USDA)-Rocky Mountain Research Station (RMRS).
- Elliot, W.J., Traeumer, D. E. (2014). "Re: TBSM Modeling Help." 27 March 2014. Email.
- Eshel, G., Levy, G. J., Mingelgrin, U., & Singer, M. J. (2004). Critical evaluation of the use of laser diffraction for particle-size distribution analysis. *Soil Science Society of America Journal*, (68), 736–743.
- Faucette, L. B., Sefton, K. A., Sadeghi, A. M., & Rowland, R. A. (2008). Sediment and phosphorus removal from simulated storm runoff with compost filter socks and silt fence, 63(4), 257–264.
- Ferro, V., & Mirabile, S. (2009). Comparing particle size distribution analysis by sedimentation and laser diffraction method. *Journal of Agricultural Engineering Research*, (2), 35–43.

- Flanagan, D. C., Frankenberger, J. R., & Ascough II, J. C. (2012). WEPP: model use, calibration, and validation. *Transactions of the ASABE*, 55(4), 1463–1477.
- Flanagan, D. C., Gilley, J. E., & Franti, T. G. (2007). Water Erosion Prediction Project (WEPP): Development History, Model Capabilities and Future Enhancements. *ASABE*, 50, 1603–1612.
- Foltz, R. B., Elliot, W. J., & Wagenbrenner, N. S. (2010). *Improving road erosion modeling for the Lake Tahoe Basin and evaluating BMP strategies for fine sediment reduction at watershed scales ( P010 ) – final report* (pp. 1–25).
- Foltz, R. B., Elliot, W. J., & Wagenbrenner, N. S. (2011). Soil erosion model predictions using parent material/soil texture-based parameters compared to using site-specific parameters, 54(4), 1347–1356.
- Foster, G. R., Toy, T. E., & Renard, K. G. (2003). *Comparison of the USLE, RUSLE1.06c, and RUSLE2 for Application to Highly Disturbed Lands* (pp. 154–160).
- Gabet, E. J. (2003). Sediment transport by dry ravel. *Journal of Geophysical Research*, 108(B1), 2049. doi:10.1029/2001JB001686
- Galetovic, J. R., Toy, T. E., & Foster, G. R. (1998). *Guidelines for the use of the Revised Universal Soil Loss Equation ( RUSLE ) version 1.06 on mined lands, construction sites, and reclaimed lands*.
- Gassman, P., Williams, J., Benson, V., Izaurrealde, R. C., Hauck, L. M., Jones, C. A., Flowers, J. D. (2005). *Historical development and applications of the EPIC and APEX models. Director* (p. 45). doi:10.13031/2013.17074
- Grismer, M. E. (2010). Rainfall simulation studies- a review of designs, performance and erosion measurement variability. *Presented at TSC Rainsim Workshop 4 March 2011*.
- Grismer, M. E. (2012). Standards vary in studies using rainfall simulators to evaluate erosion. *California Agriculture*, 66(3), 102–107. doi:10.3733/ca.v066n03p102
- Grismer, M. E., Ellis, A. L., & Fristensky, A. (2008). Runoff sediment particle sizes associated with soil erosion in the Lake Tahoe Basin, USA. *Land Degradation & Development*, 19, 331–350. Retrieved from <http://dx.doi.org/10.1002/ldr.839>
- Grismer, M. E., & Hogan, M. P. (2004). Simulated rainfall evaluation of revegetation/mulch erosion control in the Lake Tahoe Basin—1: method assessment. *Land Degradation & Development*, 15, 573–588. doi:10.1002/ldr.640
- Grismer, M. E., & Hogan, M. P. (2005a). Simulated rainfall evaluation of revegetation/mulch erosion control in the Lake Tahoe basin: 2. Bare soil assessment. *Land Degradation & Development*, 16, 397–404. doi:10.1002/ldr.689
- Grismer, M. E., & Hogan, M. P. (2005b). Simulated rainfall evaluation of revegetation/mulch erosion control in the Lake Tahoe Basin-3: soil treatment effects. *Land Degradation & Development*, 16(January), 1–13.
- Grismer, M. E., Schnurrenberger, C., Arst, R., & Hogan, M. P. (2009). Integrated monitoring and assessment of soil restoration treatments in the Lake Tahoe Basin. *Environmental Monitoring and Assessment*, 150(1-4), 365–83. doi:10.1007/s10661-008-0236-3

- Guerrant, D. G., Miller, W. W., Mahannah, C. N., & Narayanan, R. (1990). Infiltration evaluation of four mechanical rainfall simulation techniques in Sierra Nevada watersheds. *Water Resources Bulletin*, 26(1), 127–134.
- Guerrant, D. G., Miller, W. W., Mahannah, C. N., & Narayanan, R. (1991). Soil processes and chemical transport: site-specific erosivity evaluation of a Sierra Nevada forested watershed soil. *Journal of Environmental Quality*, 20(2), 396–402.
- Hamby, D. M. (1994). A review of techniques for parameter sensitivity analysis of environmental models. *Environmental Monitoring and Assessment*, 32(2), 135–54. doi:10.1007/BF00547132
- Hamed, Y., Albergel, J., Pe, Y., Nasri, S., Zante, P., & Berndtsson, R. (2002). Comparison between rainfall simulator erosion and observed reservoir sedimentation in an erosion-sensitive semiarid catchment. *Catena*, 50, 1–16.
- Helms, D. (2008). Hugh Hammond Bennett and the Creation of the Soil Erosion Service. *Historical Insights*, (8), 1–12.
- Heyvaert, A. C., Parra, A. T., Strassenburgh, C., & Townsend, P. (2008). *Brockway project area stormwater runoff and characterization study*.
- Hignett, C. T., Gusli, S., Cass, A., & Besz, W. (1995). An automated laboratory rainfall simulation system with controlled rainfall intensity, raindrop energy and soil drainage. *Soil Technology*, 8, 31–42.
- Hoffman, F. O., & Gardner, R. H. (1983). Evaluation of uncertainties in radiological assessment models. In *Radiological Assessment: A Textbook on Environmental Dose Analysis* (pp. 11–55).
- Knisel, W. G. (1980). *CREAMS: A field-scale model for chemicals, runoff and erosion from agricultural management systems*. USDA Conservation Research Report, (26).
- Krammes, J. S. (1965). Seasonal debris movement from steep mountainside slopes in southern California. In *Federal Inter-Agency Sedimentation Conference* (pp. 85–88). US Department of Agriculture.
- Laflen, J. M., Flanagan, D. C., & Engel, B. A. (2004). Soil erosion and sediment yield prediction accuracy using WEPP. *Journal of American Water Resources Association*, 1146, 289–297.
- Laflen, J. M., Lane, L. J., & Foster, G. R. (1991). A new generation of erosion prediction technology. *Journal of Soil and Water Conservation*, 46(1), 34–38. Retrieved from <http://www.ciesin.org/docs/002-215/002-215.html>
- Lahontan Water Quality Control Board (LWQCB) and the Nevada Division of Environmental Protection (NDEP). (2011). *Lake clarity crediting program handbook: for Lake Tahoe TMDL implementation v1.0*. South Lake Tahoe, CA: Prepared by Environmental Incentives, LLC.
- Lamb, M. P., Scheingross, J. S., Amidon, W. H., Swanson, E., & Limaye, A. (2011). A model for fire-induced sediment yield by dry ravel in steep landscapes. *Journal of Geophysical Research*, 116(F3), F03006. doi:10.1029/2010JF001878
- Larsen, I. J., & MacDonald, L. H. (2007). Predicting postfire sediment yields at the hillslope scale : Testing RUSLE and Disturbed WEPP, 43(August), 1–18. doi:10.1029/2006WR005560

- Laws, J. O., & Parsons, D. A. (1943). The relation of raindrop-size to intensity. *Transactions, American Geophysical Union*, 24(2), 452–460.
- Madden, L. V, Wilson, L. L., & Ntahimpera, N. (1998). Calibration and evaluation of an electronic sensor for rainfall kinetic energy. *Phytopathology*, 88(9), 950–9. doi:10.1094/PHYTO.1998.88.9.950
- Mukundan, R., Radcliffe, D. E., & Risse, L. M. (2010). Spatial resolution of soil data and channel erosion effects on SWAT model predictions of flow and sediment. *Journal of Soil and Water Conservation*, 65(2), 92–104. doi:10.2489/jswc.65.2.92
- Munn, J. R. (1974). *Development and use of a portable rainfall simulator to determine the erosion characteristics of several soils in the Lake Tahoe Basin*. University of California-Davis.
- Nash, J. E., & Sutcliffe, J. E. (1970). River flow forecasting through conceptual models. Part 1- A discussion of principles. *Journal of Hydrology*, 10, 282–290.
- Naslas, G. D., Miller, W. W., Gifford, G. F., & Fernandez, G. C. J. (1994). Effects of soil type, plot condition, and slope on runoff, and interrill erosion of two soils in the Lake Tahoe Basin. *Water Resources Bulletin*, 30(2), 319–328.
- Navas, A., Alberto, F., Machín, J., & Galán, A. (1990). Design and operation of a rainfall simulator for field studies of runoff and soil erosion. *Soil Technology*. doi:10.1016/0933-3630(90)90019-Y
- Nearing, M. A., Deer-Ascough, L., & Laflen, J. M. (1990). Sensitivity Analysis of the WEPP Hillslope Profile Erosion Model. *Transactions of the ASAE*, 33(3), 839–849.
- Nearing, M. A., Foster, G. R., Lane, L. J., & Finkner, S. C. (1989). A process-based soil erosion model for USDA-water erosion prediction project technology. *Transaction of the ASAE*, 32(5), 1587–1593.
- Pannell, D. (1997). Sensitivity analysis of normative economic models: theoretical framework and practical strategies. *Agricultural Economics*, 16(2), 139–152. doi:10.1016/S0169-5150(96)01217-0
- Pérez-Rodríguez, R., Marqués, M. J., Jiménez, L., García-ormaechea, S., & Bienes, R. (2009). Testing of rainfall simulator nozzles for suitability within soil erosion plots. In *Land degradation and rehabilitation: dryland ecosystems. Papers presented at the Fourth International Conference on Land Degradation, Cartagena, Murcia, Spain, 12-17 September 2004*. (pp. 191–199). Catena Verlag.
- Pimentel, D., Harvey, C., Resosudarmo, P., Sinclair, K., Kurz, D., McNair, M., Balir, R. (1995). Environmental and economic costs of soil erosion and conservation benefits. *Science*, 267(24), 1117–1122.
- Pollutant Load Reduction Model Development Team. (2009). *Pollutant Load Reduction Model (PLRM) user's manual* (pp. 1–151).
- Pollutant Load Reduction Model Development Team. (2010a). *Pollutant Load Reduction Model (PLRM) applications guide* (pp. 1–45).
- Pollutant Load Reduction Model Development Team. (2010b). *Pollutant Load Reduction Model (PLRM) model development document* (pp. 1–163).

- Pudasaini, M., Shrestha, S., Riley, S., Henderson, L., Geeves, G., & Pavan, N. (2004). Efficiencies of management practices in erosion control at construction sites, (408), 1–6.
- Renard, K., Foster, G., Weesies, G., McCool, D., & Yoder, D. (1997). *Predicting soil erosion by water: a guide to conservation planning with the Revised Universal Soil Loss Equation (RUSLE)*. U.S. Department of Agriculture Handbook No. 703 (p. 404).
- Renard, K. G., Yoder, D. C., Lightle, D. T., & Dabney, S. M. (2010). Chapter 8: Universal Soil Loss Equation and Revised Universal Soil Loss Equation. In R. P. C. Morgan & M. A. Nearing (Eds.), *Handbook of Erosion Modeling* (1st ed., pp. 137–167). Blackwell Publishing Ltd.
- Rice, E. C., & Grismer, M. E. (2010). Dry-season soil water repellency affects Tahoe Basin. *California Agriculture*, 64(3), 141–148.
- Robichaud, P. R., & Brown, R. E. (2002). *General Technical Report RMRS-GTR-94. Silt fences: an economical technique for measuring hillslope soil erosion* (pp. 1–28). United States Department of Agriculture (USDA), United States Forest Service (USFS) Rocky Mountain Research Station.
- Ryan, K., & Elliot, W. J. (2005). Chapter 9: Fire effects and soil erosion models. In D. G. Neary, K. C. Ryan, & L. F. DeBano (Eds.), *Wildland fire in ecosystems: effects of fire on soils and water* (Gen Tech R., Vol. 4, pp. 171–177). Ogden, UT: USDA Forest Service, Rocky Mountain Research.
- Sanchez-Moreno, J. F., Mannaerts, C. M., Jetten, V., & Löffler-Mang, M. (2012). Rainfall kinetic energy–intensity and rainfall momentum–intensity relationships for Cape Verde. *Journal of Hydrology*, 454–455, 131–140. doi:10.1016/j.jhydrol.2012.06.007
- Sawatsky, L., Dick, W., Cooper, D., Keys, M., Limited, E., & Alberta, C. (1996). Design of a rainfall simulator to measure erosion of reclaimed surfaces. In *20th Annual Columbia Mine Reclamation Symposium* (pp. 32–42). Kamloops, BC.
- Sidle, R. C., Pearce, A. J., & O' Loughlin, C. L. (1985). *Hillslope stability and land use*. Washington, D.C.: American Geophysical Union.
- Smith, S., Williams, J. R., Menzel, R. G., & Coleman, G. A. (1984). Prediction of Sediment Yield from Southern Plains Grasslands with the Modified Universal Soil Loss Equation. *Journal of Range Management*, 37(4), 295–297.
- Spaeth, K. E., Pierson, F. B., Weltz, M. A., & Blackburn, W. H. (2003). Evaluation of USLE and RUSLE estimated soil loss on rangeland. *Journal of Range Management*, 56(3), 234–246. doi:10.2307/4003812
- Stallings, J. H. (1951). *Mechanics of wind erosion*. United States Department of Agriculture, Soil Conservation Service.
- The Nevada Division of Environmental Protection (NDEP). (2011). *Final Lake Tahoe total maximum daily load* (pp. 1–338).
- Thomas, N. P., & Swamt, S. A. E. L. (1989). Construction and calibration of a rainfall simulator. *Journal of Agricultural Engineering Research*, 43, 1–9.

- Tiwari, A. K., Risse, L. M., & Nearing, M. A. (2000). Evaluation of WEPP and its comparison with USLE and RUSLE. *Transactions of the ASABE*, 43, 1129–1135.
- UC Davis Tahoe Environmental Research Center. (2013). Lake Tahoe water clarity the best in 10 years. Retrieved from [http://www.news.ucdavis.edu/search/news\\_detail.lasso?id=10511](http://www.news.ucdavis.edu/search/news_detail.lasso?id=10511)
- United States Department of Agriculture (USDA). (1993). *Soil survey manual. Soil Conservation Service. U.S. Department of Agriculture Handbook 18*. Retrieved from [http://www.nrcs.usda.gov/wps/portal/nrcs/detail/soils/planners/?cid=nrcs142p2\\_054262](http://www.nrcs.usda.gov/wps/portal/nrcs/detail/soils/planners/?cid=nrcs142p2_054262)
- United States Department of Agriculture (USDA) Natural Resources Conservation Service (NRCS). (2000). *Erosion and Sedimentation on Construction Sites* (pp. 1–5). Retrieved from [http://www.nrcs.usda.gov/Internet/FSE\\_DOCUMENTS/nrcs142p2\\_053285.pdf](http://www.nrcs.usda.gov/Internet/FSE_DOCUMENTS/nrcs142p2_053285.pdf)
- United States Department of Agriculture (USDA) Natural Resources Conservation Service (NRCS). (2003). *Revised Universal Soil Loss Equation version 2 user's guide* (Vol. 1–76).
- United States Department of Agriculture (USDA) Natural Resources Conservation Service (NRCS). (2007). *Soil survey of the Tahoe Basin Area, California and Nevada*. Retrieved from [http://soils.usda.gov/survey/printed\\_surveys/](http://soils.usda.gov/survey/printed_surveys/)
- United States Department of Agriculture (USDA) Natural Resources Conservation Service (NRCS). (2008). RUSLE2 National Database. Retrieved from [http://fargo.nserl.purdue.edu/rusle2\\_dataweb/RUSLE2\\_Index.htm](http://fargo.nserl.purdue.edu/rusle2_dataweb/RUSLE2_Index.htm)
- United States Department of Agriculture (USDA) RUSLE Development Team. (2001). *Revised Universal Soil Loss Equation version 2 handbook* (pp. 1–78). Retrieved from [http://www.nrcs.usda.gov/Internet/FSE\\_DOCUMENTS/nrcs144p2\\_025079.pdf](http://www.nrcs.usda.gov/Internet/FSE_DOCUMENTS/nrcs144p2_025079.pdf)
- United States Department of Agriculture (USDA)-Agriculture Research Service (ARS). (1995a). *NSERL Report NO. 10, chapter 1: overview of the WEPP erosion prediction model* (pp. 1–12).
- United States Department of Agriculture (USDA)-Agriculture Research Service (ARS). (1995b). *NSERL Report NO. 11: WEPP user summary* (pp. 1–141).
- United States Department of the Interior Bureau of Reclamation (USBR). (2006). *Erosion and Sedimentation Manual*. Retrieved from <http://www.usbr.gov/pmts/sediment/kb/ErosionAndSedimentation/>
- United States Environmental Protection Agency (EPA). (1992). Chapter 3: sediment and erosion control. In *Stormwater management for construction activities*. Retrieved from <http://www.epa.gov/region6/6en/w/sw/sediment.pdf>
- Van Boxel, J. H. (1998). Numerical model for the fall speed of rain drops in a rain fall simulator. In D. Gabriels & W. M. Cornelis (Eds.), *Proceedings of the International Workshop on Technical Aspects and Use of Wind Tunnels for Wind-Erosion Control: Combined Effects of Wind and Water Erosion on Processes, November 17– 18 1997, Ghent, Belgium* (pp. 77–85). ICE Spec. Rep.
- Van Dijk, A. I. J. M., Bruijnzeel, L. A., & Rosewell, C. J. (2002). Rainfall intensity-kinetic energy relationships: a critical literature appraisal. *Journal of Hydrology*, 261(1-4), 1–23. doi:10.1016/S0022-1694(02)00020-3

- Williams, J. R. (1975). Sediment-yield prediction with universal equation using runoff energy factor. In *Present and Prospective Technology for Predicting Sediment Yields and Sources* (pp. 244–252). (Proceedings of the Sediment-Yield Workshop, USDA Sedimentation Laboratory, Oxford, Mississippi, November 28-30).
- Williams, J. R. (1990). The Erosion-Productivity Impact Calculator (EPIC) Model: A Case History. *Philosophical Transactions of the Royal Society B: Biological Sciences*. doi:10.1098/rstb.1990.0184
- Williams, J. R., & Izaurrealde, R. C. (2006). Chapter 18: The APEX model. In V. P. Singh & D. K. Frevert (Eds.), *Watershed models* (pp. 437–482). CRC Press, Taylor and Francis Group, Boca Raton, FL.
- Wischmeier, W., & Smith, D. (1965). *Predicting Rainfall-Erosion Losses from Cropland East of the Rocky Mountains: Guide for Selection of Practices for Soil and Water Conservation*. U.S. Department of Agriculture Handbook No. 282 (pp. 1–47).
- Wischmeier, W., & Smith, D. (1978). *Predicting rainfall erosion losses: a guide to conservation planning*. U.S. Department of Agriculture Handbook No. 537 (pp. 1–69).



Nevada Department of Transportation  
Rudy Malfabon, P.E. Director  
Ken Chambers, Research Division Chief  
(775) 888-7220  
kchambers@dot.nv.gov  
1263 South Stewart Street  
Carson City, Nevada 89712